university of groningen

University Medical Center Groningen

University of Groningen

Cellular senescence in the ageing brain

Talma, Nynke

DOI:
10.33612/diss.206630102

IMPORTANT NOTE: You are advised to consult the publisher's version (publisher's PDF) if you wish to cite from it. Please check the document version below.

Document Version
Publisher's PDF, also known as Version of record

Publication date:
2022

Link to publication in University of Groningen/UMCG research database

Citation for published version (APA):
Talma, N. (2022). *Cellular senescence in the ageing brain: to eliminate or not to eliminate?*. University of Groningen. https://doi.org/10.33612/diss.206630102

Copyright
Other than for strictly personal use, it is not permitted to download or to forward/distribute the text or part of it without the consent of the author(s) and/or copyright holder(s), unless the work is under an open content license (like Creative Commons).

The publication may also be distributed here under the terms of Article 25fa of the Dutch Copyright Act, indicated by the "Taverne" license. More information can be found on the University of Groningen website: https://www.rug.nl/library/open-access/self-archiving-pure/taverne-amendment.

Take-down policy
If you believe that this document breaches copyright please contact us providing details, and we will remove access to the work immediately and investigate your claim.

Downloaded from the University of Groningen/UMCG research database (Pure): http://www.rug.nl/research/portal. For technical reasons the number of authors shown on this cover page is limited to 10 maximum.

Download date: 29-10-2022

Cellular senescence in the ageing brain

To eliminate or
not to eliminate?

Nynke Talma

This PhD project and the publication of this thesis were financially supported by Foundation the Cock-Hadders, the University Medical Centre Groningen, the University of Groningen and the Graduate School of Medical Sciences at the University of Groningen.

Printing Ridderprint
Layout and design Iris Reintke
Cover concept Nynke Talma
About the cover The design is based on the scene of Shakepears' Hamlet where he holds a skull and asks himself the question: To be or not to be? I have added the quote on the back because we know what the data is, but not what it might be useful for in the future. Therefore, all data is important, including the data that does not match the previously determined hypotheses.

ISBN: 978-94-6458-091-4
Elect. ISBN: 978-94-6458-106-5

Copyright © 2022 Nynke Talma
All rights reserved. No part of this publication may be reproduced or transmitted in any form or by any means without written permission of the author and, when appropriate, the publisher holding the copyrights of the published articles.

university of groningen

Cellular senescence in the ageing brain

To eliminate or not to eliminate?

PhD thesis

to obtain the degree of PhD at the
University of Groningen
on the authority of the
Rector Magnificus Prof. C. Wijmenga
and in accordance with
the decision by the College of Deans.

This thesis will be defended in public on

Wednesday 20 April 2022 at 11.00 hours

by

Nynke Talma

born on 19 June 1994
in Leeuwarden

Supervisors

Prof. B.J.L. Eggen
Dr. M. Demaria

Assessment committee

Prof. D.S. Verbeek
Prof. J.J. Oliveira Malva
Prof. V.G. Gorgoulis

Paranymphs

J. Hartung
S. Eskandar

Table of contents

Chapter 1

General introduction and outline of the thesis

Adapted from:

A Senescence-Centric View of Aging: Implications for Longevity and Disease
M. Borghesan[1,2], W.M.H. Hoogaars[1,2], M. Varela-Eirin[1,2], N. Talma[1], and M. Demaria[1,*]

[1] *European Research Institute for the Biology of Ageing (ERIBA), University Medical Center Groningen (UMCG), University of Groningen, Antonius Deusinglaan 1, 9715RA, Groningen, The Netherlands*

[2] *These authors contributed equally*

[*] *Corresponding author*

Trends in Cell Biology, October 2020, Vol. 30, No. 10 https://doi.org/10.1016/j.cb.2020.07.002

Cellular senescence

Definition and markers of cellular senescence

Cellular senescence represents a cellular state of stable and generally irreversible growth arrest originally described as one of the main processes regulating cellular and organismal ageing (Hayflick and Moorhead, 1961). Senescence acts as a potent tumor-suppressive mechanism by arresting damaged and potential tumorigenic cells. A major regulator of a senescence-associated cell cycle arrest is a chronic DNA-damage response (DDR), which derives from unresolved DNA lesions and triggers activation of cell cycle inhibitors p21 and/or p16. Senescent cells are characterized by various structural changes, including misshaped nuclei, enhanced lysosomal content and activity, altered mitochondria morphology and differential plasma membrane composition (Hernandez-Segura et al., 2018a). Other common features observed in senescent cells are profound changes in their (epi)genetic landscape and gene expression, persistent macromolecular damage, and aberrant metabolism and activation of a hypersecretory phenotype (Gorgoulis et al., 2019; Hernandez-Segura et al., 2018a).

The hypersecretory phenotype is defined as the senescence-associated secretory phenotype (SASP), a collection of chemokines, cytokines, matrix remodeling proteases, lipids and extracellular vesicles (EVs) (Hernandez-Segura et al., 2018a). The SASP is a highly heterogeneous program whose composition depends on various intrinsic and extrinsic factors (Basisty et al., 2020; Hernandez-Segura et al., 2017). Restricted and localized SASP contributes to various beneficial functions. It favors correct organ patterning during embryogenesis, halts malignant transformation by reinforcing cell cycle arrest and activating tumor immunosurveillance, and promotes tissue repair (Yun, 2018). By contrast, persistence of senescent cells and SASP has been associated with chronic inflammation, age-related pathologies, and a cancer-permissive microenvironment (Campisi, 2000). Consistently, in a young, healthy individual, senescence is successfully induced in damaged cells, to ensure correct tissue function and repair, and counteract incipient oncogenic stimuli, whereas their improper activation and disposal followed by progressive accumulation with age leads to disease (Figure 1). For this reason,

interventions selectively targeting cellular senescence hold the potential to delay ageing and alleviate multiple age-related dysfunctions.

Detection of cellular senescence

Hernandez-Segura et al. have provided protocols for the induction and validation of cellular senescence in cultured cells (Hernandez-Segura et al., 2018b). These protocols can also be adapted to detect cellular senescence in tissue *ex vivo*. Cellular senescence can be induced by replication stress, ionizing radiation, ultraviolet radiation, chemotherapy, oxidative stress and epigenetically. The induction of senescence is determined by a combination of multiple markers. A common marker of senescent cells is senescence-associated β-galactosidase (SA-β-gal) activity and it detects the increased lysosomal content and activity in senescent cells. This is accompanied by EdU incorporation assays, assessing the cell cycle arrest by a lack of DNA replication. Also, gene expression of cell cycle markers *p16* and *p21* is upregulated in senescent cells and is detected using real-time quantitative PCR (RT-qPCR). The expression of SASP factors are also detected on a gene level by RT-qPCR and can be confirmed on a protein level using ELISA. The most common SASP markers are IL6, IL8, IL1α, CXCL1, CXCL10, CCL2, CCL20, PAI1, MMP1, MMP3, MMP9, but can be expanded depending on the type pathways activated in the cells. Together, these markers confirm the induction of the senescence program in cells.

Central nervous system

Cellular composition of the brain

The central nervous system (CNS) is composed of the brain and the spinal cord, and controls most bodily functions including movement, memory and thoughts. Neurons make up about 50 percent of the brain (Herculano-Houzel, 2009) with the other 50 percent composed of different types of supporting cells (Purves et al., 2001). Neurons are the cells responsible for signal transduction and the transmission of information. The neuronal functions are supported by cells called neuroglia or glial cells in short. Besides neurons and glia, the CNS contains endothelial cells, fibroblasts, macrophages, epithelial cells, smooth muscle cells, and pericytes. The three most important glial cells are microglia, astrocytes, and oligodendrocytes. Their physiological function and what

changes occur with ageing will be discussed in more detail below.

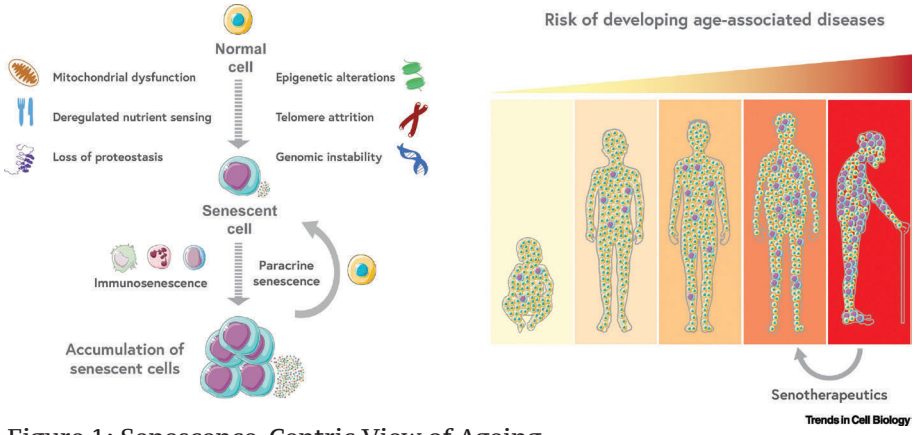

Figure 1: Senescence-Centric View of Ageing.

Some of the hallmarks of ageing (López-Otín et al., 2013) (mitochondrial dysfunction, deregulated nutrient-sensing, loss of proteostasis, epigenetic alterations, telomere attrition, and genomic instability) induce normal cells to become senescent, which in turn can induce paracrine senescence in nearby normal cells through senescence-associated secretory phenotype (SASP). Senescence-promotion through SASP together with a decline in the immune system activity, converge to induce organismal accumulation of senescent cells. In aged individuals, chronic accumulation of senescent cells contributes to tissue dysfunction and increased risk of age-associated diseases development. Nevertheless, senescent cells elimination with different senotherapeutic approaches can improve healthspan in aged individuals.

Glial cells from physiology to pathology in ageing

Microglia

Microglia are the main innate immune cells of the CNS regulating neuroimmune function. While peripheral macrophages are derived from hematopoietic stem cells, microglia originate from the yolk sac in early embryonic development (Prinz and Priller, 2014). Microglia are essential for CNS homeostasis due to their wide variety of supportive properties: synaptic pruning, shaping axonal projections, supporting activated/overactivated neurons, learning-associated synapse formation and innate immune responses amongst others (Colonna and Butovsky, 2017). Microglia, as the tissue macrophages of the brain, phagocytose dead cells and debris while also surveilling their surroundings for infections. Furthermore, during demyelination, a process discussed in more detail in the section about oligodendrocytes, microglia clear cellular

debris and stimulate the differentiation of oligodendrocyte progenitor cells (OPCs) into oligodendrocytes by secretion of signaling molecules to improve remyelination (Baror et al., 2019).

During ageing, the ability of microglia to maintain homeostasis decreases. In order to investigate this on a transcriptional level, Galatro et al analyzed the transcriptional profile of purified microglia from 39 human subjects. Age-associated changes in human microglia were detected and showed enrichment for genes involved in cell adhesion, axonal guidance, cell surface receptor expression and actin (dis)assembly (Galatro et al., 2017). In addition, during ageing, the ability of microglia to engulf protein aggregates is compromised, microglia have reduced process motility, reduced migration, reduced chemotaxis, an enhanced response to inflammatory stimuli leading to enhanced release of inflammatory cytokines, loss of neuroprotective potential (Spittau, 2017), and impaired support of remyelination (Baror et al., 2019), thereby negatively influencing the cognitive functioning in the aged brain.

Astrocytes

Astrocytes are tissue-supporting glial cells with an extensive variety of functions. Astrocytes maintain homeostasis of extracellular fluids, ions and transmitters; provide metabolites as energy substrates to neurons; regulate blood-brain-barrier function; support synapse development and plasticity; and support neural circuit function, neurological function and behavior (Sofroniew, 2020). In addition, astrocytes are capable of supporting other glial cells for example oligodendrocytes by promoting OPC differentiation into oligodendrocytes (Willis et al., 2020).

With age, this support that can be conveyed via extracellular vesicles, is diminished in ageing astrocytes (Willis et al., 2020). Moreover, ageing astrocytes upregulate genes associated with synaptic transmission or elimination, widely recognized Alzheimer's disease (AD) risk genes, peptidase-inhibitor genes, genes involved in inflammatory pathways, and downregulate genes involved in cholesterol synthesis (Boisvert et al., 2018; Pan et al., 2020). However, with age, astrocytes maintain homeostatic and neurotransmission-regulating genes. The loss of astrocyte function and gain of neuroinflammatory function of astrocytes might influence cell function in age-associated neurodegenerative disease (Cohen and Torres, 2019).

Oligodendrocytes

Oligodendrocytes are the myelinating cells of the CNS and are derived from oligodendrocyte precursor cells, OPCs (Bergles and Richardson, 2016). OPCs are one of the few progenitors that remain abundant during adulthood in the CNS, where they retain the ability to generate new oligodendrocytes. The new oligodendrocytes wrap myelin sheets around unmyelinated axons of neurons to function as an electric insulator resulting in enhanced signal transduction speed (Simons and Nave, 2016). Regeneration of myelin, also called remyelination, occurs after myelin loss, known as demyelination, through normal ageing or disease, as well as changing patterns of myelination in response to life experience.

With ageing, myelin thickness decreases and remyelination is reduced (Neumann et al., 2019). One of the main reasons of diminished remyelination is the reduced differentiation of OPCs into oligodendrocytes. One of the causes of impaired oligodendrocyte differentiation is unresolved DNA damage in aged oligodendrocytes (Tse and Herrup, 2017). Interestingly, age-related deficits in memory were shown to be improved by stimulating oligodendrocyte differentiation from OPCs and thereby myelin renewal (Wang et al., 2020). Renewed myelin sheaths are thinner compared to myelin that was formed during development. Thin myelin is an indicator of remyelination which retains axonal function (Duncan et al., 2017). Impaired myelination during ageing is associated with decreased brain function and impaired recovery in demyelinating diseases such as multiple sclerosis (MS) (Sim et al., 2002).

Cellular senescence in the central nervous system

Cellular senescence in neurodegeneration

In the past decade, the senescence research field has grown exponentially. The past 5 years, many studies have been performed on the role of cellular senescence in the CNS and especially on the effect of senescence on age-related neurodegenerative diseases. Here, the current view on the role of senescent cells in neurodegenerative disease will be summarized, and senescence in Alzheimer's disease, amyotrophic lateral sclerosis, Parkinson's disease and multiple sclerosis will be highlighted.

Alzheimer's disease

Alzheimer's disease (AD) is a multifactorial neurodegenerative disease causing progressive dementia (Guerreiro and Bras, 2015). It is characterized by extracellular plaques composed of amyloid-β aggregates and intracellular neurofibrillary tangles composed of aggregated hyperphosphorylated tau (Gallardo and Holtzman, 2019). Early-onset familial AD accounts for 5-10 % of all cases and is strongly linked to causal gene mutations in amyloid precursor protein (APP) and presenilin (PSEN1/2) genes (Ayodele et al., 2021). Sporadic, or late-onset AD is a multifactorial disease for which age is the most important risk factor (Armstrong, 2019).

Cellular senescence in AD has been observed in post-mortem human brain tissues and has been further characterized using mouse models containing tau or amyloid pathology. $p16^{INK4a}$ upregulation, one of the most common and specific senescence markers, has been described in astrocytes of AD patients (Bhat et al., 2012). Also, senescence markers *p21*, p16 proteins, and SA-β-gal were detected in OPCs in human AD tissues (Zhang et al., 2019). Moreover, in laser capture micro-dissected cortical neurons containing neurofibrillary tangles from AD brains, transcriptional upregulation of senescence-associated genes was observed (Musi et al., 2018). To study AD, many transgenic mouse models have been generated representing familial AD, however no mouse model fully recapitulates both the pathological aspects and behavioral phenotypes of AD (Myers and McGonigle, 2019). Increased $p16^{INK4a}$ levels were detected in hippocampal neurons (Wei et al., 2016) and in oligodendrocyte progenitor cells (Bussian et al., 2018) in amyloid mouse models. In addition, elimination of senescent oligodendrocyte progenitor cells improved cognitive function and reduced amyloid load (Zhang et al., 2019). In AD models of dysfunctional tau protein, genetic or pharmacological elimination of senescent cells have also been shown to ameliorate disease progression (Bussian et al., 2018; Musi et al., 2018). This suggests that elimination of senescent cells from the AD brain might be beneficial for familial AD. More research needs to be performed to investigate if the same holds true for sporadic cases.

Amyotrophic lateral sclerosis

Amyotrophic lateral sclerosis (ALS) is a progressive motor neuron disease. Mutations in the c9orf72, TDP-43, superoxide dismutase-1 (SOD-1) and fused

in sarcoma (FUS) genes in combination with environmental factors result in formation of intracellular aggregates (Bos et al., 2019). These aggregates together with other disturbed molecular pathways result in neuronal cell death and activation of glial cells which in turn can also lead to neurotoxicity.

Cellular senescence markers have been identified in patient tissues as well as in a rat model for ALS. Stainings for p16 and p21 in human port-mortem brain tissues from ALS patients showed increased p16 and p21 in glial cells, mainly astrocytes, and increased p21 in neurons compared to tissues of control donors (Vazquez-Villaseñor et al., 2019). In the SOD1G93A ALS rat model, containing a mutation in the SOD-1 gene, mostly microglia but also astrocytes and neurons have been found positive for multiple senescence markers (Trias et al., 2019). All the data together suggests the accumulation of senescent cells during ALS disease progression.

Parkinson's disease

The prevalence of Parkinson's disease (PD), the second most common neurodegenerative disorder, increases with advanced age (de Lau and Breteler, 2006). PD progression is characterized by tremor, rigidity, and bradykinesia. Pathologically, PD is characterized by a loss of dopaminergic neurons from the substantia nigra and neuronal accumulation of aggregated α-synuclein in Lewy bodies (Kouli et al., 2018).

A recent study with an incident PD cohort identified that both inflammatory and senescence markers ($p16^{INK4a}$) derived from blood are valuable predictors of clinical progression in PD patients (Martin-Ruiz et al., 2020). In experimental PD models, pathology can be induced either genetically or with neurotoxins (Terzioglu and Galter, 2008). Senescent dopaminergic neurons have been detected in a model of familial PD (Riessland et al., 2019). In addition, preformed alpha-synuclein fibrils have been shown to induce cellular senescence in both astrocytes and microglia in alpha-synuclein injected mouse brains (Verma et al., 2021). Moreover, in PD mouse models, elimination of senescent cells has been shown to improve neurological functions. Neurotoxin-induced PD has been shown to be accompanied by accumulation of senescent cells, while the elimination of senescent astrocytes by the use of a transgene protected against neuropathology (Chinta et al., 2018). Furthermore, inhibition of astrocyte senescence with the antioxidant astragaloside IV confirmed the beneficial

effect of removing senescent astrocytes in PD (Xia et al., 2020).

Multiple Sclerosis

The auto-immune disease multiple sclerosis (MS) is characterized by lesions of: demyelination, inflammation, axonal injury and axonal loss. The disease appears as abrupt onset of focal sensory disturbances that is accompanied by damage of vision, limb weakness, unsteadiness of gait, and bowel or bladder symptoms (Huang et al., 2017). In animal models, MS is mostly investigated using experimental autoimmune encephalomyelitis (EAE) and cuprizone intoxication (Palumbo and Pellegrini, 2017). EAE is used to study the inflammatory aspects of MS, whereas cuprizone is used to study the demyelination and remyelination that occurs in lesions.

Cellular senescence has been proposed as a target for the treatment of MS (Oost et al., 2018). In the cuprizone model, senescence markers have been detected in the white matter of the brain. DNA damage response was present in glial cell nuclei and SA-β-gal was found in demyelinated lesions (Papadopoulos et al., 2017). Moreover, neural progenitor cells from primary progressive multiple sclerosis patients were shown to be senescent and elimination of, the by senescent cells secreted, high-mobility group box-1 (HMBG1) protein restored oligodendrocyte differentiation (Nicaise et al., 2019).

Taken together, it has been shown that senescent cells play a role in the progression of neurodegenerative diseases.

Cellular senescence in the ageing brain

Over time, the risk of developing a neurodegenerative disease increases dramatically. It is important to understand what changes in the brain cause pathology. To gain insight in these mechanisms, we need to know what occurs during chronological ageing in the brain. Little is known about the healthy aged brain and the effect of chronological ageing on senescence in the CNS.

To investigate the transcriptional profile of senescent cells in the aged CNS, single cell RNA sequencing was performed on aged mouse brains. The data showed that cerebro-microvascular endothelial cells expressed cellular senescence markers (Kiss et al., 2020). Moreover, it was shown that vascular cell senescence compromised blood-brain-barrier integrity (Yamazaki et al.,

2016). This is highlighting the significance of studying the effect of senescent cells in the CNS already before development of neurodegenerative diseases.

In adulthood, neurons are only replenished in very limited brain regions. Neurogenesis occurs in the hippocampus, however Jin and colleagues have shown that due to the SASP expression of the neuroblasts in the dendrite gyrus, Natural killer (NK) cells get attracted and eliminate these neuroblasts halting the neurogenesis (Jin et al., 2021). Elimination of senescent neuroblasts by NK cells has been shown to negatively impact the ageing brain, due to excessive removal of neuroblasts. Senotherapy by eliminating specifically senescent neuroblasts or modulation of the SASP might improve the neurogenesis by preventing NK cell attraction and the elimination of neuroblasts. Taken together, these studies show that there is still a large gap in the knowledge of the impact of senescence cells and removal of these cells on the ageing brain.

Outline of the thesis

Cellular senescence has been shown to play an important role in the progression of age-related tissue dysfunction in the periphery and removal of these cells has been shown to improve the health span of aged animals. However, less is known about the effects of (accelerated) ageing on cellular senescence in the central nervous system. The goal of this thesis was to gain more insight into the senescence phenotypes of glial cells and identify which cells become senescent in the aged brain. This information brings us closer to the question: should senescent brain cells be removed from the brain or are they beneficial? In other words: to eliminate senescent brain cells or not to eliminate senescent brain cells?

In chapter 1, an introduction to senescent cells in the central nervous system is given. First, cellular senescence is explained. Next, the cellular composition of the CNS with the focus on glial cells in physiology and ageing is described. Lastly, the current knowledge of senescent cells in the brain with age and disease is provided.

In chapter 2, the effect of the modulation of lysosomes on senescent cells is investigated. First, the effects of senescence induction on lysosomal gene expression is tested. Next, the effect of three lysosomal modulating drugs on senescence markers is studied. In addition, the effect of lysosomal modulation

on lysosomal trapped drug-induced senescence is investigated.

In chapter 3, single-cell RNA sequencing is used to identify distinct age-dependent $p16^{high}$ subpopulations in the murine brain. First, fluorescence-activated cell sorting is used to isolate and quantify the amount of $p16^{high}$ cells in the young and old mouse brain. Next, bulk sequencing is used to identify differentially expressed gene between $p16^{high}$ and $p16^{low}$ cells. Single-cell RNA sequencing is used to identify the cell types that express p16 and assess the differences in subpopulations within cell types.

In chapter 4, the direct and indirect effect of genotoxic stress-induced senescence in glial cells *in vitro* and in mice *in vivo* are characterized. First, the effect of genotoxic stress inducers on microglia, astrocytes and oligodendrocytes was assessed. Next, the indirect effect of conditioned medium from senescence cells on *ex vivo* organotypic slice cultures was studied. Finally, the direct and indirect effects of chemotherapy-induced genotoxic stress in mice was investigated.

In chapter 5, the data presented in experimental chapters 2-4 are summarized and further discussed. Also, future prospects are described.

References

Armstrong, R.A. (2019). Risk factors for Alzheimer's disease. Folia Neuropathol. 57, 87–105.

Ayodele, T., Rogaeva, E., Kurup, J.T., Beecham, G., and Reitz, C. (2021). Early-Onset Alzheimer's Disease: What Is Missing in Research? Curr. Neurol. Neurosci. Rep. 21.

Baror, R., Neumann, B., Segel, M., Chalut, K., Fancy, S., Schafer, D., and Franklin, R. (2019). Transforming growth factor-beta renders ageing microglia inhibitory to oligodendrocyte generation by CNS progenitors. Glia 67, 1374–1384.

Basisty, N., Kale, A., Jeon, O.H., Kuehnemann, C., Payne, T., Rao, C., Holtz, A., Shah, S., Sharma, V., Ferrucci, L., et al. (2020). A proteomic atlas of senescence-associated secretomes for aging biomarker development. PLoS Biol. 18, e3000599.

Bergles, D.E., and Richardson, W.D. (2016). Oligodendrocyte Development and Plasticity. Cold Spring Harb. Perspect. Biol. 8.

Bhat, R., Crowe, E.P., Bitto, A., Moh, M., Katsetos, C.D., Garcia, F.U., Johnson, F.B., Trojanowski, J.Q., Sell, C., and Torres, C. (2012). Astrocyte Senescence as a Component of Alzheimer's Disease. PLoS One 7, e45069.

Boisvert, M.M., Erikson, G.A., Shokhirev, M.N., and Allen, N.J. (2018). The Aging Astrocyte Transcriptome from Multiple Regions of the Mouse Brain. Cell Rep. 22, 269.

Bos, M.A.J. van den, Geevasinga, N., Higashihara, M., Menon, P., and Vucic, S. (2019). Pathophysiology and Diagnosis of ALS: Insights from Advances in Neurophysiological Techniques. Int. J. Mol. Sci. 20.

Bussian, T.J., Aziz, A., Meyer, C.F., Swenson, B.L., van Deursen, J.M., and Baker, D.J. (2018). Clearance of senescent glial cells prevents tau-dependent pathology and cognitive decline. Nature 562, 578–582.

Campisi, J. (2000). Cancer, aging and cellular senescence. In Vivo 14, 183–188.

Chinta, S.J., Woods, G., Demaria, M., Rane, A., Zou, Y., McQuade, A., Rajagopalan, S., Limbad, C., Madden, D.T., Campisi, J., et al. (2018). Cellular Senescence Is Induced by the Environmental Neurotoxin Paraquat and Contributes to Neuropathology Linked to Parkinson's Disease. Cell Rep. 22, 930–940.

Cohen, J., and Torres, C. (2019). Astrocyte senescence: Evidence and significance. Aging Cell 18.

Colonna, M., and Butovsky, O. (2017). Microglia Function in the Central Nervous System During Health and Neurodegeneration. Annu. Rev. Immunol. 35, 441–468.

Duncan, I., Marik, R., Broman, A., and Heidari, M. (2017). Thin myelin sheaths as the hallmark of remyelination persist over time and preserve axon function. Proc. Natl. Acad. Sci. U. S. A. 114, E9685–E9691.

Galatro, T.F., Holtman, I.R., Lerario, A.M., Vainchtein, I.D., Brouwer, N., Sola, P.R., Veras, M.M., Pereira, T.F., Leite, R.E.P., Möller, T., et al. (2017). Transcriptomic analysis of purified human cortical microglia reveals age-associated changes. Nat. Neurosci. 20, 1162–1171.

Gorgoulis, V., Adams, P.D., Alimonti, A., Bennett, D.C., Bischof, O., Bishop, C., Campisi, J., Collado, M., Evangelou, K., Ferbeyre, G., et al. (2019). Cellular Senescence: Defining a Path Forward. Cell 179, 813–827.

Guerreiro, R., and Bras, J. (2015). The age factor in Alzheimer's disease. Genome Med. 7, 1–3.

Hayflick, L., and Moorhead, P.S. (1961). The serial cultivation of human diploid cell strains. Exp. Cell Res. 25, 585–621.

Herculano-Houzel, S. (2009). The Human Brain in Numbers: A Linearly Scaled-up Primate Brain. Front. Hum. Neurosci. 3.

Hernandez-Segura, A., de Jong, T. V, Melov, S., Guryev, V., Campisi, J., and Demaria, M. (2017). Unmasking Transcriptional Heterogeneity in Senescent Cells.

Hernandez-Segura, A., Nehme, J., and Demaria, M. (2018a). Hallmarks of Cellular Senescence. Trends Cell Biol. 28, 436–453.

Hernandez-Segura, A., Brandenburg, S., and Demaria, M. (2018b). Induction and Validation of Cellular Senescence in Primary Human Cells. JoVE (Journal Vis. Exp. 2018, e57782.

Huang, W.J., Chen, W.W., and Zhang, X. (2017). Multiple sclerosis: Pathology, diagnosis and treatments. Exp. Ther. Med. 13, 3163.

Jin, W., Shi, K., He, W., Sun, J., Van Kaer, L., Shi, F., and Liu, Q. (2021). Neuroblast senescence in the aged brain augments natural killer cell cytotoxicity leading to impaired neurogenesis and cognition. Nat. Neurosci. 24, 61–73.

Kiss, T., Nyúl-Tóth, Á., Balasubramanian, P., Tarantini, S., Ahire, C., DelFavero, J., Yabluchanskiy, A., Csipo, T., Farkas, E., Wiley, G., et al. (2020). Single-cell RNA sequencing identifies senescent cerebromicrovascular endothelial cells in the aged mouse brain. GeroScience 42, 429–444.

Kouli, A., Torsney, K.M., and Kuan, W.-L. (2018). Parkinson's Disease: Etiology, Neuropathology, and Pathogenesis. Park. Dis. Pathog. Clin. Asp. 3–26.

de Lau, L.M., and Breteler, M.M. (2006). Epidemiology of Parkinson's disease. Lancet Neurol. 5, 525–535.

López-Otín, C., Blasco, M.A., Partridge, L., Serrano, M., and Kroemer, G. (2013). The Hallmarks of Aging. Cell 153, 1194–1217.

Martin-Ruiz, C., Williams-Gray, C.H., Yarnall, A.J., Boucher, J.J., Lawson, R.A., Wijeyekoon, R.S., Barker, R.A., Kolenda, C., Parker, C., Burn, D.J., et al. (2020). Senescence and Inflammatory Markers for Predicting Clinical Progression in Parkinson's Disease: The ICICLE-PD Study. J. Parkinsons. Dis. 10, 193–206.

Musi, N., Valentine, J.M., Sickora, K.R., Baeuerle, E., Thompson, C.S., Shen, Q., and Orr, M.E. (2018). Tau protein aggregation is associated with cellular senescence in the brain. Aging Cell 17, e12840.

Neumann, B., Segel, M., Chalut, K., and Franklin, R. (2019). Remyelination and ageing: Reversing the ravages of time. Mult. Scler. 25, 1835–1841.

Nicaise, A.M., Wagstaff, L.J., Willis, C.M., Paisie, C., Chandok, H., Robson, P., Fossati, V., Williams, A., and Crocker, S.J. (2019). Cellular senescence in progenitor cells contributes to diminished remyelination potential in progressive multiple sclerosis. Proc. Natl. Acad. Sci. 116, 9030–9039.

Oost, W., Talma, N., Meilof, J.F., and Laman, J.D. (2018). Targeting senescence to delay progression of multiple sclerosis. J. Mol. Med. 96, 1153–1166.

Palumbo, S., and Pellegrini, S. (2017). Experimental In Vivo Models of Multiple Sclerosis: State of the Art. Mult. Scler. Perspect. Treat. Pathog. 173–183.

Pan, J., Ma, N., Yu, B., Zhang, W., and Wan, J. (2020). Transcriptomic profiling of microglia and astrocytes throughout aging. J. Neuroinflammation 17.

Papadopoulos, D., Karamita, M., Mitsikostas, D.D., Gorgoulis, V., Probert, L., and Nicholas, R. (2017). Accelerated cellular senescence in a model of multiple sclerosis (S50.004). Neurology 88.

Prinz, M., and Priller, J. (2014). Microglia and brain macrophages in the molecular age: from origin to neuropsychiatric disease. Nat. Rev. Neurosci. 15, 300–312.

Purves, D., Augustine, G.J., Fitzpatrick, D., Katz, L.C., LaMantia, A.-S., McNamara, J.O., and Williams, S.M. (2001). The Cellular Components of the Nervous System.

Riessland, M., Kolisnyk, B., Kim, T.W., Cheng, J., Ni, J., Pearson, J.A., Park, E.J., Dam, K., Acehan, D., Ramos-Espiritu, L.S., et al. (2019). Loss of SATB1 Induces p21-Dependent Cellular Senescence in Post-mitotic Dopaminergic Neurons. Cell Stem Cell.

Sim, F., Zhao, C., Penderis, J., and Franklin, R. (2002). The age-related decrease in CNS remyelination efficiency is attributable to an impairment of both oligodendrocyte progenitor recruitment and differentiation. J. Neurosci. 22, 2451–2459.

Simons, M., and Nave, K.-A. (2016). Oligodendrocytes: Myelination and Axonal Support. Cold Spring Harb. Perspect. Biol. 8, a020479.

Sofroniew, M. (2020). Astrocyte Reactivity: Subtypes, States, and Functions in CNS Innate Immunity. Trends Immunol. 41, 758–770.

Spittau, B. (2017). Aging microglia-phenotypes, functions and implications for age-related neurodegenerative diseases. Front. Aging Neurosci. 9.

Terzioglu, M., and Galter, D. (2008). Parkinson's disease: genetic versus toxin-induced rodent models. FEBS J. 275, 1384–1391.

Trias, E., Beilby, P.R., Kovacs, M., Ibarburu, S., Varela, V., Barreto-Núñez, R., Bradford, S.C., Beckman, J.S., and Barbeito, L. (2019). Emergence of microglia bearing senescence markers during paralysis progression in a rat model of inherited ALS. Front. Aging Neurosci. 10.

Tse, K., and Herrup, K. (2017). DNA damage in the oligodendrocyte lineage and its role in brain aging. Mech. Ageing Dev. 161, 37–50.

Vazquez-Villaseñor, I., Garwood, C.J., Heath, P.R., Simpson, J.E., Ince, P.G., and Wharton, S.B. (2019). Expression of p16 and p21 in the frontal association cortex of ALS / MND brains suggest neuronal cell cycle dysregulation and astrocyte senescence in early stages of the disease. Neuropathol. Appl. Neurobiol. nan.12559.

Wang, F., Ren, S.-Y., Chen, J.-F., Liu, K., Li, R.-X., Li, Z.-F., Hu, B., Niu, J.-Q., Xiao, L., Chan, J.R., et al. (2020). Myelin degeneration and diminished myelin renewal contribute to age-related deficits in memory. Nat. Neurosci. 23, 481.

Wei, Z., Chen, X.C., Song, Y., Pan, X.D., Dai, X.M., Zhang, J., Cui, X.L., Wu, X.L., and Zhu, Y.G. (2016). Amyloid β protein aggravates neuronal senescence and cognitive deficits in 5XFAD mouse model of Alzheimer's disease. Chin. Med. J. (Engl). 129, 1835–1844.

Willis, C., Nicaise, A., Bongarzone, E., Givogri, M., Reiter, C., Heintz, O., Jellison, E., Sutter, P., TeHennepe, G., Ananda, G., et al. (2020). Astrocyte Support for Oligodendrocyte Differentiation can be Conveyed via Extracellular Vesicles but Diminishes with Age. Sci. Rep. 10.

Xia, M.-L., Xie, X.-H., Ding, J.-H., Du, R.-H., and Hu, G. (2020). Astragaloside IV inhibits astrocyte senescence: implication in Parkinson's disease. J. Neuroinflammation 17, 105.

Yamazaki, Y., Baker, D.J., Tachibana, M., Liu, C.-C., van Deursen, J.M., Brott, T.G., Bu, G., and Kanekiyo, T. (2016). Vascular Cell Senescence Contributes to Blood-Brain Barrier Breakdown. Stroke 47, 1068–1077.

Yun, M.H. (2018). Cellular senescence in tissue repair: every cloud has a silver lining. Int. J. Dev. Biol. 62, 591–604.

Zhang, P., Kishimoto, Y., Grammatikakis, I., Gottimukkala, K., Cutler, R.G., Zhang, S., Abdelmohsen, K., Bohr, V.A., Misra Sen, J., Gorospe, M., et al. (2019). Senolytic therapy alleviates Aβ-associated oligodendrocyte progenitor cell senescence and cognitive deficits in an Alzheimer's disease model. Nat. Neurosci. 22, 719–728.

Chapter 2

Modulation of lysosomes in senescent cells

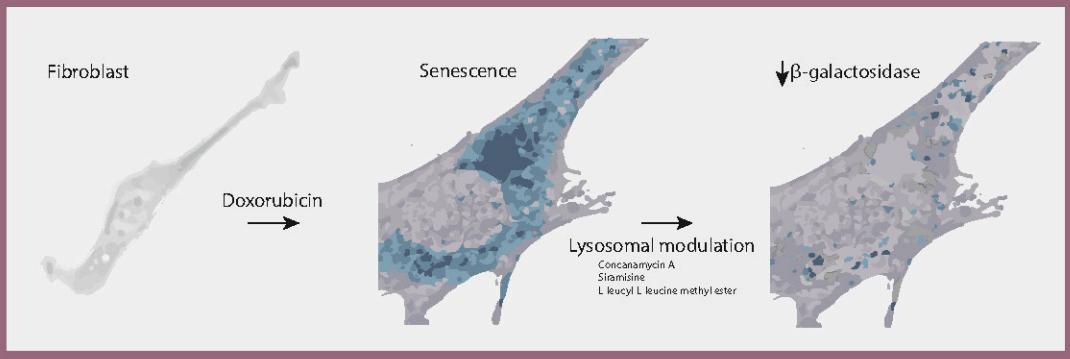

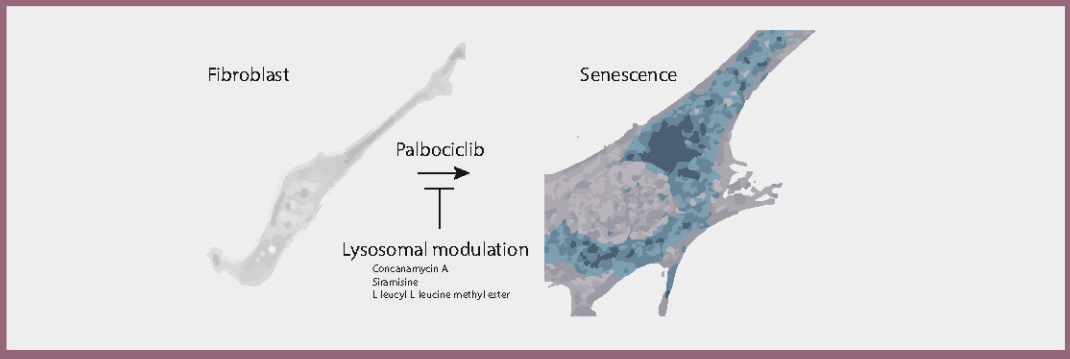

N. Talma[1,2], T. Gheorghe[1] , B.J.L. Eggen[2], M. Demaria[1]

1. European Institute for the Biology of Ageing, University Medical Center Groningen, University of Groningen, Groningen, The Netherlands
2. Section of Molecular Neurobiology, Department of Biomedical Sciences of Cells & Systems, University Medical Center Groningen, University of Groningen, Groningen, The Netherlands

Abstract

Lysosomes are membrane-bound organelles involved in degrading and recycling macromolecules. Lysosomal activity and accumulation of lysosomal content are two hallmarks of senescent cells. To investigate the effect of lysosomal modulation on senescent human fibroblasts, and on senescence induction in these cells, three lysosomorphic agents were used: Concanamycin A, Siramesine and L-Leucyl-L-Leucine-O-Methyl esther (LLOMe). Senescence induction by doxorubicin showed an increase in lysosomal gene expression, especially LAPTM4A. This increase was not altered by lysosomal modulation, whereas it did reduce the activity of senescence associated β-galactosidase. The reduced activity occurred by modulating the lysosomes both after and before the induction of senescence. Overall, this study showed that senescence-associated β-galactosidase activity might be subject to lysosomal modulation.

Introduction

Lysosomes are the main degradative compartments of the cell. They are single membrane bound organelles containing at least 50 different types of lytic enzymes which are optimally active at an acidic pH. The pH of the internal lysosomal environment is maintained between 4.5-5 primarily through the activity of V-type ATPases which actively pump protons through the lysosomal membrane (Mindell, 2012). Lysosomes mature from endocytic vesicles through acquisition of specific lysosomal proteins. Lysosomal enzyme precursors are sorted and delivered through the trans-golgi network and become (auto)catalytically activated upon their release into the acidic lysosomes (Wang et al., 2018). Lysosomes obtain content aimed for degradation through several pathways including endocytosis, crinophagy (fusion with secretory vesicles), (macro)autophagy, microautophagy (internalization of cytoplasmic components through invaginations of the lysosomal membrane), and chaperone mediated autophagy (direct transport of proteins through the lysosomal membrane) (Cuervo and Dice, 2000). Most substrates are processed efficiently by the lysosome culminating in the release of small molecules that can be recycled by the cell and used as building blocks for macromolecules. However, under conditions of stress, lysosomes can accumulate non-degradable material in the form of oxidized and highly cross-linked protein and lipid aggregates generally termed lipofuscin (Höhn and Grune, 2013). As

cells have no means to dispose of this content, its accumulation increases as a function of time in non-dividing cells, including senescent cells.

Alterations in lysosomal content and activity is a typical feature of ageing. The accumulation of lipofuscin –consisting of lipid-soluble, brown to yellow, and auto- fluorescent pigments– with ageing was already reported in 1842 (Wolf, 1993). Interestingly, lysosomal changes are also clear in senescent cells. Senescence-associated β-galactosidase (SA-β-gal) activity is often used to distinguish senescent cells from quiescent and proliferating cells (Dimri et al., 1995). SA-β-gal is defined as lysosomal β-D-galactosidase activity detected at suboptimal pH 6, typically with the use of a chromogenic substrate. Proliferating and quiescent cells express β-galactosidase activity most optimal at pH 4, whereas senescent cells also express β-galactosidase activity at pH 6. Positive staining of SA-β-gal in senescent cells is explained by the highly increased lysosomal accumulation of the active enzyme, which allows the development of a visible effect even in unfavorable pH conditions in which normal cells do not reach the threshold for detection (Kurz et al., 2000). In senescent cells, the lysosomal compartment typically expands, likely due to both increased biosynthesis of lysosomes and impaired elimination of old lysosomes. Enhanced lysosomal biogenesis is supported by the increased expression of multiple lysosomal proteins, while accumulation of dysfunctional lysosomes can be deduced from the detectable increase in lipofuscin content (Hernandez-Segura et al., 2018). Despite the enlarged hydrolase content, lysosomal activity is not necessarily enhanced in senescence. In fact, overexpression of lysosomal proteins might be a compensatory mechanism employed to cope with an increasingly dysfunctional lysosomal system. It has been suggested that older, lipofuscin filled lysosomes unable to degrade their contents act as a sink for newly synthesized enzymes (Park et al., 2018). In order to eliminate cells with accumulated damage and inactive lysosomes, altered lysosomal activity has been exploited for the targeting and removal of senescent cells (Dörr et al., 2013). To expand the knowledge on lysosomal function in senescent cells, the aim of this study was to investigate the effect of lysosomal modulation on (pre-) senescent cells.

Results

Lysosomal gene expression in doxorubicin-induced senescent fibroblasts

To further investigate lysosomal content and activity in senescent cells, we used senescent IMR90 fibroblasts. Senescence was induced in IMR90 cells by a 24 hour treatment with 250 nM of the topoisomerase II inhibitor doxorubicin. The chemotherapeutic has been shown to induce senescence in multiple cell types such as cardiac progenitor cells and microglia (Marques et al., 2020; Piegari et al., 2013). Induction of senescence in IMR90 cells was evaluated by measuring various senescence markers.

The doxorubicin treated cells exhibited decreased EdU incorporation, indicative of reduced DNA synthesis, and increased lysosomal activity measured by SA-β-gal positivity (Figure 1A-D and Figure S1A). Interestingly, a small percentage of cells with SA-β-gal activity was observed that incorporated EdU, indicating these cells were still proliferative, but displayed high lysosomal activity (Figure S1B).

Real-time qPCR for senescent marker genes showed the increase of *p16*, *p21* and *MMP1* expression and decrease of *LMNB1* expression in doxorubicin-treated cells (Figure 1E). Next, the expression of various lysosomal genes was examined: a lysosomal ABC transporter involved in cholesterol transport (*ABCA2*) (Szakacs and Abele, 2020); lysosomal membrane protein 2 (*LAMP2*); V-ATPase subunit (*ATP6AP1*); lysosomal enzyme beta-hexosaminidase (*HEXB*); trafficking receptor sortilin 1 (*SORT1*); lysosomal enzyme alpha-galactosidase A (*GLA*); lysosomal protein transmembrane 4 alpha (*LAPTM4A*); and lysosomal enzyme arylsulfatase B (*ARSB*). Interestingly, the expression of various lysosomal genes seemed to be upregulated in the doxorubicin treated cells (Figure 1F). Taken together, this data shows that expression of lysosomal genes is altered in senescent IMR90 cells and is reflective of higher lysosomal content and activity.

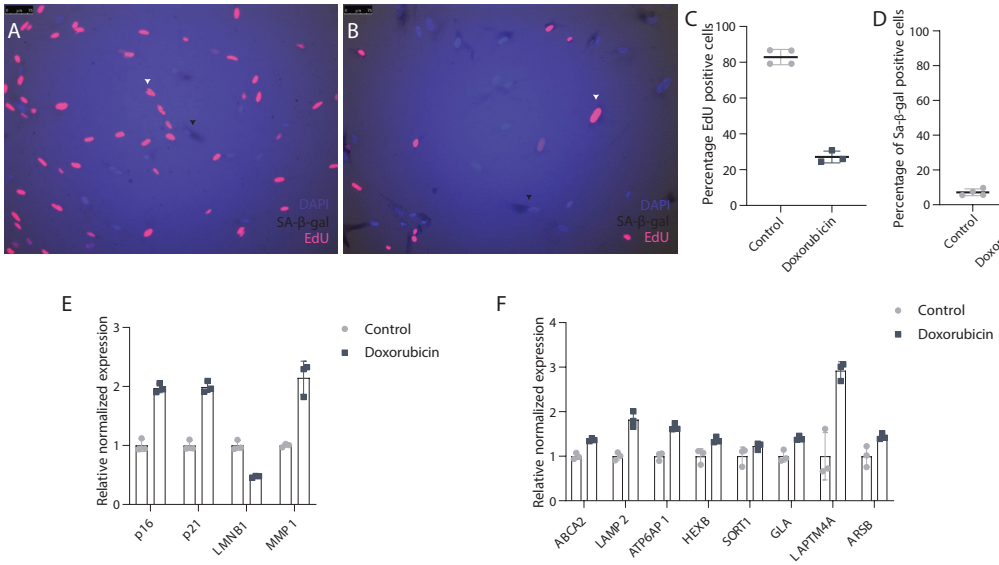

Figure 1: Effect of doxorubicin-induced senescence on lysosomal gene transcription.

A: Representative image of a combination staining of EdU and SA-β-gal in proliferating IMR90 cells B: Representative image of a combination staining of EdU and SA-β-gal in IMR90 cells one week after 24h treatment with 250 nM doxorubicin. Quantification of C: EdU and D: SA-β-gal positive cells between doxorubicin treated cells and proliferating controls. E: Expression of senescence markers p16, p21, LMNB1 and MMP1 measured by qPCR in IMR90s one week after doxorubicin treatment and proliferating controls. F: Expression of lysosomal genes ABCA2, LAMP2, ATP6AP1, HEXB, SORT1, GLA, LAPTM4A and ARSB measured by qPCR in IMR90s one week after doxorubicin treatment and

Effect of lysosomal modulation on senescent phenotypes

To investigate the biological function of lysosomes in senescent cells, we pharmacologically modulated lysosomal activity. We used three different lysosomal modulating drugs: Concanamycin A, Siramesine and L-Leucyl-L-Leucine-O-Methyl esther (LLOMe). Concanamycin A is a specific high-affinity inhibitor of V-ATPases on the lysosomes (Huss et al., 2002). Inhibition of V-ATPases increases the lysosomal pH, perturbing lysosomal enzyme function. Siramesine accumulates in lysosomes and causes a rapid but transient increase in lysosomal pH, but its exact mechanism of action is not fully understood (Hafner Česen et al., 2013; Ostenfeld et al., 2008). LLOMe causes rapid lysosomal membrane permeabilization due to increased intra-lysosomal osmotic pressure (Repnik et al., 2017).

To determine which concentration of lysosomal modulating drugs was tolerated by IMR90 cells, a viability assay was performed with a concentration

range of each drug (Figure 2A-C). Treatments with lysosomal modulators were performed for 24 hr, one week after senescence induction by 24 hr of treatment with 250 nM doxorubicin. Three concentrations were used to study the effect of lysosomal modulation on lysosome activity, in particular in regards to SA-β-gal (Figure 2D-P). The loss in SA-β-gal staining shown by each drug is indicative of an increase in pH or lysosomal disruption. However, alteration of lysosomal activity was not associated to changes in the expression of senescence-associated or lysosomal genes (Figure 2Q-V). Interestingly, when we combined the qPCR data of figure 1F with the data of figures 3T-V, we observed that *LAPTM4A* is the only lysosomal gene that was consistently upregulated in doxorubicin-treated IMR90 cells. Overall, lysosomal dysfunction was observed by a loss of SA-β-gal staining, but did not seem to influence gene expression shortly after 24 hr of lysosomal modulation.

Effects of altered lysosomal pH on palbociclib-induced senescence

The previous section demonstrated that pharmacological perturbations of lysosomal activity lead to reduced activity of senescence marker SA-β-gal of cells already in a senescent state. To address whether lysosomal activity can modulate the induction of senescence, we used another model of drug induced-senescence. Palbociclib is a selective cyclin-dependent kinase 4 and 6 (CDK4/6) inhibitor and a well characterized senescence inducer (Bueno et al., 2019). Palbociclib has been shown to be trapped in lysosomes (Llanos et al., 2019) and thereby potentially prolonging its activity. The trapping might possibly be an important mediator of the pro-senescence functions of palbociclib. To investigate if lysosomal modulation had an effect on the efficiency of senescence induction by palbociclib, we pre-treated BJ fibroblasts, another cell line that is commonly used to study senescence (Hernandez-Segura et al., 2017), with 2 different concentrations of concanamycin A and measured the EdU incorporation and SA-β-gal staining with increasing concentration of palbociclib. The concentrations for concanamycin A that were chosen had no effect on the viability of the BJ cells (Figure S2A).

Interestingly, concanamycin A pre-treatment seemed to partly protect cells against the induction of cell cycle arrest by higher concentrations of palbociclib (Figure 3A-B). In addition, the SA-β-gal staining is reduced by concanamycin A pre-treatment (Figure 3C-D). In conclusion, altered lysosomal pH might

reduce pro-senescence effects of certain stressors, in particular of drugs such as palbociclib which are normally trapped in lysosomes.

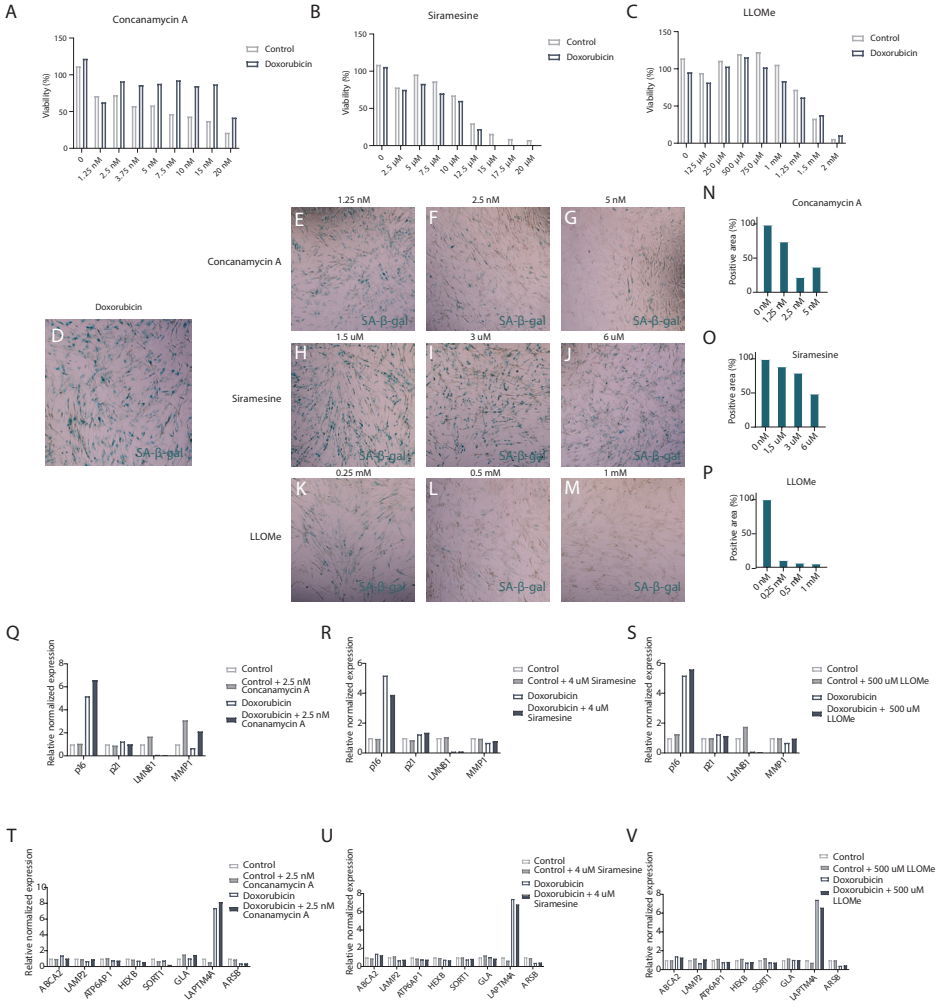

Figure 2: Effects of lysosome modulating agents on the phenotype of senescent cells.

Treatments were applied for 24h, one week after induction of senescence. A-C: MTS viability assay 24h after increasing concentrations of concanamycin A, siramesine or LLOMe respectively. D-M: Representative images of SA-β-gal staining of early senescent IMR90 cells immediately after concanamycin A, siramesine or LLOMe treatment respectively. 10x magnification. N-P: Quantification of SA-β-gal positive area after concanamycin A, siramesine or LLOMe treatment respectively, normalized to the doxorubicin control. Q-S: Expression of senescence markers p16, p21, LMNB1 and MMP1 measured by qPCR in IMR90s after concanamycin A, siramesine or LLOMe treatment respectively. T-V: Expression of lysosomal genes ABCA2, LAMP2, ATP6AP1, HEXB, SORT1, GLA, LAPTM4A and ARSB measured by qPCR in IMR90s after concanamycin A, siramesine or LLOMe treatment respectively.

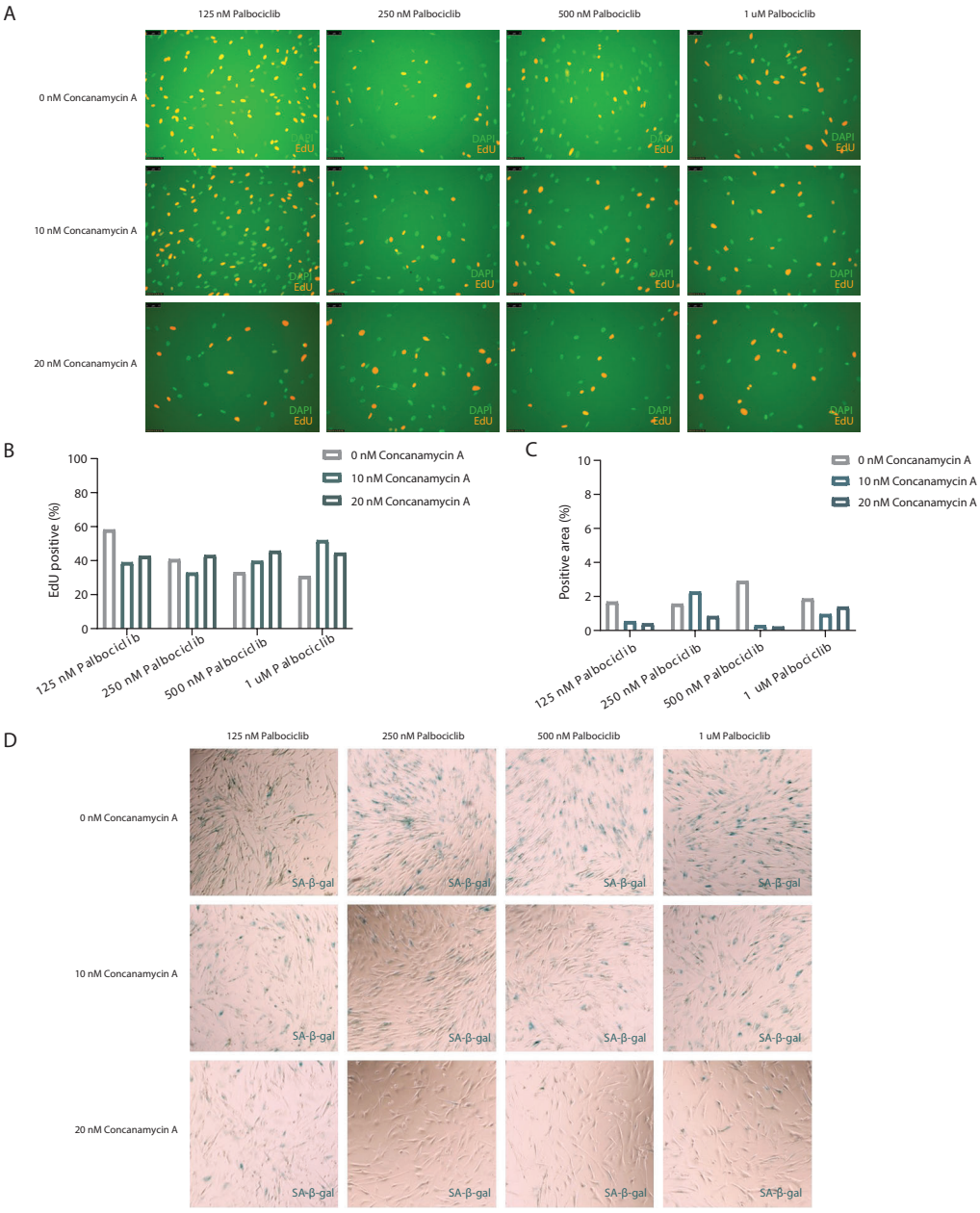

Figure 3: Effects of Concanamycin A pre-treatment on palbociclib-induced senescence.

BJ cells with 24h exposure to concanamycin A prior to treatment of 7 days with palbociclib. A: Representative images of EdU incorporation immediately after removal of palbociclib. B: Quantification of EdU incorporation shown in Figure 4A. C: Quantification of area positive for SA-β-gal staining shown in Figure 4D. D: Representative images of SA-β-gal staining immediately after removal of palbociclib. 10x magnification.

Discussion

Senescent fibroblasts show increased expression of lysosomal genes, which was not altered by lysosomal modulation. On the contrary, the activity of senescence marker SA-β-gal was altered by lysosomal modulation, both before and after the induction of senescence. SA-β-gal is dispensable for senescence (Lee et al., 2006), but the presence of SA-β-gal activity in proliferating, EdU incorporating cells showed that it is not restricted to senescence cells. This supports the need for more specific and stable markers of senescence and future studies aimed at identifying biomarkers for senescent cells should be performed.

A limitation of this study is that the *in vitro* experiments have been performed once, with technical triplicates, and should be considered as preliminary data. The experiments should be repeated for the validation of the findings. For example, the data that suggested that lysosomal modulation can influence the induction of senescence by lysosomal trapped drugs. In the literature, this was confirmed by showing that interference with the accumulation of palbociclib into lysosomes reduced the minimal dose of palbociclib required for cell cycle arrest and senescence (Llanos et al., 2019). Lysosomal trapping is an important mechanism that has been proposed as a mechanism of multidrug resistance in cancer cells, because it lowers the cytotoxic potential of chemotherapeutics (Halaby, 2019). Future studies should investigate the potential synergistic or inhibitory effects of treatment combinations of lysosomotropic drugs and chemotherapeutics.

Interestingly, the lysosomal gene *LAPTM4A* was consistently high expressed in doxorubicin-induced senescent IMR90 fibroblasts. To examine if *LAPTM4A* was also upregulated with other types of senescence, we consulted a dataset regarding transcriptional heterogeneity in senescent cells by Alejandra Hernandez-Segura and colleagues. *LAPTM4A* was upregulated with replicative senescence in two fibroblast cell lines (IMR90 and HFF) (Hernandez-Segura et al., 2017). The role of LAPTM4A is not yet completely understood. It is a multispanning membrane protein mostly located in lysosomes and late endosomes. It was shown to be involved in the synthesis of glycosphingolipids, which are part of the cell membrane. LAPTM4A loss resulted in decrease of biosynthesis of globotriaosylceramide (Gb3), the Shiga toxin receptor, in a

post-transcriptional mechanism (Yamaji et al., 2019). Recent studies showed that LAPTM4A is a short lived protein (Zhang et al., 2021). It is possible that senescent cells upregulate the transcript of this short-lived protein as a response to the degradation of LAPTM4A in the high number of lysosomes these cells contain. Future studies on the dynamics of LAPTM4A are needed to confirm this hypothesis.

LAPTM4A was identified as one of nine macrophage phenotypic switch-related genes correlated to the prognosis of pancreatic adenocarcinoma patients (Li et al., 2021). This suggests that cells with high *LAPTM4A* expression are harmful in the case of pancreatic adenocarcinoma, making it an interesting candidate to study in more detail. If future experiments confirm the high expression of *LAPTM4A* in senescent cells, the possibility of *LAPTM4A* as a target for senescent cells might be valuable to explore.

Overall, this chapter shows the effect of lysosomal modulation on senescence. Even though the data is preliminary, it provides novel interesting hypotheses that can be tested with future experiments.

With time, the lysosomes accumulate as well as the content in the lysosomes. Senolytics such as 2-DG (Dörr et al., 2013) and SSK1-Gemcitabine, a β-galactosidase-targeted prodrug, (Cai et al., 2020) exploit the altered lysosomal phenotype of senescent cells to eliminate them. In addition, new mouse models such as the α-l-fucosidase exploiting model termed QM-NHαfuc (Koo et al., 2021) make it possible to detect, and in this case image, senescent cells in vivo by harnessing the lysosomal activity of the cells. Moreover, the model is able to identify senescent cell lacking SA-β-gal expression. These are examples illustrating the utility of exploring lysosomal biomarkers and targets for senescence. However, lysosomes do not only accumulate in senescent cells, but also in non-senescent post-mitotic cells as a result of the accumulation of damage over time. More research needs to be done to investigate the consequences of detecting and especially elimination of these non-senescent cells.

Materials and methods

Cell culture

Human fetal lung fibroblasts IMR-90 (CCL-186; ATCC) and human foreskin fibroblasts BJ (CRL-2522; ATCC) were maintained in DMEM + GlutaMAX (Thermo Fisher Scientific) enriched with 10% FBS and 1% penicillin/streptomycin, incubated at 37°C in 5% CO_2 and 5% O_2.

Senescence was induced by treatment with 250nM doxorubicin for 24h. Cells were used 7 to 14 days after treatment. For experiments with cells in the course of entering senescence, a 7-day treatment with palbociclib was subjected to the fibroblasts, with 1μM palbociclib considered the standard dosage for inducing senescence and lower dosages used for comparison.

Concanamycin A, Siramesine and L-Leucyl-L-Leucine-O-Methyl esther (LLOMe) treatments were performed for 24 hours one week after doxorubicin-induced senescence, except for the concanamycin A pre-treatment.

SA-β-gal assay in fibroblasts

Cells plated in 6-well or 24-well plates were washed with PBS, fixed in formaldehyde 2% + glutaraldehyde 0.2% in PBS for 5 minutes and stained overnight (16-20 hours) in a 37°C incubator. Staining solution was freshly prepared to a composition of 5mM potassium ferricyanide, 5mM potassium ferrocyanide, 150mM sodium chloride, 2mM magnesium chloride, 5% dimethylformamide+0.1% 5-bromo-4-chloro-3-indolyl β D-galactopyranoside (X-gal) in 40mM citric acid / sodium phosphate buffer at pH 6. Bright field images were obtained with an EVOS XL Core Cell Imaging System (Invitrogen) using a 10x objective.

EdU incorporation assay

Cells were cultured in medium containing 10μM 5-ethynyl-2'-deoxyuridine (EdU, Lumiprobe) for 24 hours, then washed with PBS, fixed with formaldehyde 4% in PBS for 10 minutes and stored in PBS at 4°C for a maximum of 2 weeks. In preparation for staining, cells were incubated in 100mM Tris(hydroxymethyl) aminomethane (Tris) at pH 7.6 for 5 minutes, then permeabilized with 0.1% Triton X-100 in PBS for 10 minutes and washed with PBS. Staining solution was freshly prepared from 10% sodium ascorbate solution 200mg/ml, 1% copper(II) sulphate pentahydrate (Sigma) and 0.1% sulfo-cyanine3 azide (Lumiprobe) in PBS. Coverslips were incubated in staining solution in the dark for 30 minutes,

then washed with PBS and stained additionally with 1μg/ml 4',6-diamino-2-phenylindole (DAPI, Sigma-Aldrich) for 10-15 minutes. Coverslips were mounted on glass slides in ProLong Gold Antifade Mountant (Thermo Fisher Scientific) and imaged with a fluorescence microscope (DMI4000 B, Leica).

MTS assay

Cells were seeded in 96-well plates at a density of 2500 cells per well. Drug treatments were performed directly in the plate. 20μl MTS reagent (CellTiter 96 AQueous One Solution Cell Proliferation Assay, Promega) dissolved in 100μl culture medium was added to each well either immediately or 24h after removal of drug containing medium. Cells were incubated with the reagent for 3-4h at 37^{o}C. Absorbance was recorded at 450nm and normalized with respect to the absorbance measured in the acellular wells. Where applicable, cell number was estimated with the use of a calibration curve plotted from measurements of wells seeded with 0, 500, 1000, 1500, 2000, 2500, 5000 and 7500 cells respectively.

Real Time-PCR

Cells were washed with PBS and harvested by scraping in the presence of RLY lysis buffer with 1% β-mercaptoethanol. Samples were processed either immediately or after several days of storage at -80^{o}C. Total RNA was purified using a commercial kit (Isolate II RNA Mini Kit, Bioline) according to the manufacturers protocol. Depending on the amount of RNA extracted, either 75ng, 250ng or 500ng of RNA were reverse transcribed into cDNA in a 30μl reaction volume using the High-Capacity cDNA Reverse Transcription Kit (Applied Biosystems). qRT-PCR reactions were performed in a 10μl reaction volume with a cDNA concentration of 0.5ng/μl, using the Universal Probe Library system (Roche) and the SensiFAST Probe No-ROX Kit (Bioline). Tested genes were *p16(Cdkn2a), p21(Cdkn1a), MMP1, LMNB1, HEXB, SORT1, GLA, ATP6AP1, ABCA2, LAMP2, LAPTM4A, ARSB* and the expression was normalized to the expression of two reference genes, *Vamp7* and *L3mbtl2*. A list of primers is available in Supplemental Table 1.

References

Bueno, A.M., Aramillo, J.B., Mosquera, J.J.G., Capitan, A.G., Codony-Servat, J., Aguilar, A., Román, S.G., Casas, C.M. de las, Viteri, S., and Molina, M.A. (2019). Palbociclib-induced senescence upregulates the expression of IL-8 and may enhance the response to inmunotherapy. Ann. Oncol. 30, iii15–iii16.

Cai, Y., Zhou, H., Zhu, Y., Sun, Q., Ji, Y., Xue, A., Wang, Y., Chen, W., Yu, X., Wang, L., et al. (2020). Elimination of senescent cells by β-galactosidase-targeted prodrug attenuates inflammation and restores physical function in aged mice. Cell Res. 2020 307 30, 574–589.

Cuervo, A., and Dice, J. (2000). When lysosomes get old. Exp. Gerontol. 35, 119–131.

Dimri, G.P., Leet, X., Basile, G., Acosta, M., Scorrt, G., Roskelley, C., Medrano, E.E., Linskensi, M., Rubeljii, I., Pereira-Smithii, O., et al. (1995). A biomarker that identifies senescent human cells in culture and in aging skin in vivo (replicative senescence/tumor suppression/18-galactosidase) Communicated by Arthur. Cell Bioiogy 92, 9363–9367.

Dörr, J.R., Yu, Y., Milanovic, M., Beuster, G., Zasada, C., Däbritz, J.H.M., Lisec, J., Lenze, D., Gerhardt, A., Schleicher, K., et al. (2013). Synthetic lethal metabolic targeting of cellular senescence in cancer therapy. Nat. 2013 5017467 501, 421–425.

Hafner Česen, M., Repnik, U., Turk, V., and Turk, B. (2013). Siramesine triggers cell death through destabilisation of mitochondria, but not lysosomes. Cell Death Dis. 2013 410 4, e818–e818.

Halaby, R. (2019). Influence of lysosomal sequestration on multidrug resistance in cancer cells. Cancer Drug Resist. 2, 31–42.

Hernandez-Segura, A., de Jong, T. V, Melov, S., Guryev, V., Campisi, J., and Demaria, M. (2017). Unmasking Transcriptional Heterogeneity in Senescent Cells.

Hernandez-Segura, A., Nehme, J., and Demaria, M. (2018). Hallmarks of Cellular Senescence. Trends Cell Biol. 28, 436–453.

Höhn, A., and Grune, T. (2013). Lipofuscin: formation, effects and role of macroautophagy. Redox Biol. 1, 140.

Huss, M., Ingenhorst, G., König, S., Gassel, M., Dröse, S., Zeeck, A., Altendorf, K., and Wieczorek, H. (2002). Concanamycin A, the specific inhibitor of V-ATPases, binds to the V(o) subunit c. J. Biol. Chem. 277, 40544–40548.

Koo, S., Won, M., Li, H., Kim, W.Y., Li, M., Yan, C., Sharma, A., Guo, Z., Zhu, W.-H., Sessler, J.L., et al. (2021). Harnessing α-L-fucosidase for in vivo cellular senescence imaging. Chem. Sci. 12, 10054–10062.

Kurz, D., Decary, S., Hong, Y., and Erusalimsky, J. (2000). Senescence-associated (beta)-galactosidase reflects an increase in lysosomal mass during replicative ageing of human endothelial cells. J. Cell Sci. 113 (Pt 2, 3613–3622.

Lee, B.Y., Han, J.A., Im, J.S., Morrone, A., Johung, K., Goodwin, E.C., Kleijer, W.J., DiMaio, D., and Hwang, E.S. (2006). Senescence-associated β-galactosidase is lysosomal β-galactosidase. Aging Cell 5, 187–195.

Li, M., Wang, H., Yuan, C., Ma, Z., Jiang, B., Li, L., Zhang, L., and Xiu, D. (2021).

Establishment of a Macrophage Phenotypic Switch Related Prognostic Signature in Patients With Pancreatic Cancer. Front. Oncol. 11.

Llanos, S., Megias, D., Blanco-Aparicio, C., Hernández-Encinas, E., Rovira, M., Pietrocola, F., and Serrano, M. (2019a). Lysosomal trapping of palbociclib and its functional implications. Oncogene 2019 3820 38, 3886–3902.

Marques, L., Johnson, A.A., and Stolzing, A. (2020). Doxorubicin generates senescent microglia that exhibit altered proteomes, higher levels of cytokine secretion, and a decreased ability to internalize amyloid β. Exp. Cell Res. 395, 112203.

Mindell, J.A. (2012). Lysosomal Acidification Mechanisms. Annu. Rev. Physiol. 74, 69–86.

Ostenfeld, M.S., Høyer-Hansen, M., Bastholm, L., Fehrenbacher, N., Olsen, O.D., Groth-Pedersen, L., Puustinen, P., Kirkegaard-Sørensen, T., Nylandsted, J., Farkas, T., et al. (2008). Anti-cancer agent siramesine is a lysosomotropic detergent that induces cytoprotective autophagosome accumulation. Autophagy 4, 487–499.

Park, J.T., Lee, Y.S., Cho, K.A., and Park, S.C. (2018). Adjustment of the lysosomal-mitochondrial axis for control of cellular senescence. Ageing Res. Rev. 47, 176–182.

Piegari, E., Angelis, A., Cappetta, D., Russo, R., Esposito, G., Costantino, S., Graiani, G., Frati, C., Prezioso, L., Berrino, L., et al. (2013). Doxorubicin induces senescence and impairs function of human cardiac progenitor cells. Basic Res. Cardiol. 108, 334.

Repnik, U., Borg Distefano, M., Speth, M.T., Ng, M.Y.W., Progida, C., Hoflack, B., Gruenberg, J., and Griffiths, G. (2017). L-leucyl-L-leucine methyl ester does not release cysteine cathepsins to the cytosol but inactivates them in transiently permeabilized lysosomes. J. Cell Sci. 130, 3124–3140.

Szakacs, G., and Abele, R. (2020). An inventory of lysosomal ABC transporters. FEBS Lett. 594, 3965–3985.

Wang, F., Gómez-Sintes, R., and Boya, P. (2018). Lysosomal membrane permeabilization and cell death. Traffic 19, 918–931.

Wolf, G. (1993). Lipofuscin, the Age Pigment. Nutr. Rev. 51, 205–206.

Yamaji, T., Sekizuka, T., Tachida, Y., Sakuma, C., Morimoto, K., Kuroda, M., and Hanada, K. (2019). A CRISPR Screen Identifies LAPTM4A and TM9SF Proteins as Glycolipid-Regulating Factors. IScience 11, 409–424.

Zhang, W., Yang, X., Chen, L., Liu, Y., Venkatarangan, V., Reist, L., Hanson, P., Xu, H., Wang, Y., and Li, M. (2021). A conserved ubiquitin- and ESCRT-dependent pathway internalizes human lysosomal membrane proteins for degradation. PLoS Biol. 19.

Supplemental Table

Gene	Forward primer	Reverse primer
Vamp7	CAAACATGCTTGGTGTGGAG	AAATTAAAGGCTCGGGAACG
L3mbtl2	CCAAGACCAAGAGGTTCTGC	TTTGGTCGGTGGTTTTCC
Abca2	CTATGGCATCCTCACGTGGT	GACTTCTGCAGTGGGAAGTACC
Arsb	CTGCTCACTGGCCGCTAC	GGGTAGTATAACCTGCTTCTTTTAGGA
Atp6ap1	CCATCTTGCTCCCTCTTCAG	CACCTTGTTGGGAGAGATGG
Cdkn1a	TCACTGTCTTGTACCCTTGTGC	GGCGTTTGGAGTGGTAGAAA
Cdkn2a	GAGCAGCATGGAGCCTTC	CGTAACTATTCGGTGCGTTG
Gla	TGGAAAATTTGGCAGATGGT	AAAGAGGCCACTCACAGGAG
Hexb	ACCTCTTGATTTTGGCGGTA	CATCCACATATTCTCCCCATAGA
Lamp2	TTTAACTAAAAACAAAAGTTCCCAAAG	CTTGGAATGAATAACCAACTCACTT
Laptm4a	GCCTTTGAAGCACCTCCTC	CAGAATTTCTTCAGGCAGGTAAG
Lmnb1	GTGCTGCGAGCAGGAGAC	CCATTAAGATCAGATTCCTTCTTAGC
Mmp1	GCTAACCTTTGATGCTATAACTACGA	TTTGTGCGCATGTAGAATCTG
Sort1	AAGATATCCTTGAAAGGAACTGTGA	CGCAGAAACTGTTCTTTGTAGC

Table 1: *Primers used for amplification of reverse-transcribed transcripts of the genes of interest.*

Supplemental figures

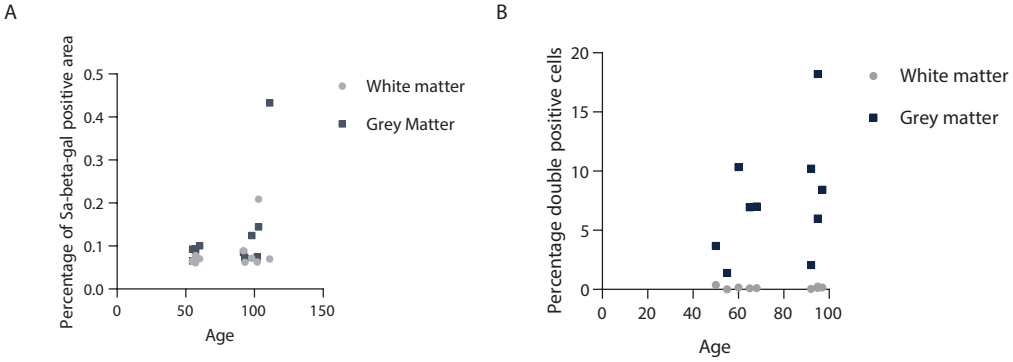

Figure S1: Quantification of EdU and SA-β-gal double staining.
A: Quantification of EdU negative and SA-β-gal positive cells from figure 2A-B. B: Quantification of double positive cells from figure 2A-B.

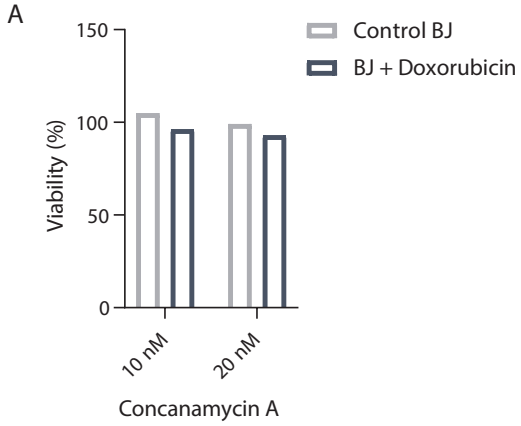

Figure S2: Viability of BJ cells after Concanamycin A treatment.
A: Viability measured by an MTS assay 24h after the 24h treatment.

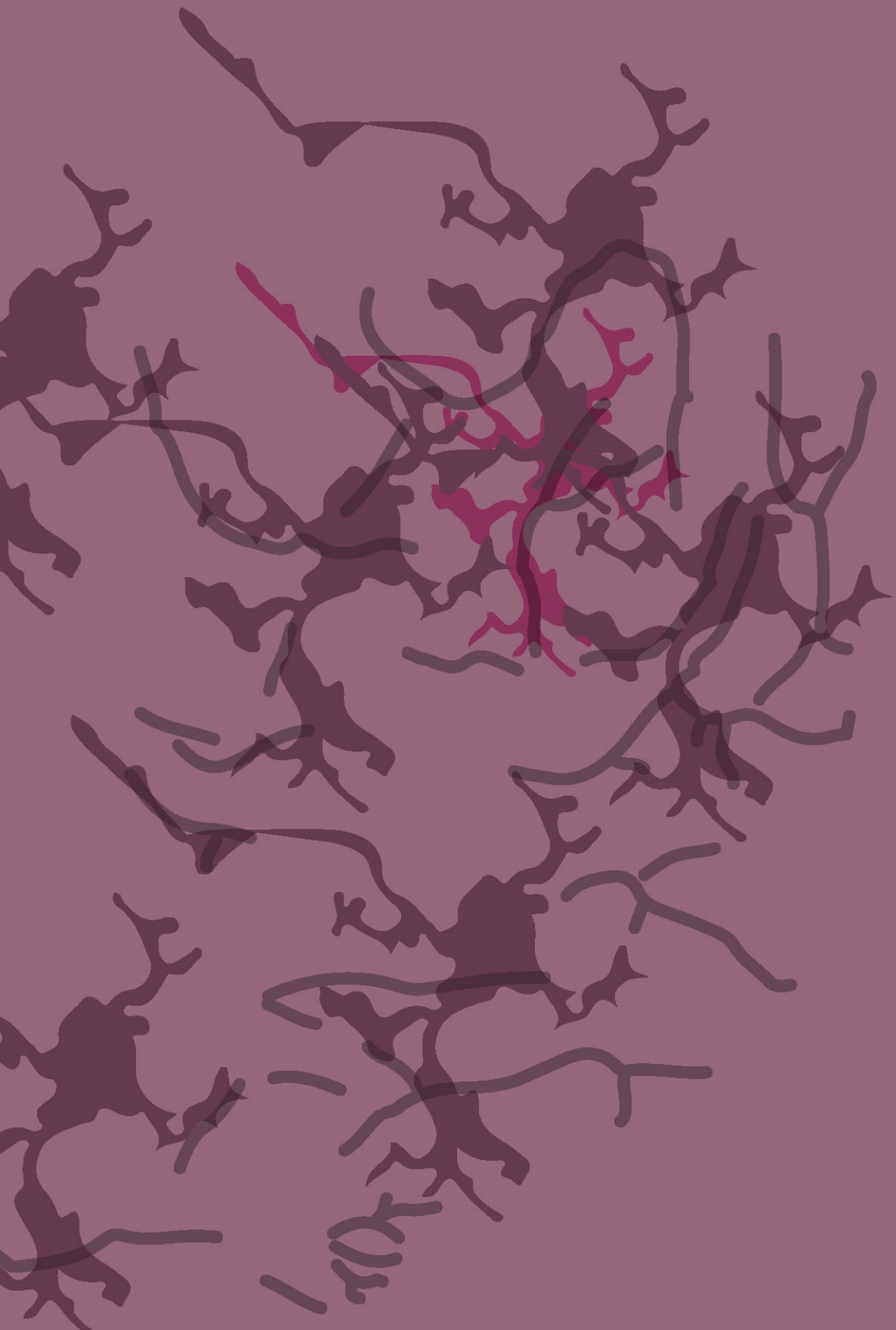

Chapter 3

Identification of distinct and age-dependent p16^{High} microglia subtypes

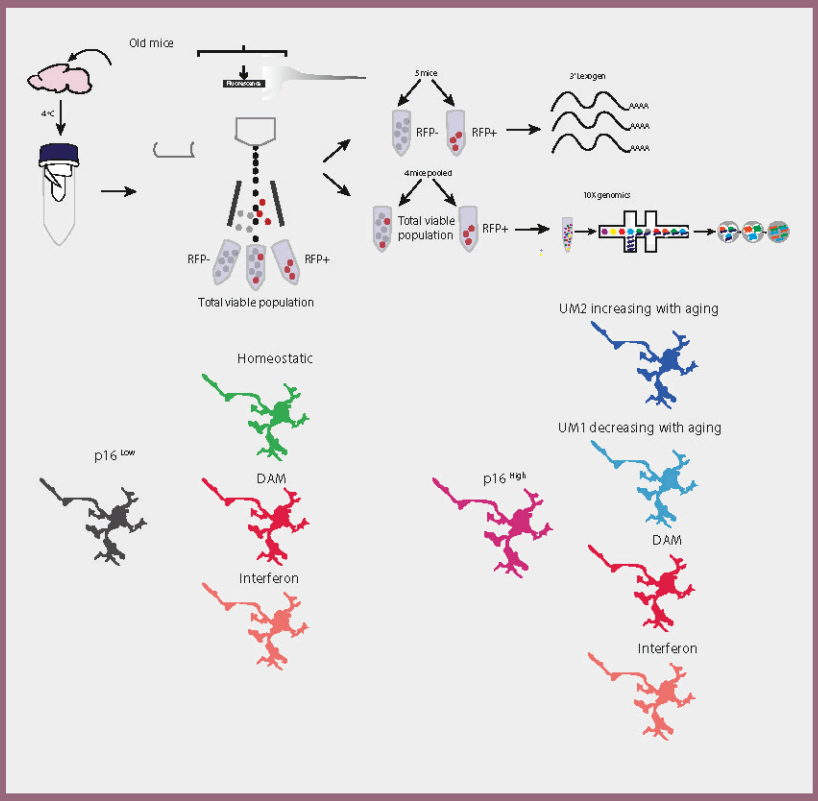

Adapted from:

Identification of distinct and age-dependent p16^{High} microglia subtypes

Nynke Talma[1,2], Emma Gerrits[1], Boshi Wang[2], Bart J.L. Eggen[1], Marco Demaria[2*]*

[1] Department of Biomedical Sciences of Cells & Systems, Section Molecular Neurobiology, University of Groningen, University Medical Center Groningen, Groningen, The Netherlands
[2] European Research Institute for the Biology of Ageing, University of Groningen, University Medical Center Groningen, Groningen, The Netherlands

[*] These authors have contributed equally

Aging Cell, October 2021, Vol. 30, No. 10 https://doi.org/10.1111/acel.13450

Abstract

Cells expressing high levels of the cyclin-dependent kinase (CDK)4/6 inhibitor p16 ($p16^{High}$) accumulate in ageing tissues and promote multiple age-related pathologies, including neurodegeneration. Here, we show that the number of $p16^{High}$ cells is significantly increased in the central nervous system (CNS) of 2-year-old mice. Bulk RNAseq indicated that genes expressed by $p16^{High}$ cells were associated with inflammation and phagocytosis. Single-cell RNAseq of brain cells indicated $p16^{High}$ cells were primarily microglia, and their accumulation was confirmed in brains of aged humans. Interestingly, we identified two distinct subpopulations of $p16^{High}$ microglia in the mouse brain, with one being age-associated and one present in young animals. Both $p16^{High}$ clusters significantly differed from previously described disease-associated microglia and expressed only a partial senescence signature. Taken together, our study provides evidence for the existence of two p16-expressing microglia populations, one accumulating with age and another already present in youth that could positively and negatively contribute to brain homeostasis, function, and disease.

Introduction

Cyclin-dependent kinase (CDK)4/6 inhibitor $p16^{INK4a}$ (from now on referred to as p16) levels gradually increase with age in multiple tissues and organisms (Herbig et al., 2006; Liu et al., 2009; Melk et al., 2004; Yousefzadeh et al., 2020). $p16^{High}$ cells actively contribute to ageing and age-associated dysfunctions by restricting the regenerative potential of the tissue (Martin et al., 2014) and promoting chronic inflammation (Sanada et al., 2018). Genetic or pharmacological ablation of $p16^{High}$ cells is able to increase health- and lifespan in mice (Baker et al., 2016; Xu et al., 2018). p16 expression is a common feature of cellular senescence (Liu et al., 2019), a state of stable and generally irreversible growth arrest originally described as a key process regulating cellular and organismal ageing (Hayflick and Moorhead, 1961). Senescent cells are characterized by various structural changes, including misshaped nuclei, enhanced lysosomal content and phagocytic activity, altered mitochondria morphology, and changed plasma membrane composition (Hernandez-Segura et al., 2018). In addition, senescent cells acquire a pro-inflammatory phenotype by releasing cytokines and chemokines (a phenotype collectively

defined as the SASP—senescence-associated secretory phenotype) (Gorgoulis et al., 2019). Virtually, all cells can up-regulate p16 levels, but this induction is not always reflected by a fully senescent state. For example, p16 expression is significantly increased in aged macrophages (Hall et al., 2016), but p16 overexpression can also be observed in young macrophages responding to physiological stimuli (Hall et al., 2017), (Behmoaras and Gil, 2021). Ageing leads to a reduction in brain volume and cognition (Peters, 2006) and is the main risk factor for dementia and neurodegeneration (Wyss-Coray, 2016). Ageing and neurodegenerative conditions induce a common gene expression signature in microglia, the resident immune cells of the CNS (Galatro et al., 2017). Microglia exhibit a hypersensitive and pro-inflammatory phenotype, known as priming, in particular during ageing and neurodegeneration (Norden and Godbout, 2013; Perry and Holmes, 2014; Raj et al., 2014). These primed microglia exert an increased inflammatory response and thereby alter CNS function (Norden and Godbout, 2013). In addition to primed immune cells, the accumulation of pro-inflammatory senescent cells in the CNS may also predispose elderly to neurodegenerative diseases or aggravate disease etiology (Kritsilis et al., 2018). In the CNS, p16 expression increases during natural ageing and in brains affected by pathologies such as Parkinson's disease (PD), multiple sclerosis (MS), and Alzheimer's disease (AD) (Martin-Ruiz et al., 2020; Nicaise et al., 2019; Zhang et al., 2019). Removal of p16^{High} cells ameliorates the progression of neurodegeneration in amyloid and tau AD mouse models and in mice exposed to the neurotoxin paraquat (Bussian et al., 2018; Chinta et al., 2018; Zhang et al., 2019). In a neurodegenerative context, different cell types become p16^{High} and influence disease progression. A recent study has attempted to identify senescent cell types naturally occurring in the murine ageing brain using single-cell transcriptomic profiling, and identified an enrichment of p16^{High} cells in microglia and OPCs (Ogrodnik et al., 2021). However, a limitation of single-cell RNA sequencing (scRNAseq) is its ability to detect low abundant transcripts, which is the case of the p16 transcript. Here, we aimed to identify p16^{High} cell populations in the ageing brain by using a transgenic mouse model that allows for the isolation of cells expressing p16 at the protein level, and then perform validation of the findings in wild-type mice and humans.

Results

RFP^{High} cells expressing inflammatory and phagocytosis-related genes accumulate in the ageing brain of p16-3MR mice

The p16-3MR mouse contains a monomeric red fluorescent protein (mRFP) fused to Renilla Luciferase and a truncated herpes simplex virus (HSV)-1 thymidine kinase (tTK), under control of the p16 promoter (Demaria et al., 2014). In order to evaluate whether the levels of the 3MR transgene and the number of 3MR^{High} cells increase in the brain with age, we measured RFP signal and percentage of cells expressing high levels of RFP in 7- to 12-week (defined young) and 105- to 116-week (defined old) mice by flow cytometry (Figure S1a). The mean mRFP intensity was significantly higher in old mice (Figure 1a), and the percentage of cells expressing high levels of RFP (RFP^{High}) cells increased >sevenfold with ageing, from ~0.2% in young to ~1.5% in old mouse brains (Figure 1b). Importantly, the purified RFP^{High} population was enriched in cells expressing high levels of the p16 transcript (Figure S1b). We then isolated RFP^{Low} and RFP^{High} cells from aged brains and generated gene expression profiles of both populations using bulk RNA sequencing (RNAseq). Principal component analysis (PCA) showed significant transcriptional differences between the RFP^{Low} and RFP^{High} populations as indicated by the first principal component (Figure 1c).

Differential gene expression analysis revealed 1459 differentially expressed genes between the two populations (Figure 1d). Among the most enriched genes in the RFP^{High} samples (Table S1) were Cass4 and Apba2 (or Mint2), which are involved in amyloid synthesis and AD (Beck et al., 2014; Ho et al., 2008) and genes associated with macrophage activation, like Akr1b3, Angptl7, and Ticam2 (Qian et al., 2016; Ramana et al., 2006; Seya et al., 2005). To determine whether gene networks in RFP^{High} samples associated with specific biological or cellular functions, a weighted gene correlation network analysis (WGCNA) (Langfelder and Horvath, 2008a) was performed, resulting in branches, or modules, of highly correlating genes (Figure S1c; Table S2). One of these modules (the “blue” module), involved in phagocytosis and cytokine production, was significantly enriched in the RFP^{High} samples, as reflected by the Module Eigengene, or first principal component, of the module (Figure 1e; Figure S1d-h). These data suggest that RFP^{High} cells accumulate in the ageing

brain and are enriched in expression of genes associated with inflammation and phagocytosis pathways.

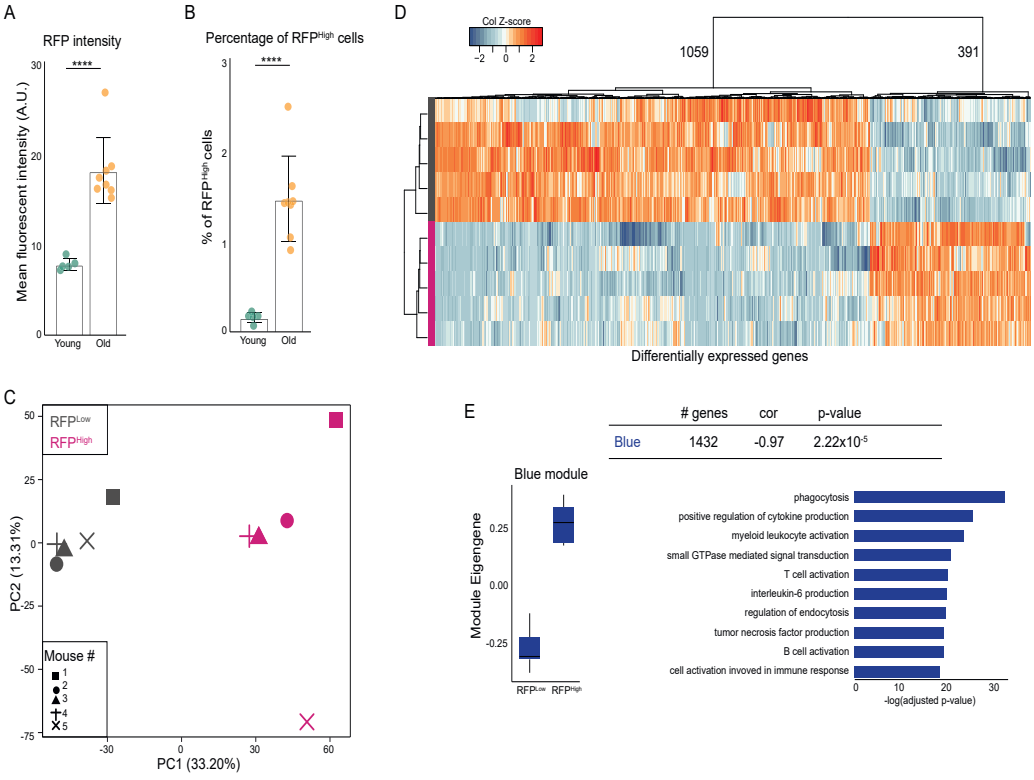

Figure 1: p16-RFP ew express inflammatory and microglia genes.

*A: Mean fluorescent RFP intensity of all viable cells in young compared to old brains. ****P<0,0001 B: Percentage of viable cells positive for RFP in young mouse brains compared to old. ****P<0,0001 C: PCA plot of bulk sequenced RFPLow and RFPHigh cells from old mouse brains. D: Heatmap of all differentially expressed gene between the RFPLow and RFPHigh samples. E: Expression and gene-ontology analysis of a WGCNA module enriched in RFPHigh samples.*

Single-cell transcriptomic profiling demonstrates accumulation of RFP^{High} microglia with ageing in p16-3MR mice

To further characterize the phenotype of the RFP^{High} cell population in the aged mouse CNS, we compared scRNAseq profiles of purified RFP^{High} cells to unsorted CNS cell samples (Figure S2a-d; Table S3). We identified 14 clusters in the dataset, using unsupervised, graph-based clustering analysis where each cluster corresponds to a distinct cell type (Figure 2a). The cell types were identified based on the expression of well-known cell type marker genes: *P2ry12*, *Cx3cr1*, and *Tgfbr1* for microglia; *Cldn5* for endothelial cells; *Gfap*, *Aqp4*, and *Atp1b2* for astrocytes; *Grid2* for Purkinje neurons; *Npy* and *Fabp7* for glial restricted progenitors (GRP); *Cd3g* for T/NK cells; *H2-Aa* for monocytes; *F13a1* for CNS-associated macrophages (CAMs); *Pdgfrb* for mural cells; *Acta2* for neutrophils; *Map1b* for neurons; *Dcn* and *Col1a1* for fibroblasts; *Olig1*, *Mobp*, and *Plp1* for oligodendrocytes; *Ms4a1* for B cells; *Ttr* for unidentified population 1 (unknown 1); and *Ak7* for unidentified population 2 (unknown 2) (Figure 2b; Table S4). Next, for the total viable and the RFP^{High} populations, the distribution of cell types within each sample was compared. Microglia, astrocytes, and endothelial cells were the most abundant cell types obtained with our isolation method (total viable population) from aged mouse brains, while other cell types such as neurons and oligodendrocytes were less abundant, and most likely underrepresented compared to their normal physiological distribution in the CNS (Valério-Gomes et al., 2018). Strikingly, the RFP^{High} sample was almost exclusively comprised of microglia (94.6%) and some glial restricted progenitors (2.6%) (Figure 2c and d). The scRNAseq data confirmed that microglia expressed *Cdkn2a*, the genomic locus containing *p16*, more abundantly compared to other cell types in the CNS (Figure 2e). To investigate whether microglia showed additional markers of cellular senescence, the expression levels of a list of 162 senescence-associated genes in each cell type were evaluated (Table S5). These genes were variably expressed and not abundantly present in the microglia population (Figure 2f). These data suggest that RFP^{High} microglia accumulate in the ageing brain of p16-3MR mice and that their transcriptional profile differs from a classical senescence-associated gene signature.

Figure 2: RFP^{High} cells are highly enriched for microglia.

A: UMAP depicting mouse CNS with cluster annotations based on cell types. B: Heatmap showing the expression of cell type markers in each cluster. C: Bar plot of cluster distribution of total viable cells and RFP^{High} cells. D: Bar plot showing the percentage of RFP^{High} cells for each cell type E: Cdkn2a plotted in UMAP of all sequenced single cells. F: Dot plot showing the expression of senescence markers in each cluster.

Microglia are enriched in p16 in the brains of wild-type mice and humans

To confirm the presence of RFP^{High} microglia in aged brains, we used different methods. First, from the bulk RNAseq list, we investigated the expression level of cell type-specific genes in the RFP^{High} fraction: *Hexb, Cxcr1, P2ry12,* and *Tmem119* for microglia; *Aqp4* and *Gfap* for astrocytes; *Cldn5* and *Vcan* for endothelial cells; *Rbfox3* for neurons; *F13a1* for CNS-associated macrophages; *Plp1* for oligodendrocytes; and *Pdgfra* for oligodendrocyte progenitor cells and fibroblasts (Figure 3a). The expression level of microglia genes was consistently higher in the RFP^{High} samples, while in the RFP^{Low} samples, endothelial cell, oligodendrocyte, and oligodendrocyte progenitor cell markers were more abundantly expressed. Second, we deconvoluted transcriptomes of the bulk RFP^{High} samples with CIBERSORT, using our single-cell data as the reference matrix (Table S4). Again, a pattern of enrichment for microglia in the RFP^{High} cell population was observed (Figure 3b). To validate the correlation between *p16* and RFP positivity in a non-transgenic background, we measured *p16* levels in wild-type animals. We isolated microglia, astrocytes, and non-microglia/non-astrocyte (defined as "the rest") cells from the brain of young and old wild-type C57BL/6 mouse brains and evaluated the *p16* transcript levels of the isolated populations. Only microglia of old mice revealed a significant *p16* upregulation, while no significant differences between young and old mice were detected neither in astrocytes, a cell population that was minimally represented in the RFP^{High} cells isolated from aged p16-3MR mice, nor in other mixed cell types mainly consisting of endothelial cells (Figure 3c). Next, we evaluated the level of *p16* expression in human microglia and cortical CNS tissue (Galatro et al., 2017). Strikingly, we measured a significant enrichment for *CDKN2A,* the genomic locus containing *p16*, in the microglia population compared to the total brain samples (Figure 3d). In addition, we determined the expression levels of *CDKN2A* in a single-nucleus RNA sequencing data set of human AD cases and healthy donors (Gerrits et al., 2021). Also, in this dataset, *CDKN2A* was most abundantly expressed by microglia (Figure 3e). Interestingly, lymphocytes and oligodendrocytes, underrepresented in our mouse scRNAseq, also expressed *CDKN2A* in human brains. Altogether, these data confirm that both in the mouse and in the human aged brain, p16^{High} cells are mostly present in the microglia population.

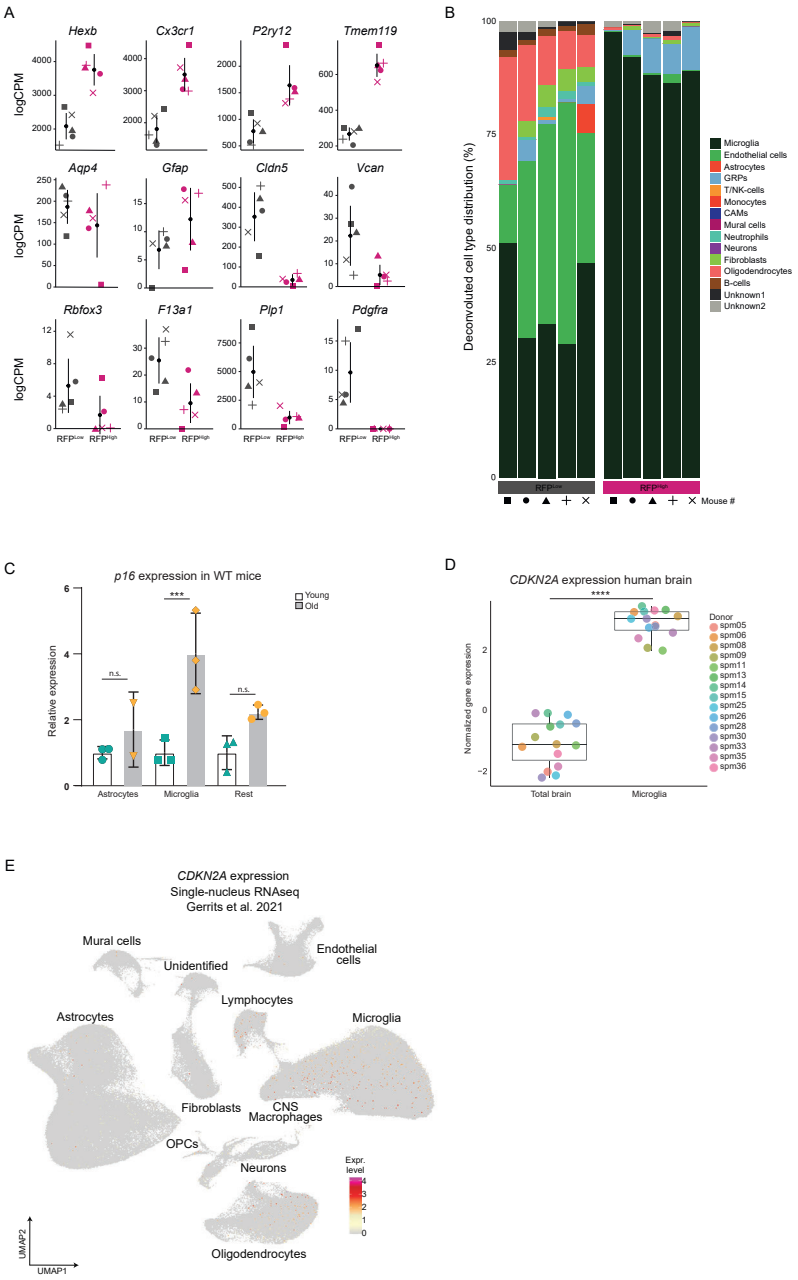

Figure 3: Increased expression of p16 in mouse and human microglia.

*A: Gene expression of cell marker genes in RFP^{Low} compared to RFP^{High} mouse samples. B: Bar plot showing the distribution of cells types in the mouse CNS bulk dataset after deconvolution. C: p16 expression measured by qPCR in cells isolated from young and old mouse brains. ****P<0,0001 D: CCKN2A expression in human microglia and total cortical tissue from Galatro et al. (Galatro et al., 2017). ****P<0,0001E: UMAP depicting CDKN2A expression in 450,000 CNS cell nuclei (Gerrits et al., 2021).*

RFP^{High} cells cluster in two distinct and previously unreported microglia populations

Recent reports based on single-cell transcriptomes identified context-dependent microglia subtypes (Masuda et al., 2020; Sierksma et al., 2020). Sub clustering analysis of the entire microglia population from our single-cell dataset (RFP^{High} and unpurified) revealed 5 distinct subpopulations: 3 previously described—a population which surveils the surroundings and maintains homeostasis through clearance of cellular debris, called homeostatic (HOM); a more reactive population, which acquires pro-inflammatory and antigen-presenting properties, called disease-associated microglia (DAM); and activated microglia with high interferon signaling (IFN)—and 2 additional clusters, named unknown microglia clusters 1 and 2 (UM1 and UM2), which segregated from the known clusters and were almost exclusively derived from the RFP^{High} samples (Figure 4a; Figure S3a). The HOM cluster was depleted in the RFP^{High} microglia, while DAM and IFN clusters were equally present in both RFP^{High} and RFP^{Low}

Differential gene expression analysis revealed a clear distinction of the RFP^{High} microglia from the total viable population (Figure 4b), even if the expression of selected senescence-associated genes was not specifically enriched in the UM1 and UM2 clusters, but seems to be slightly increased in the DAM cluster (Figure 4c; Figure S3d). Single-cell regulatory network inference and clustering (SCENIC) analysis identified 43 gene networks differentially expressed between RFP^{High} and total microglia. Interestingly, expression of genes regulated by Ets2, a transcription factor that positively regulates *p16* expression (Kotake et al., 2015), was enriched in RFP^{High} microglia (Figure 4d; Figure S3b). We then investigated the predicted functions of genes upregulated in the RFP^{High} microglia. In line with our bulk RNAseq results, two AD risk genes were upregulated in the RFP^{High} microglia. *Gsap* selectively increases amyloid-β production (He et al., 2010), a protein that is aggregated in AD, and inositol polyphosphate5-phosphatase D (*Inpp5d*) is suggested to contribute to AD in a non-amyloid-β-dependent fashion (Efthymiou and Goate, 2017). Additionally, we found genes involved in macrophage motility and myelination. *Plxnb2* has been shown to negatively regulate cell motility (Roney et al., 2011), while *Kif13b* regulates myelination in the CNS (Noseda et al., 2016)(Table S4). In addition, we examined the genes upregulated in each UM cluster. Gene ontology

analysis for genes enriched in the UM1 cluster showed an enrichment for genes involved in the ERK/MAPK pathways (Figure 4e) suggested to underlie CNS inflammation (Kaminska et al., 2009). Genes highly expressed in UM2 microglia were associated with cell cycle response and Rho GTPase signaling (Figure 4f), a pathway necessary for process motility, which is important for scanning of the parenchyma (Neubrand et al., 2014). Finally, we compared the gene expression profile of the RFP^{High} microglia to previously reported disease- and ageing-associated microglia profiles (Table S5). While both the DAM and the IFN clusters significantly overlap with previously reported profiles, none of the investigated gene sets was significantly enriched in our UM1 and UM2 clusters (Figure S3c). Interestingly, when we looked at the expression levels of UM1 and UM2 cluster marker genes in ageing wild-type mice from the dataset of Zhang et al. 2020 (Zhang et al., 2020), we observed that UM1 cluster markers were expressed in microglia at all ages albeit lower at 19 months, while the expression of UM2 cluster marker genes progressively increased with age in these wild-type mice (Figure 4g). In summary, these data show that RFP^{High} microglia cluster in two distinct subpopulations with previously unreported gene signatures which we named UM1 and UM2. UM1 negatively correlates with age and is characterized by expression of inflammatory genes. In contrast, UM2 is age-associated and characterized by differential expression of genes involved in cell cycle regulation and cell motility.

Figure 4: p16^{High} microglia express genes associated with inflammation, cell cycle response and cell motility.

A: UMAP plots where colors indicate the different clusters within all the sequenced microglia cells. DAM= damage associated microglia. B: Volcano plot depicting differential expressed genes between the RFP^{High} microglia and total viable microglia. C: Violin plot showing the expression of senescence genes in each microglia cluster. D: Heatmap showing the differentially expressed regulons in the SCENIC analysis between all RFP^{High} and total viable microglia. E: GOs significantly enriched in the p16-UM1 cluster. F: GOs significantly enriched in the p16-UM2 cluster. G. Violin plot depicting the expression of UM1 and UM2 cluster markers with age in wild type mice of the dataset from Zhang et al. (Zhang et al., 2020).

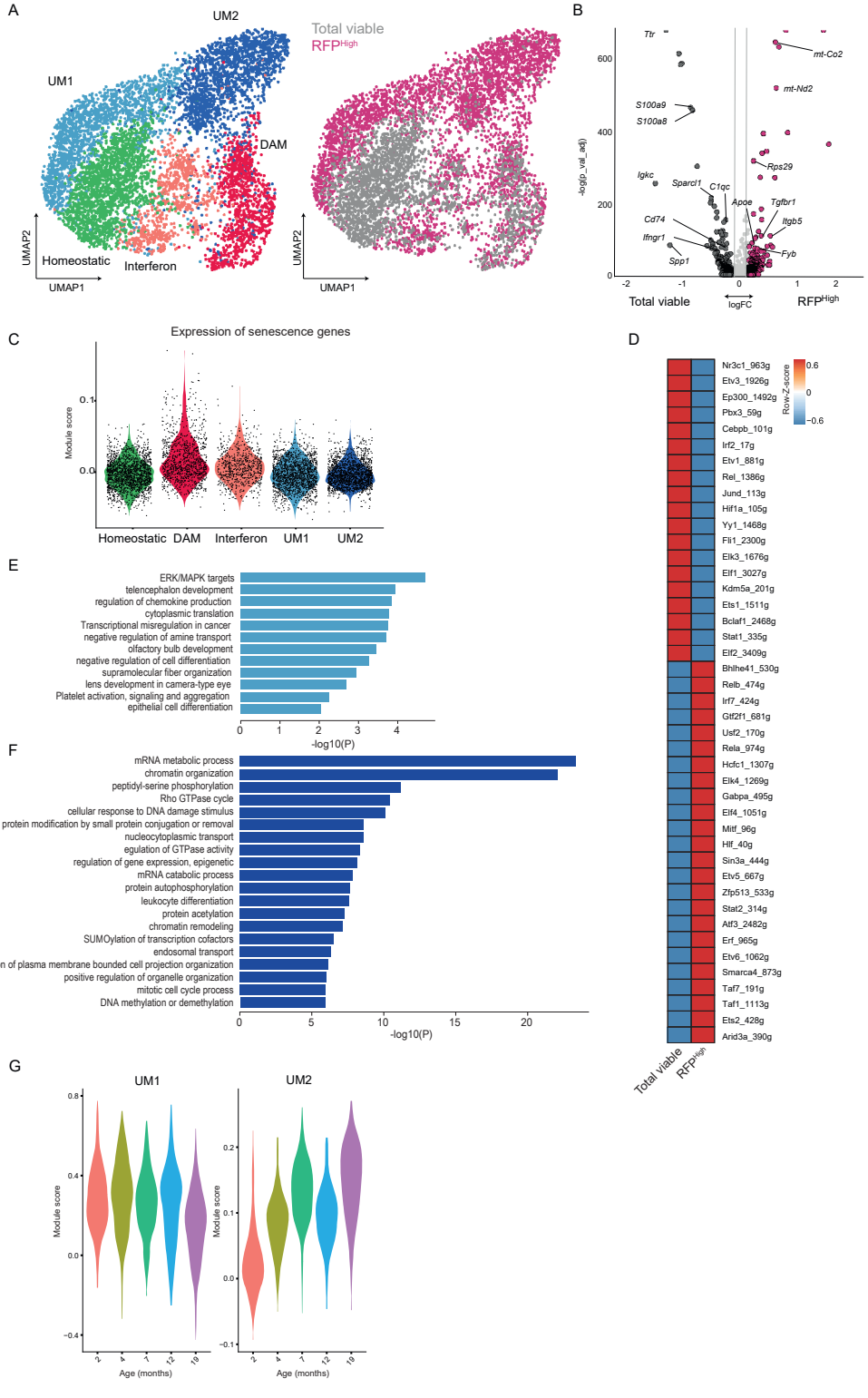
A
UM2
UM1
DAM
Homeostatic
Interferon
UMAP2
UMAP1
Total viable
RFPHigh
B
Ttr
mt-Co2
mt-Nd2
S100a9
S100a8
Igkc
Sparcl1
C1qc
Apoe
Tgfbr1
Cd74
Itgb5
Ifngr1
Fyb
Spp1
-log(p_val_adj)
Total viable
logFC
RFPHigh
C
Expression of senescence genes
Module score
Homeostatic
DAM
Interferon
UM1
UM2
D
Nr3c1_963g
Etv3_1926g
Ep300_1492g
Pbx3_59g
Cebpb_101g
Irf2_17g
Etv1_881g
Rel_1386g
Jund_113g
Hif1a_105g
Yy1_1468g
Fli1_2300g
Elk3_1676g
Elf1_3027g
Kdm5a_201g
Ets1_1511g
Bclaf1_2468g
Stat1_335g
Elf2_3409g
Bhlhe41_530g
Relb_474g
Irf7_424g
Gtf2f1_681g
Usf2_170g
Rela_974g
Hcfc1_1307g
Elk4_1269g
Gabpa_495g
Elf4_1051g
Mitf_96g
Hlf_40g
Sin3a_444g
Etv5_667g
Zfp513_533g
Stat2_314g
Atf3_2482g
Erf_965g
Etv6_1062g
Smarca4_873g
Taf7_191g
Taf1_1113g
Ets2_428g
Arid3a_390g
Row-Z-score
Total viable
RFPHigh
E
ERK/MAPK targets
telencephalon development
regulation of chemokine production
cytoplasmic translation
Transcriptional misregulation in cancer
negative regulation of amine transport
olfactory bulb development
negative regulation of cell differentiation
supramolecular fiber organization
lens development in camera-type eye
Platelet activation, signaling and aggregation
epithelial cell differentiation
-log10(P)
F
mRNA metabolic process
chromatin organization
peptidyl-serine phosphorylation
Rho GTPase cycle
cellular response to DNA damage stimulus
protein modification by small protein conjugation or removal
nucleocytoplasmic transport
egulation of GTPase activity
regulation of gene expression, epigenetic
mRNA catabolic process
protein autophosphorylation
leukocyte differentiation
protein acetylation
chromatin remodeling
SUMOylation of transcription cofactors
endosomal transport
egulation of plasma membrane bounded cell projection organization
positive regulation of organelle organization
mitotic cell cycle process
DNA methylation or demethylation
-log10(P)
G
UM1
UM2
Module score
Age (months)

Discussion

Microglia, tissue-resident macrophages of the CNS, is a heterogeneous cell population that change over the course of an organism lifespan. Microglia heterogeneity decreases with age, but several states—for example chemokine-enriched inflammatory microglia— remain unchanged or increase in aged brains (Hammond et al., 2019). Moreover, microglia are reported to age in a regional-dependent manner (Grabert et al., 2016). However, there is still little understanding of the phenotypical characteristics of microglia subpopulations in the aged brain. The current study reveals two previously unreported p16-expressing microglia subpopulations, one with a quite stable expression across different life stages and one which accumulation significantly increases with age. Elevated p16 expression is a marker of cellular senescence and has been used to identify the accumulation of senescent astrocytes (Bhat et al., 2012; Chinta et al., 2018; Yabluchanskiy et al., 2020), oligodendrocyte progenitor cells (Nicaise et al., 2019; Zhang et al., 2019), and neurons in the human ageing brain (Kang et al., 2015) and in mouse models of neurodegeneration.

Moreover, recent data indicated that microglia accumulate p16^{High} cells in aged mouse brains (Ogrodnik et al., 2021). In this study, using both transgenic and wild-type mice, and various publicly available mouse and human transcriptomic datasets, we identified two distinct subpopulations of p16^{High} microglia, one constantly present and one age-associated, that did not express a classical senescence-associated gene signature. Absence of a senescence profiling is in line with a previous study showing that while murine microglia in vitro show markers of replicative senescence, the microglia of aged mice express higher levels of *p16* but no other typical senescence-associated changes (Stojiljkovic et al., 2019). Distinct transcriptional changes in each cell population were found during single-cell sequencing of the aged murine brain (Ximerakis et al., 2019), indicating that each cell type ages differently. In our single-cell study, only astrocytes, endothelial cells, and microglia were represented in large quantities, while other cell types were underrepresented due to our cold protease isolation procedure. Since we also identified higher expression of *CDKN2A* in lymphocytes and oligodendrocytes by analyzing a dataset derived from RNAseq of single nuclei isolated from human brains (Gerrits et al., 2021), it remains to be seen whether other less represented populations also express *p16* with age. Our data suggest a clear separation of the p16^{High} microglia from

other microglia populations and the existence of two distinct subsets—one expressed across the entire lifespan and the other age-associated. A subset of $p16^{High}$ microglia may be part of a homeostatic mechanism aimed at reducing damage propagation, via cell cycle arrest and improved phagocytic properties, and at promoting immune surveillance, via activation of specific secretory and proinflammatory phenotypes. On the other side, the accumulation of a subset of $p16^{High}$ cells with age may represent the byproduct of excessive damage and reduced clearance capacity, which could contribute to detriment accumulation and loss of tissue homeostasis. Future studies need to address this issue by evaluating the effects of specifically eliminating specific $p16^{High}$ microglia subsets, and to further characterize the presence and function of these subsets in the human brain. It will also be important to evaluate whether current senolytic approaches are eliminating these $p16^{High}$ microglia subsets, and the balance between benefits and toxicities of removing such populations.

Materials and Methods

Mice

p16–3MR mice with a C57BL/6 background or wild type C57BL/6 were used for all experiments (Demaria et al., 2014). Young mice were between 7 and 12 weeks of age, and old mice between 105 and 116 weeks of age. The young mice were a mix of males and females (n=5), male old mice were used for bulk sequencing (n=5) and female mice for single cell sequencing (n=4). Young, 18 weeks of age, (n=3) and old, 101 and 104 weeks of age, (n=3) wild-type mice were used for the isolation of astrocytes, microglia and rest cells. Mice were raised on a 12-hr light/dark cycle with food and water available *ad libitum* and were individually housed. All experiments were performed in the Central Animal Facility (CDP) of the UMCG, with protocol (15339-02-001) approved by the Animal Care and Use Committee (DEC) of the University of Groningen.

Cell isolation from mouse brain tissue

Cells were isolated from adult mouse brain using an enzymatic protocol at 4°C. The brains were isolated and dissociated by three rounds of GentleMACS (m_brain_01, m_brain_02, and m_brain_03) in enzyme mix of 15 mg/ml Protease (Sigma P5380), 1 mM L-cysteine hydrochloride (Sigma C7477), 0.5 µg/µl DNase (Roche 10104159001) with 10 min incubation in the mix on ice in

between GentleMACS programs. The homogenized brain samples were passed through a 100 µM cell strainer to obtain a single cell suspension. The cells were centrifuged at 300 rcf for 10 min at 4°C and the pellet was resuspended in 24% Percoll gradient buffer. 3 mL dPBS was pipetted onto the gradient buffer and myelin was removed by centrifuging at 950 rcf for 20 min at 4°C. The cell pellets were incubated with DAPI and Draq5. Viable cells were FACS sorted as DAPI^{neg}Draq5^{pos} events. RFP^{High} and RFP^{Low} bulk samples were sorted from individual mice, but for the single cell sequencing, RFP^{High} (21,500) and total viable cells (45,000) from four mice were combined each into one lane of a 10X Genomics Chromium chip.

For the isolation of astrocytes, microglia and rest cells, cell pellets were incubated with the antibodies CD11b-BV421 (clone M1/70, Biolegend, San Diego, CA, USA), CD45-FITC (clone 30-F11, Biolegend, San Diego, CA, USA), CD49d-PE (clone R1-2, Miltenyi Biotec), Acsa2-FITC (clone REA969, Miltenyi Biotec), PI and Draq5. Microglia were FACS sorted as PI^{neg} Draq5^{pos} CD11b^{high} CD45^{int} CD49d^{neg} events. Astrocytes were FACS sorted as PI^{neg} Draq5^{pos} CD11b^{neg} CD45^{neg} Acsa2^{pos} events and rest cells as PI^{neg} Draq5^{pos} CD11b^{neg} CD45^{neg} Acsa2^{neg} events. Bulk samples were sorted from individual mice.

FACS analysis

Flowjo V.10 was used to analyze the mean, median RFP expression, number of RFP positive cells and viability of cells. Unpaired t-tests were used to compare the mean, median and number of positive cells. Paired t-test was used to compare viability.

Real-Time PCR

Total RNA was prepared using the AllPrep DNA/RNA Micro Kit (Qiagen, 80284). RNA was reverse transcribed into cDNA using a kit (Applied Biosystems). Quantitative RT-PCR (qRT-PCR) reactions were performed as described (Demaria et al., 2010) using the Universal Probe Library system (Roche).

Primers used:

p16 #91 -F	AATCTCCGCGAGGAAAGC	-R	GTCTGCAGCGGACTCCAT
Hprt1 #62 -F	ATCACATTGTGGCCCTCTG	-R	GTCATGGGAATGGATCTATCACT
Hmbs #91 -F	AGAAAAGTGCCGTGGGAAC	-R	TGTTGAGGTTTCCCCGAAT

Bulk RNAseq library construction and sequencing

RNA was isolated from cell pellets with the AllPrep DNA/RNA Micro Kit (Qiagen, 80284). RNA concentrations were measured on a Qubit using a HS RNA kit. 2,5 ng of the samples was used for library preparation with the Lexogen QuantSeq 3' mRNA-Seq Library Prep Kit (FWD) from Illumina. All libraries were pooled equimolarly and sequenced on a NextSeq 500 at the sequencing facility in the UMCG.

scRNAseq library construction and sequencing

The single cell cDNA libraries were constructed using the Chromium Single Cell 3' Reagents Kit v3 and corresponding user guide (10x Genomics). All samples were pooled in equimolar ratios and sequenced on a NextSeq 500 at the sequencing facility in the UMCG.

Gene sets from literature

To compare our microglia clusters with reported microglia phenotypes in literature, several gene sets were downloaded. From (Sierksma et al., 2020), EV7 was downloaded and genes with a p_val_adj < 0.05 and logFC > 0.15 were selected (304 genes) and from EV6 the CPM gene set (521 genes). From (Hammond et al., 2019), table S1 was downloaded and marker genes from clusters OA2 and OA3 were selected (136 and 37 genes, respectively). From (Keren-Shaul et al., 2017), table S2 was downloaded and upregulated genes of "Microglia3" with a p_val_adj < 0.05 were selected (469 genes). From (Butovsky and Weiner, 2018), upregulated genes listed in figure 2 were used (29 genes). From (Gerrits et al., 2020), genes from table S4 with a p_val_adj < 0.05 and logFC > 0.15 were selected (188 genes). From Galatro et al. (2017), Voom Normalized counts were downloaded from GEO. From Gerrits et al. 2021, the exact same analyzed data objects as reported in the paper were used as these were generated by ourselves.

Bulk RNAseq data analysis

Data preprocessing was performed with the Lexogen Quantseq 2.3.1 FWD UMI pipeline on the BlueBee Genomics Platform (1.10.18). Count files were loaded into R and DAFS filtering was performed to remove lowly expressed genes (George and Chang, 2014). A negative binomial generalized log-linear model was used to model gene expression levels, as implemented in edgeR, adjusted for mouse since the RFP^{Low} and RFP^{High} cells were obtained from the same mice

and differentially expressed genes were determined using a likelihood ratio test (Robinson et al., 2010). Thresholds were set at abs(logFC) > 1 and p < 0.05. Principal component analysis was performed on logCPM transformed counts. Visualizations were made with the CRAN package 'ggplot2'. Heatmaps were made with the CRAN package 'gplots' and rows and columns were clustered using hierarchical clustering with the ward.D2 method on pearson correlations. For WGCNA analysis, VST-transformed counts obtained from DESeq2 were used as input (Langfelder and Horvath, 2008b; Love et al., 2014). Signed WGCNA was performed using biweight mid-correlations and the max number of excluded outliers was restricted to 10%. Since we were dealing with binary data (i.e. two experimental groups) the robust treatment for the y variable of the biweight mid-correlation was turned off (Langfelder and Horvath, 2012). Gene ontology analysis was performed on significantly differentially expressed genes (p < 0.05 and logFC > 0.15) using 'clusterProfiler' with a p- and q-value cutoff of 0.05.

scRNAseq data analysis

Raw reads were processed using Cell Ranger 3.0.0 with default settings and aligned to the mouse mm10 genome. Barcode filtering was performed with DropletUtils with a threshold on > 250 UMIs. Counts from cellular barcodes were then extracted from the raw output count matrix from Cell ranger. Cells with a mitochondrial content >10% were removed from the dataset. Counts from the different sample groups were merged into one using the 'Merge' function from Seurat (v3). Then, the data was SCTransformed with regression on mitochondrial and ribosomal content and subsequently PCA, UMAP, finding neighbors and clustering was performed as implemented by Seurat (Hafemeister and Satija, 2019). For differential gene expression analysis, raw counts were normalized using the 'NormalizeData' function, then DE genes were identified with MAST. Geneset scores were calculated using the 'AddModuleScore' function. Average gene expression per cluster was calculated using the 'AverageExpression' function. Median of expressed genes that were mitochondrial per cell: 2.2%; ribosomal: 5.6%; median number of genes detected per cell: 755.

Regulatory gene network (regulon) analysis was performed using SCENIC, normalized counts from Seurat were used as input (Aibar et al., 2017). Only

genes with more than 3 counts and present in at least 0.5% of all cells were included. GENIE3 and SCENIC were used with default settings (Aibar et al., 2017; Huynh-Thu et al., 2010). Enrichment of gene sets and regulons in our scRNAseq data was quantified using AUCell. AUC values are plotted as an average per group. Regulons with a median AUC < 0.01 were excluded in the downstream analysis.

From Zhang et al. (2020), the raw count matrices of all mice were downloaded and raw reads were processed using Cell Ranger 3.0.0 with default settings and the pre-mRNA package. From the bam file, exonic reads and intronic reads mapping in the same direction as the mRNA were counted per barcode with Abacus in order to distinguish barcodes containing nuclear RNA from ambient and cytoplasmic RNA (Xi et al., 2020). The counts corresponding to these barcodes were extracted from the raw count matrix generated by Cell Ranger and loaded in R with Seurat (3.0.3). Nuclei with a mitochondrial content > 5% were removed from the dataset. Count matrices of all mice were merged. The data was normalized for library size, by a scale factor of 10,000 and log-transformed. Scrublet was used to identify and remove doublets (Wolock et al., 2019). Highly variable features (HVGs) were determined using the VST method. The data was scaled and heterogeneity associated with number of UMIs and mitochondrial content was regressed out and the data was clustered using the graph-based clustering approach implemented in Seurat. The microglia cluster was identified based on expression of P2ry12, Csf1r and Cx3cr1. Then, only WT mice were used for further analysis. Geneset scores were calculated using the 'AddModuleScore' function from Seurat.

References

Aibar, S., González-Blas, C.B., Moerman, T., Huynh-Thu, V.A., Imrichova, H., Hulselmans, G., Rambow, F., Marine, J.-C., Geurts, P., Aerts, J., et al. (2017). SCENIC: Single-cell regulatory network inference and clustering. Nat. Methods 14, 1083.

Baker, D.J., Childs, B.G., Durik, M., Wijers, M.E., Sieben, C.J., Zhong, J., A. Saltness, R., Jeganathan, K.B., Verzosa, G.C., Pezeshki, A., et al. (2016). Naturally occurring p16 Ink4a-positive cells shorten healthy lifespan. Nature 530, 184–189.

Beck, T.N., Nicolas, E., Kopp, M.C., and Golemis, E.A. (2014). Adaptors for disorders of the brain? The cancer signaling proteins NEDD9, CASS4, and PTK2B in Alzheimer's disease. Oncoscience 1, 486–503.

Behmoaras, J., and Gil, J. (2021). Similarities and interplay between senescent cells and macrophages. J. Cell Biol. 220.

Bhat, R., Crowe, E.P., Bitto, A., Moh, M., Katsetos, C.D., Garcia, F.U., Johnson, F.B., Trojanowski, J.Q., Sell, C., and Torres, C. (2012). Astrocyte Senescence as a Component of Alzheimer's Disease. PLoS One 7, e45069.

Bussian, T.J., Aziz, A., Meyer, C.F., Swenson, B.L., van Deursen, J.M., and Baker, D.J. (2018). Clearance of senescent glial cells prevents tau-dependent pathology and cognitive decline. Nature 1.

Butovsky, O., and Weiner, H.L. (2018). Microglial signatures and their role in health and disease. Nat. Rev. Neurosci. 19, 622–635.

Chinta, S.J., Woods, G., Demaria, M., Rane, A., Zou, Y., McQuade, A., Rajagopalan, S., Limbad, C., Madden, D.T., Campisi, J., et al. (2018). Cellular Senescence Is Induced by the Environmental Neurotoxin Paraquat and Contributes to Neuropathology Linked to Parkinson's Disease. Cell Rep. 22, 930–940.

Demaria, M., Giorgi, C., Lebiedzinska, M., Esposito, G., D'angeli, L., Bartoli, A., Gough, D.J., Turkson, J., Levy, D.E., Watson, C.J., et al. (2010). A STAT3-mediated metabolic switch is involved in tumour transformation and STAT3 addiction. Aging (Albany. NY). 2, 823–842.

Demaria, M., Ohtani, N., Youssef, S.A., Rodier, F., Toussaint, W., Mitchell, J.R., Laberge, R.-M., Vijg, J., Van Steeg, H., Dollé, M.E.T., et al. (2014). An Essential Role for Senescent Cells in Optimal Wound Healing through Secretion of PDGF-AA. Dev. Cell 31, 722–733.

Efthymiou, A.G., and Goate, A.M. (2017). Late onset Alzheimer's disease genetics implicates microglial pathways in disease risk. Mol. Neurodegener. 12, 43.

Galatro, T.F., Holtman, I.R., Lerario, A.M., Vainchtein, I.D., Brouwer, N., Sola, P.R., Veras, M.M., Pereira, T.F., Leite, R.E.P., Möller, T., et al. (2017). Transcriptomic analysis of purified human cortical microglia reveals age-associated changes. Nat. Neurosci. 20, 1162–1171.

George, N.I., and Chang, C.-W. (2014). DAFS: a data-adaptive flag method for RNA-sequencing data to differentiate genes with low and high expression. BMC Bioinformatics 15, 92.

Gerrits, E., Heng, Y., Boddeke, E.W.G.M., and Eggen, B.J.L. (2020). Transcriptional profiling of microglia; current state of the art and future perspectives. Glia 68, 740–755.

Gerrits, E., Brouwer, N., Kooistra, S.M., Woodbury, M.E., Vermeiren, Y., Lambourne, M., Mulder, J., Kummer, M., Möller, T., Biber, K., et al. (2021). Distinct amyloid-β and tau-associated microglia profiles in Alzheimer's disease. Acta Neuropathol. 141, 681–696.

Gorgoulis, V., Adams, P.D., Alimonti, A., Bennett, D.C., Bischof, O., Bishop, C., Campisi, J., Collado, M., Evangelou, K., Ferbeyre, G., et al. (2019). Cellular Senescence: Defining a Path Forward. Cell 179, 813–827.

Grabert, K., Michoel, T., Karavolos, M.H., Clohisey, S., Kenneth Baillie, J., Stevens, M.P., Freeman, T.C., Summers, K.M., and McColl, B.W. (2016). Microglial brain regionâ 'dependent diversity and selective regional sensitivities to aging. Nat. Neurosci. 19, 504–516.

Hafemeister, C., and Satija, R. (2019). Normalization and variance stabilization of single-cell RNA-seq data using regularized negative binomial regression. Genome Biol. 20, 296.

Hall, B.M., Balan, V., Gleiberman, A.S., Strom, E., Krasnov, P., Virtuoso, L.P., Rydkina, E., Vujcic, S., Balan, K., Gitlin, I., et al. (2016). Aging of mice is associated with p16(Ink4a)- and β-galactosidasepositive macrophage accumulation that can be induced in young mice by senescent cells. Aging (Albany. NY). 8, 1294–1315.

Hall, B.M., Balan, V., Gleiberman, A.S., Strom, E., Krasnov, P., Virtuoso, L.P., Rydkina, E., Vujcic, S., Balan, K., Gitlin, I.I., et al. (2017). p16(Ink4a) and senescence-associated β-galactosidase can be induced in macrophages as part of a reversible response to physiological stimuli. Aging (Albany. NY). 9, 1867–1884.

Hammond, T.R., Dufort, C., Dissing-Olesen, L., Giera, S., Young, A., Wysoker, A., Walker, A.J., Gergits, F., Segel, M., Nemesh, J., et al. (2019). Single-Cell RNA Sequencing of Microglia throughout the Mouse Lifespan and in the Injured Brain Reveals Complex Cell-State Changes. Immunity 50, 253-271.e6.

Hayflick, L., and Moorhead, P.S. (1961). The serial cultivation of human diploid cell strains. Exp. Cell Res. 25, 585–621.

He, G., Luo, W., Li, P., Remmers, C., Netzer, W.J., Hendrick, J., Bettayeb, K., Flajolet, M., Gorelick, F., Wennogle, L.P., et al. (2010). Gamma-secretase activating protein is a therapeutic target for Alzheimer's disease. Nature 467, 95–98.

Herbig, U., Ferreira, M., Condel, L., Carey, D., and Sedivy, J.M. (2006). Cellular senescence in aging primates. Science (80-.). 311, 1257.

Hernandez-Segura, A., Nehme, J., and Demaria, M. (2018). Hallmarks of Cellular Senescence. Trends Cell Biol. 28, 436–453.

Ho, A., Liu, X., and Südhof, T.C. (2008). Deletion of Mint proteins decreases amyloid production in transgenic mouse models of Alzheimer's disease. J. Neurosci. 28, 14392–14400.

Huynh-Thu, V.A., Irrthum, A., Wehenkel, L., and Geurts, P. (2010). Inferring Regulatory Networks from Expression Data Using Tree-Based Methods. PLoS One 5, e12776.

Kaminska, B., Gozdz, A., Zawadzka, M., Ellert-Miklaszewska, A., and Lipko, M. (2009). MAPK Signal Transduction Underlying Brain Inflammation and Gliosis as Therapeutic Target. Anat. Rec. Adv. Integr. Anat. Evol. Biol. 292, 1902–1913.

Kang, C., Xu, Q., Martin, T.D., Li, M.Z., Demaria, M., Aron, L., Lu, T., Yankner, B.A., Campisi, J., and Elledge, S.J. (2015). The DNA damage response induces inflammation and

senescence by inhibiting autophagy of GATA4. Science (80-.). 349, aaa5612.

Keren-Shaul, H., Spinrad, A., Weiner, A., Matcovitch-Natan, O., Dvir-Szternfeld, R., Ulland, T.K., David, E., Baruch, K., Lara-Astaiso, D., Toth, B., et al. (2017). A Unique Microglia Type Associated with Restricting Development of Alzheimer's Disease. Cell 169, 1276-1290.e17.

Kotake, Y., Naemura, M., Murasaki, C., Inoue, Y., and Okamoto, H. (2015). Transcriptional regulation of the p16 tumor suppressor gene. Anticancer Res. 35, 4397–4402.

Kritsilis, M., Rizou, S. V., Koutsoudaki, P.N., Evangelou, K., Gorgoulis, V.G., and Papadopoulos, D. (2018). Ageing, cellular senescence and neurodegenerative disease. Int. J. Mol. Sci. 19.

Langfelder, P., and Horvath, S. (2008a). WGCNA: An R package for weighted correlation network analysis. BMC Bioinformatics 9.

Langfelder, P., and Horvath, S. (2008b). WGCNA: an R package for weighted correlation network analysis. BMC Bioinformatics 9, 559.

Langfelder, P., and Horvath, S. (2012). Fast R Functions for Robust Correlations and Hierarchical Clustering. J. Stat. Softw. 46, 1–17.

Liu, J.Y., Souroullas, G.P., Diekman, B.O., Krishnamurthy, J., Hall, B.M., Sorrentino, J.A., Parker, J.S., Sessions, G.A., Gudkov, A. V., and Sharpless, N.E. (2019). Cells exhibiting strong p16 INK4a promoter activation in vivo display features of senescence. Proc. Natl. Acad. Sci. U. S. A. 116, 2603–2611.

Liu, Y., Sanoff, H.K., Cho, H., Burd, C.E., Torrice, C., Ibrahim, J.G., Thomas, N.E., and Sharpless, N.E. (2009). Expression of p16INK4a in peripheral blood T-cells is a biomarker of human aging. Aging Cell 8, 439–448.

Love, M.I., Huber, W., and Anders, S. (2014). Moderated estimation of fold change and dispersion for RNA-seq data with DESeq2. Genome Biol. 15, 550.

Martin-Ruiz, C., Williams-Gray, C.H., Yarnall, A.J., Boucher, J.J., Lawson, R.A., Wijeyekoon, R.S., Barker, R.A., Kolenda, C., Parker, C., Burn, D.J., et al. (2020). Senescence and Inflammatory Markers for Predicting Clinical Progression in Parkinson's Disease: The ICICLE-PD Study. J. Parkinsons. Dis. 10, 193–206.

Martin, N., Beach, D., and Gil, J. (2014). Ageing as developmental decay: Insights from p16INK4a. Trends Mol. Med. 20, 667–674.

Masuda, T., Sankowski, R., Staszewski, O., and Prinz, M. (2020). Microglia Heterogeneity in the Single-Cell Era. Cell Rep. 30, 1271–1281.

Melk, A., Schmidt, B.M.W., Takeuchi, O., Sawitzki, B., Rayner, D.C., and Halloran, P.F. (2004). Expression of p16INK4a and other cell cycle regulator and senescence associated genes in aging human kidney. Kidney Int. 65, 510–520.

Neubrand, V.E., Pedreño, M., Caro, M., Forte-Lago, I., Delgado, M., and Gonzalez-Rey, E. (2014). Mesenchymal stem cells induce the ramification of microglia via the small RhoGTPases Cdc42 and Rac1. Glia 62, 1932–1942.

Nicaise, A.M., Wagstaff, L.J., Willis, C.M., Paisie, C., Chandok, H., Robson, P., Fossati, V., Williams, A., and Crocker, S.J. (2019). Cellular senescence in progenitor cells contributes

to diminished remyelination potential in progressive multiple sclerosis. Proc. Natl. Acad. Sci. 116, 9030–9039.

Norden, D.M., and Godbout, J.P. (2013). Review: Microglia of the aged brain: Primed to be activated and resistant to regulation. Neuropathol. Appl. Neurobiol. 39, 19–34.

Noseda, R., Guerrero-Valero, M., Alberizzi, V., Previtali, S.C., Sherman, D.L., Palmisano, M., Huganir, R.L., Nave, K.-A., Cuenda, A., Feltri, M.L., et al. (2016). Kif13b Regulates PNS and CNS Myelination through the Dlg1 Scaffold. PLOS Biol. 14, e1002440.

Ogrodnik, M., Evans, S.A., Fielder, E., Victorelli, S., Kruger, P., Salmonowicz, H., Weigand, B.M., Patel, A.D., Pirtskhalava, T., Inman, C.L., et al. (2021). Whole-body senescent cell clearance alleviates age-related brain inflammation and cognitive impairment in mice. Aging Cell.

Perry, V.H., and Holmes, C. (2014). Microglial priming in neurodegenerative disease. Nat. Rev. Neurol. 10, 217–224.

Peters, R. (2006). Ageing and the brain. Postgrad. Med. J. 82, 84–88.

Qian, T., Wang, K., Cui, J., He, Y., and Yang, Z. (2016). Angiopoietin-Like Protein 7 Promotes an Inflammatory Phenotype in RAW264.7 Macrophages Through the P38 MAPK Signaling Pathway. Inflammation 39, 974–985.

Raj, D.D.A., Jaarsma, D., Holtman, I.R., Olah, M., Ferreira, F.M., Schaafsma, W., Brouwer, N., Meijer, M.M., De Waard, M.C., Van der Pluijm, I., et al. (2014). Priming of microglia in a DNA-repair deficient model of accelerated aging. Neurobiol. Aging 35, 2147–2160.

Ramana, K. V., Fadl, A.A., Tammali, R., Reddy, A.B.M., Chopra, A.K., and Srivastava, S.K. (2006). Aldose reductase mediates the lipopolysaccharide-induced release of inflammatory mediators in RAW264.7 murine macrophages. J. Biol. Chem. 281, 33019–33029.

Robinson, M.D., McCarthy, D.J., and Smyth, G.K. (2010). edgeR: a Bioconductor package for differential expression analysis of digital gene expression data. Bioinformatics 26, 139–140.

Roney, K.E., O'Connor, B.P., Wen, H., Holl, E.K., Guthrie, E.H., Davis, B.K., Jones, S.W., Jha, S., Sharek, L., Garcia-Mata, R., et al. (2011). Plexin-B2 Negatively Regulates Macrophage Motility, Rac, and Cdc42 Activation. PLoS One 6, e24795.

Sanada, F., Taniyama, Y., Muratsu, J., Otsu, R., Shimizu, H., Rakugi, H., and Morishita, R. (2018). Source of Chronic Inflammation in Aging. Front. Cardiovasc. Med. 5, 12.

Seya, T., Oshiumi, H., Sasai, M., Akazawa, T., and Matsumoto, M. (2005). TICAM-1 and TICAM-2: Toll-like receptor adapters that participate in induction of type 1 interferons. Int. J. Biochem. Cell Biol. 37, 524–529.

Sierksma, A., Lu, A., Mancuso, R., Fattorelli, N., Thrupp, N., Salta, E., Zoco, J., Blum, D., Buée, L., De Strooper, B., et al. (2020). Novel Alzheimer risk genes determine the microglia response to amyloid-β but not to TAU pathology. EMBO Mol. Med. 12.

Stojiljkovic, M.R., Ain, Q., Bondeva, T., Heller, R., Schmeer, C., and Witte, O.W. (2019). Phenotypic and functional differences between senescent and aged murine microglia. Neurobiol. Aging 74, 56–69.

Valério-Gomes, B., Guimarães, D.M., Szczupak, D., and Lent, R. (2018). The absolute number of oligodendrocytes in the adult mouse brain. Front. Neuroanat. 12.

Wolock, S.L., Lopez, R., and Klein, A.M. (2019). Scrublet: Computational Identification of Cell Doublets in Single-Cell Transcriptomic Data. Cell Syst. 8, 281-291.e9.

Wyss-Coray, T. (2016). Ageing, neurodegeneration and brain rejuvenation. Nature 539, 180–186.

Xi, S., Gibilisco, L., Kummer, M., Biber, K., Wachter, A., and Woodbury, M. (2020). ABACUS: A flexible UMI counter that leverages intronic reads for single-nucleus RNAseq analysis. BioRxiv 2020.11.13.381624.

Ximerakis, M., Lipnick, S.L., Innes, B.T., Simmons, S.K., Adiconis, X., Dionne, D., Mayweather, B.A., Nguyen, L., Niziolek, Z., Ozek, C., et al. (2019). Single-cell transcriptomic profiling of the aging mouse brain. Nat. Neurosci. 22, 1696–1708.

Xu, M., Pirtskhalava, T., Farr, J.N., Weigand, B.M., Palmer, A.K., Weivoda, M.M., Inman, C.L., Ogrodnik, M.B., Hachfeld, C.M., Fraser, D.G., et al. (2018). Senolytics improve physical function and increase lifespan in old age. Nat. Med. 24, 1246–1256.

Yabluchanskiy, A., Tarantini, S., Balasubramanian, P., Kiss, T., Csipo, T., Fülöp, G.A., Lipecz, A., Ahire, C., DelFavero, J., Nyul-Toth, A., et al. (2020). Pharmacological or genetic depletion of senescent astrocytes prevents whole brain irradiation–induced impairment of neurovascular coupling responses protecting cognitive function in mice. GeroScience.

Yousefzadeh, M.J., Zhao, J., Bukata, C., Wade, E.A., McGowan, S.J., Angelini, L.A., Bank, M.P., Gurkar, A.U., McGuckian, C.A., Calubag, M.F., et al. (2020). Tissue specificity of senescent cell accumulation during physiologic and accelerated aging of mice. Aging Cell 19.

Zhang, J., Velmeshev, D., Hashimoto, K., Huang, Y.H., Hofmann, J.W., Shi, X., Chen, J., Leidal, A.M., Dishart, J.G., Cahill, M.K., et al. (2020). Neurotoxic microglia promote TDP-43 proteinopathy in progranulin deficiency. Nature 588, 459–465.

Zhang, P., Kishimoto, Y., Grammatikakis, I., Gottimukkala, K., Cutler, R.G., Zhang, S., Abdelmohsen, K., Bohr, V.A., Misra Sen, J., Gorospe, M., et al. (2019). Senolytic therapy alleviates Aβ-associated oligodendrocyte progenitor cell senescence and cognitive deficits in an Alzheimer's disease model. Nat. Neurosci. 22, 719–728.

Supplemental tables

Excel file containing Tables S1 to S7

(acel13450-sup-0002-TableS1-S7.xlsx)

Table S1: Differential gene expression analysis between RFP^{High} and RFP^{Low} samples

Table S2: WGCNA modules significantly correlated with cell population

Table S3: Stats of single cell sequencing

Table S4: Differential gene expression analysis between cell types

Table S5: Senescence gene list

Table S6: Differential gene expression analysis of RFP^{High} microglia versus total viable microglia population

Table S7: List of ageing-associated microglia profiles

Supplemental figures

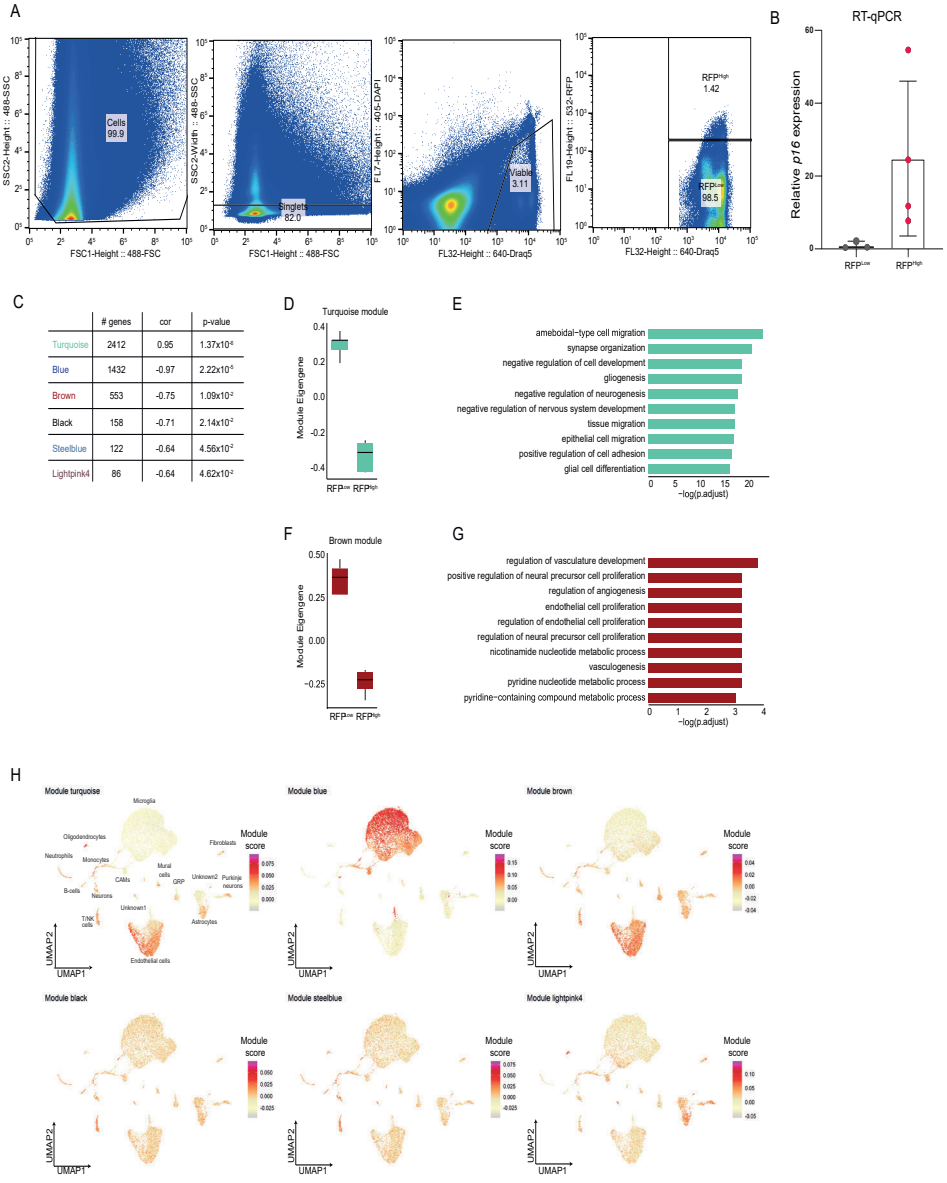

Figure S1: WGCNA module expression between cell types.

A: Gating strategy for sorting RFP^{High} cells by FACS. B: p16 expression measured by qPCR in old mouse brains. C: List of significant weighted gene correlation network analysis (WGCNA) modules between RFP^{Low} and RFP^{High} samples. D-G: ModuleEigengene expression levels and gene ontology analysis of WGCNA modules enriched in RFP^{Low} samples. H: UMAPs depicting the expression of WGCNA modules in all isolated cell types in single cell data set.

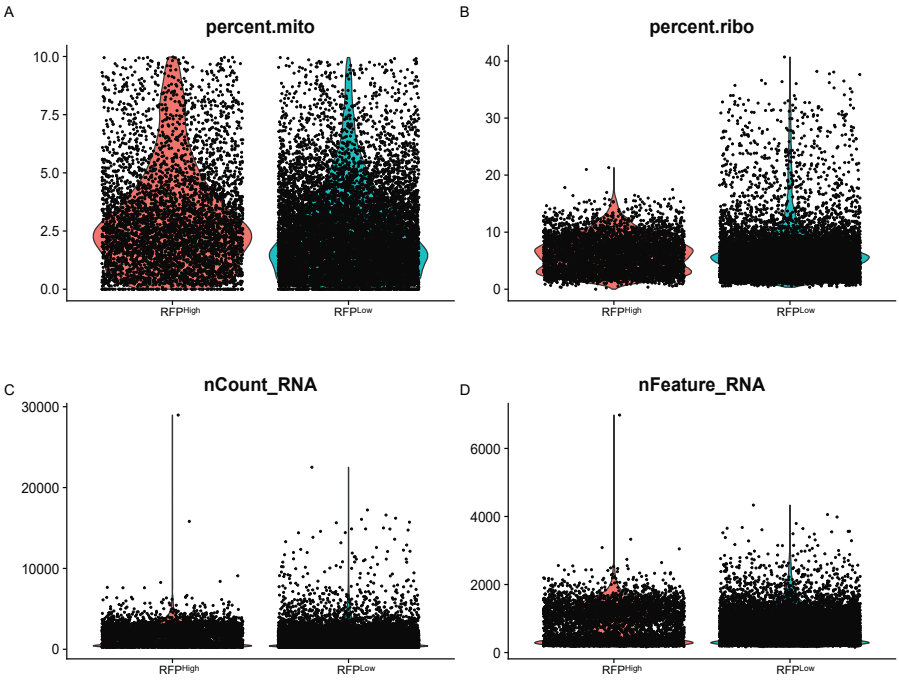

Figure S2: Quality control of scRNAseq.

A: Percentage mitochondrial RNA, B: percentage ribosomal RNA, C: read counts and D: number of unique genes detected in RFP^{Low} and RFP^{High} samples

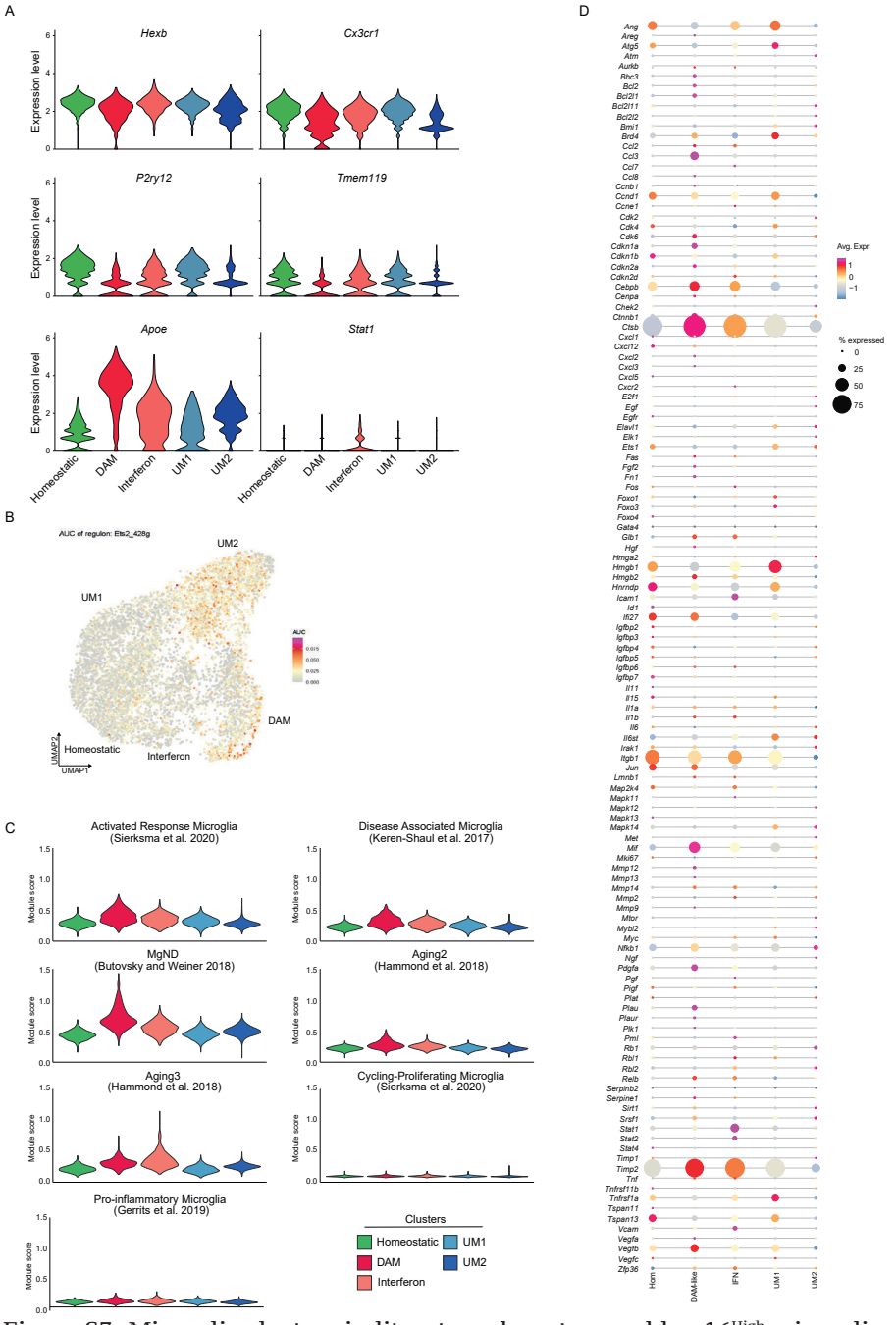

Figure S3: Microglia clusters in literature do not resemble p16^{High} microglia.

A: Violin plot depicting the expression of Hexb, Cxcr1, P2ry12, Tmem119, Apoe and Stat1 respectively in each cell of the microglia cluster. B: UMAP depicting Ets2 regulon expression in all microglia. C: Violin plots showing the expression of subtype signatures from the literature in each cluster. D: Dot plot showing expression of senescence genes in microglia clusters.

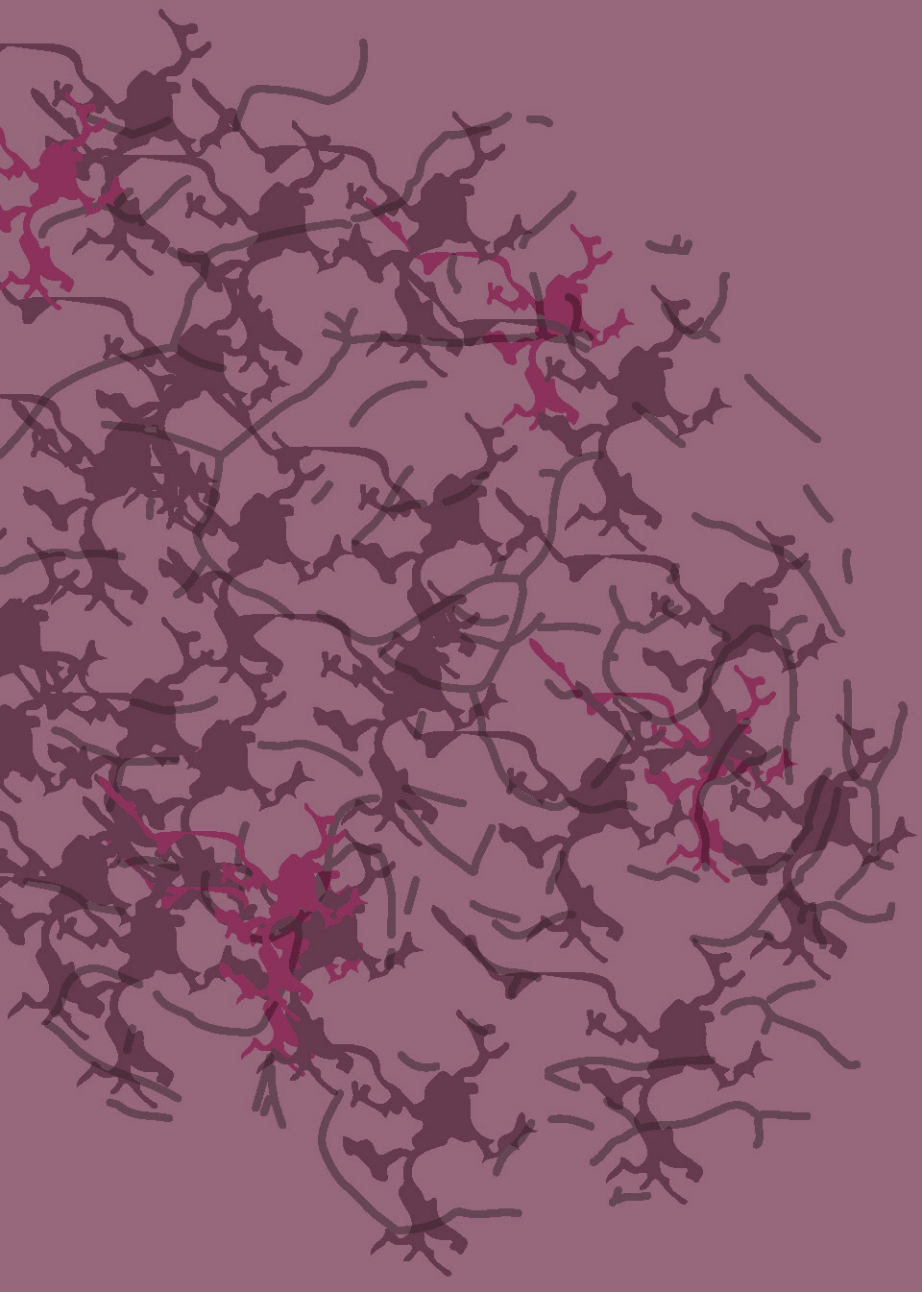

Chapter 4

Direct and indirect effects of genotoxic stress-induced senescence in glial cells

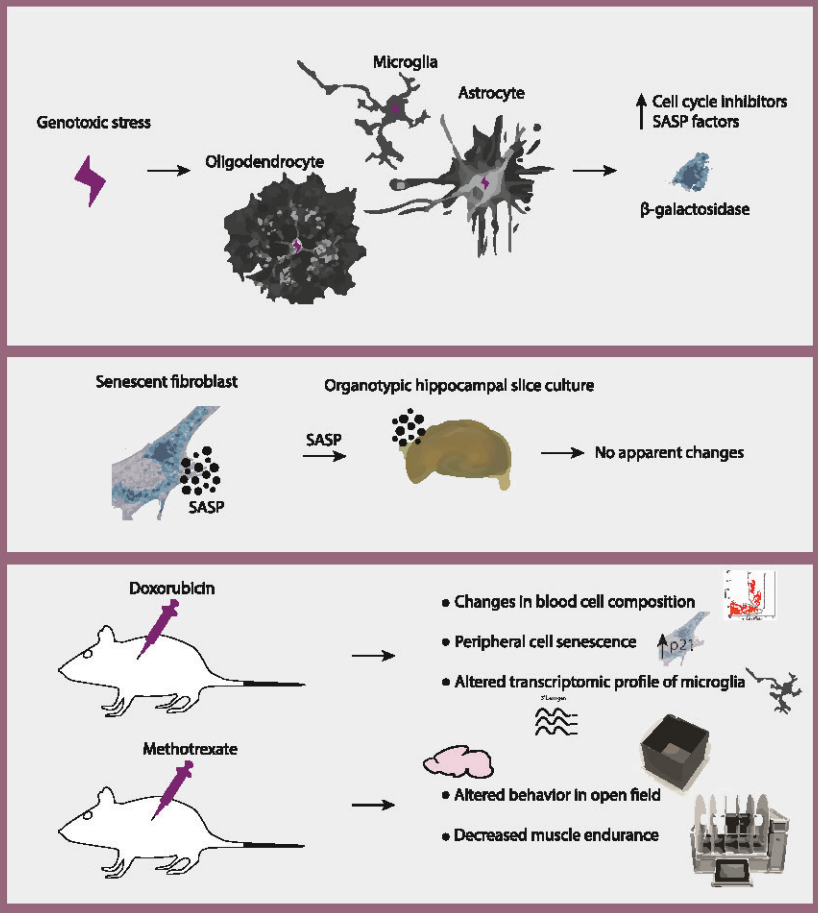

N. Talma[1,2], J. L. Geertsma[1], J. W. A. Sijbesma[3], A. Dethmers-Ausema[1], E. Gerrits[2], J. Doorduin[3], B.J.L. Eggen[2], M. Demaria[1]

1. European Institute for the Biology of Ageing, University Medical Center Groningen, University of Groningen, Groningen, The Netherlands

2. Section of Molecular Neurobiology, Department of Biomedical Sciences of Cells & Systems, University Medical Center Groningen, University of Groningen, Groningen, The Netherlands

3. Department of Nuclear Medicine and Molecular Imaging, University Medical Center Groningen, University of Groningen, Groningen, The Netherlands

Abstract

Cancer treatments have significantly improved specificity and efficacy in the past decades in particular with the advent targeted and immunotherapies. However, less specific interventions based on inflicting genotoxic stress remain the gold standard for the treatment of cancer patients. Despite their efficacy, the lack of specificity of genotoxic agents is associated with various side effects. Among the side effects is the chemobrain, where patients suffer from cognitive deficits after chemotherapy treatment. The direct and indirect effects of genotoxic stress on brain cells and cognitive function in cancer patients is not fully understood. To study the effect of genotoxic stress on brain cell function, we examined the effect of irradiation and genotoxic agents on glial cells *in vitro*, the *ex vivo* effects of conditioned medium from genotoxic stress-induced senescent cells on organotypic slice cultures, and the effects of the chemotherapeutics doxorubicin and methotrexate *in vivo*. Markers of cellular senescence were increased in glial cells after the induction of genotoxic stress, but conditioned medium from senescent cells did not induce major changes in the slice cultures. Doxorubicin was shown to change blood cell composition and was shown to have an indirect effect on microglial gene expression. However, doxorubicin treatment did not result in alterations in behavior. On the other hand, methotrexate was shown to decrease muscle endurance and induced atypical behavior in an open field test, but did not show changes in blood cell composition. Overall, the data shows that genotoxic stress can induce direct cellular senescence in glial cells *in vitro* and indirect changes in glial cells *in vivo*, which together might play a role in induction of cognitive deficits after cancer treatments.

Introduction

Cancer treatments have improved dramatically in the past decades, and consequently the population of cancer survivors has steadily increased (Siegel et al., 2018). By studying this population, it has become clear that cancer and its treatment, such as chemotherapy and irradiation, have long-term unresolved and debilitating side-effects, which often resemble ageing phenotypes (Tao et al., 2015). Thus, cancer treatment might accelerate ageing and the onset of a number of age-related pathologies. A common marker in chemotherapy-treated and ageing organisms is the accumulation of senescent

cells. Cellular senescence can be induced by multiple stressors such as DNA damage (genotoxic stress), telomere loss, oncogene activation, excessive production of reactive oxygen species or treatment with chemotherapeutic agents. This cell fate is characterized by an irreversible growth arrest and these cells often secrete a spectrum of inflammatory and other factors, also called the senescence associated secretory phenotype (SASP) (Watanabe et al., 2017). The growth arrest is exerted via two main effector pathways, the p53/p21 and $p16^{INK4A}$/pRb pathways, which block cell cycle progression through the inhibition of cyclin dependent kinases. Other hallmarks of senescence include gross morphological changes, nuclear modifications, metabolic reprogramming, changes in the structure and function of mitochondria and lysosomes, and increased resistance to apoptosis (Hernandez-Segura et al, 2018). Senescent cells are important for embryonic development (Muñoz-Espín et al., 2013), tissue repair (Jun and Lau, 2010; Krizhanovsky et al., 2008), and tumor suppression (Serrano et al., 1997). However, during ageing, accumulation of senescent cells can contribute to a decline in regenerative potential, decline in the function of tissues, increased inflammation, and promote tumorigenesis (Hernandez-Segura et al, 2018). Clearance of senescent cells has been shown to improve the symptomatology of several diseases such as atherosclerosis, lung fibrosis or diabetes mellitus, making them an attractive therapeutic target (Kirkland et al, 2017).

Cognitive deficits due to cancer treatment is a common phenomenon and is referred to as 'chemobrain' (Walczak and Janowski, 2019). The side effects described by patients as brain fog include loss of memory, attention, processing speed, and executive function. The duration of chemo brain symptoms ranges from short to long, with around one third of patients reporting side effects for months to as long as 5 to 10 y after the cessation of their treatments (Kovalchuk and Kolb, 2017). Some chemotherapeutics were shown to be even more toxic to healthy brain cells than to the cancer cells they were designed to treat (Han et al., 2008). A common denominator between chemotherapeutics is the induction of genotoxic stress in cancerous, highly proliferative cells, making them go into apoptosis or senescence. This however, does not only happen in cancer cells. The effect of genotoxic stress on the brain directly, but also indirectly is not yet fully understood. Therefore, the goal of this study was to investigate the effects of genotoxic stress on glial cells.

Results

Genotoxic stress induces senescence-associated phenotypes in glial cells

To determine how senescence-associated phenotypes evolve in microglia, we exposed the murine microglia cell line BV2 to different doses of gamma irradiation: 5, 10, and 20 Gray (Gy). To assess the effect of irradiation on BV-2 proliferation, EdU incorporation was quantified after increasing gamma dosages. A decrease in EdU incorporation was already observed at 5 Gy, which did not further decrease at higher doses (Figure 1A-B). Furthermore, 10 and 20 Gy of irradiation induced Senescence-Associated (SA) β-galactosidase (gal) activity (Figure 1C-D). The expression of the cell cycle inhibitors *p21* (Figure1E) and p16 (Figure 1F-G and Figure S1A), and of the nuclear lamina protein *Lmnb1* (Figure1E) was not significantly altered. A significant increase in the expression of the senescence associated secretory phenotype (SASP) marker *Il6* was observed after exposure to 10 Gy radiation (Figure1E). Taken together, gamma irradiation induced senescence in BV2 cells with most profound expression of senescence markers in cells exposed to 10 Gy.

To study senescence-associated features of other glial cell types exposed to stress, oligodendrocytes were isolated from the white matter (non-cortical region) and grey matter (cortical region) of the rat brain. Oligodendrocytes were subjected to genotoxic stress to promote premature senescence. At first, we exposed the cells to paraquat, which has been shown to induce senescence in mouse astrocytes (Chinta et al., 2018). Paraquat induces reactive oxygen species (ROS) which can damage macromolecules and cellular organelles. Small changes in senescence gene expression levels and larger changes in SASP factor *Il6* expression levels were observed 10 days after paraquat treatment (Figure 2A-B). Next, we looked at the effect of ionizing radiation by exposing cells to 0.5, 2.5, 5, and 10 Gy of y-radiation. Irradiation induced changes in senescence gene expression, in particular an upregulation of *p21* and a decrease of *Lmnb1* were observed (Figure 2C). Together, these data suggest that cellular stress can induce senescence in oligodendrocytes and that the senescent phenotype depends on the stressor.

To study astrocyte senescence, primary astrocytes were treated with different concentrations of the chemotherapeutic agent methotrexate and gene

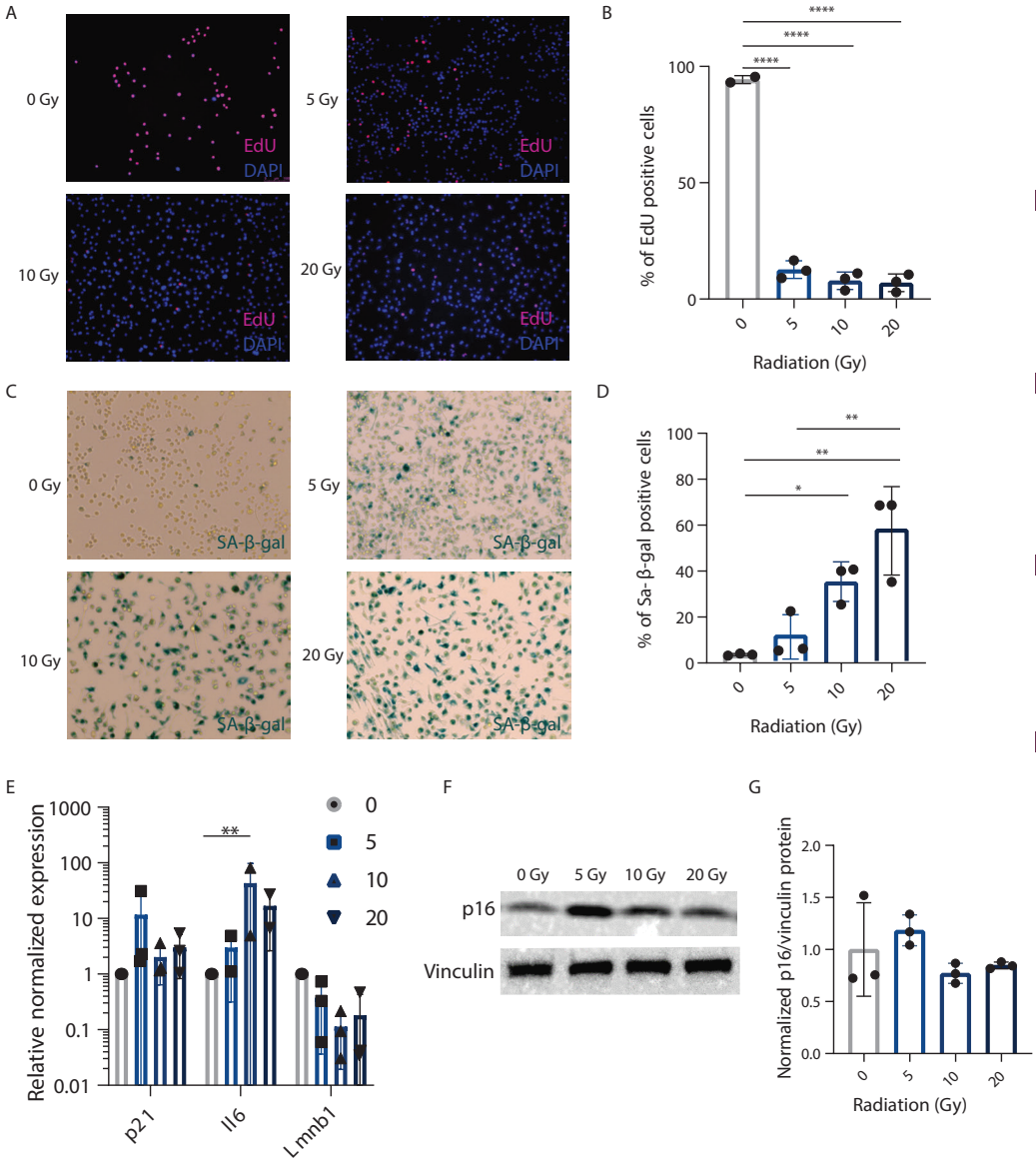

Figure 1: Characterization of radiation-induced senescence in microglia.

*A: Representative images of EdU staining in BV2 cells irradiated with 0, 5, 10 or 20 Gy. B: Quantification of EdU incorporation in BV2 cells irradiated with 0, 5, 10 or 20 Gy. ****p<0.0001. C: Representative images of SA-β-gal staining in BV2 cells irradiated with 0, 5, 10 or 20 Gy. D: Quantification of SA-β-gal staining in BV2 cells irradiated with 0, 5, 10 or 20 Gy. *p<0.05 **p<0.01. E: p21, Il6, and Lmnb1 expression measured by qPCR in BV2 cells irradiated with 0, 5, 10 or 20 Gy. **p<0.01. F: Representative image of the western blot for p16 of BV2 cells subjected to 0, 5, 10 or 20 Gy of ionizing radiation. G: Quantification of the western blot for p16 of BV2 cells subjected to 0, 5, 10 or 20 Gy of ionizing radiation.*

expression changes were determined by qPCR. Methotrexate has been shown to cause cognitive decline through microglial activation, oligodendrocyte lineage disruption, and astrocyte reactivity, but whether it also induces senescence is unresolved (Gibson et al., 2019). Methotrexate treatment resulted in minor changes in the expression of senescence genes in primary astrocytes (Figure 2D-E).

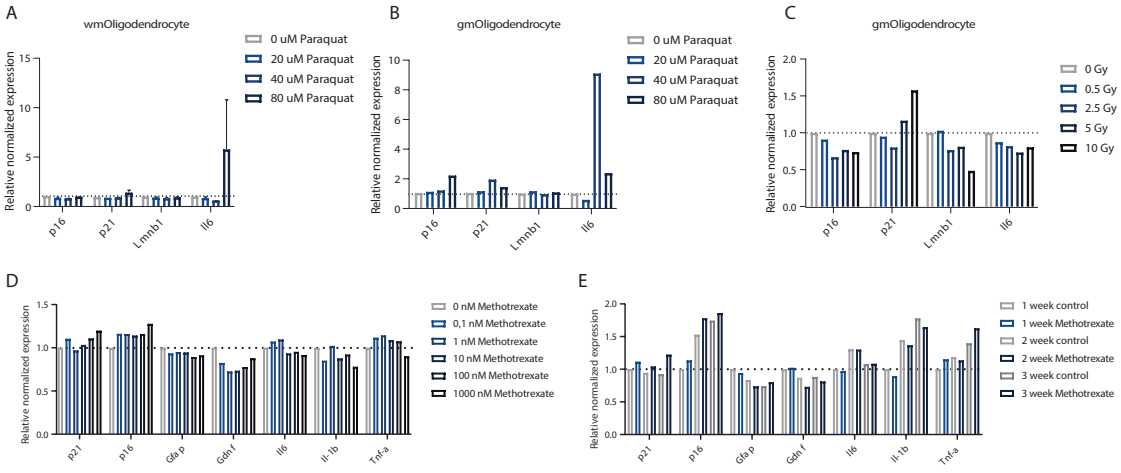

Figure 2: Characterization of stress-induced senescence in oligodendrocytes and astrocytes.

A: p21, p16, Lmnb1 , and Il6 expression measured by qPCR in white matter oligodendrocytes 10 days after treatment with 0, 20, 40 or 80 μM paraquat. B: p21, p16, Lmnb1, and Il6 expression measured by qPCR in grey matter oligodendrocytes 10 days after treatment with 0, 20, 40 or 80 μM paraquat. C: p21, p16, Lmnb1, and Il6 expression measured by qPCR in grey matter oligodendrocytes 10 days after 0, 0.5, 2.5, 5 or 20 Gy ionizing radiation. D: Normalized values of mRNA expression of senescence and astrocyte markers measured by RT-qPCR in primary rat astrocytes 7 days after 48h methotrexate treatment. E: Normalized values of mRNA expression of senescence and astrocyte markers measured by RT-qPCR in primary rat astrocytes after 1, 2 or 3 rounds of 48h 1μM methotrexate treatment.

Replication stress induces senescence-associated phenotypes in glial cells

To further explore the induction and maturation of senescence in glial cells, we used a model of replicative exhaustion. The expression levels of senescence genes were determined in primary rat microglia, oligodendrocytes, and astrocytes short term (3-5 days) and around three weeks (21-26 days) after plating the cells. Primary microglia were studied at 4 and 25 days in culture. An increase in mRNA expression of cell cycle inhibitors *p21* and *p16*, and SASP factor *Il6* was observed, but unexpectedly also an increase in *Lmnb1* expression, a gene which is typically downregulated in classical senescence (Figure S2A) (Freund et al., 2012). The expression of SASP factors *Il1b, Tnf-a* and *Tgf-b* seemed to be reduced, but further experiments are required to confirm this observation.

In oligodendrocytes from the white matter and grey matter of the brain, the expression of senescence genes was compared between cells that were cultured for 5 days or 21 days. The expression of cell cycle inhibitors *p16, p21,* SASP factor *Il6*, and oligodendrocyte differentiation marker *Mpb1* were increased and *Lmnb1* was decreased in oligodendrocytes after 21 days in culture (Figure S2B-C). In addition, a decrease in progenitor gene *Pdgfra* was observed in non-cortical oligodendrocytes after 21 days. In comparison to microglia and oligodendrocytes, astrocytes seemed less affected by replication stress. After 26 days of culture, more than half of the primary astrocytes were still replicating (Figure S2D-E). Overall, in glial cells senescence was observed, but additional experiments are required to better characterize the senescent signatures of glial cells and its functional ramifications.

The SASP of genotoxic stress-induced senescent cells does not alter on the phenotype of organotypic hippocampal slice cultures

To determine the indirect effect of genotoxic stress-induced senescence on the brain, we investigated the effect of the SASP in conditioned media of senescent cells on organotypic hippocampal slice cultures (OHSC). Mouse embryonic fibroblasts (MEFs) were made senescent by doxorubicin treatment which was confirmed by the expression of senescence-associated genes by qPCR (Figure 3A).

Expression of genes involved in senescence (*p21*), inflammation (*Tnf-a*), glial activation (*Hexb, Gfap*) and neuro-protection (*Bdnf*) were measured by qPCR after 1, 3 and 5 days of treatment with conditioned medium from senescent MEFs (Figure 3B-F). No significant differences were observed in gene expression levels. To study the effect of the treatment on the number and morphology of the cells, stainings for Iba1, a microglia marker, and NeuN, a neuronal marker, were performed (Figure 3G-H). Again, no differences in cell numbers were observed. This data suggests that short term exposure of OHSC to SASP did not change their gene expression or number of cells.

Genotoxic drugs exert variable effect on cognitive and physical functions *in vivo*

Methotrexate is a chemotherapeutic agent used to treat cancer in children, and as an immuno-suppressant drug in chronic inflammatory disorders (Genestier et al., 1998). In astrocytes *in vitro*, we detected a small increase in senescent markers, however induction of senescence *in vivo* by methotrexate has not yet been investigated. We used a treatment paradigm that resulted in cognitive decline in mice, where mice received 3 times a weekly dose of 100 mg methotrexate starting at an age of 3 weeks (Gibson et al., 2019). We compared the effects of methotrexate, a known inducer of cognitive deficits (Gibson et al., 2019), to doxorubicin, a known senescence inducer, to investigate the effects of genotoxic stress on physical and cognitive functioning *in vivo*. The topo isomerase II inhibitor doxorubicin has been previously reported to induce senescence in peripheral organs in p16 reporter mice (Demaria et al., 2017) and thereby promoting chemotherapy related side effects. Weight gain was not affected by methotrexate treatment (Figure S3A), however, as expected, mice treated with doxorubicin lost weight after treatment (Figure S3B).

In order to determine if methotrexate induced senescence in the periphery, we investigated the expression of senescence markers in the liver of methotrexate treated animals compared to their littermate controls. No differences in *p21* or *p16* expression were observed between both groups (Figure 4A-B), while the induction of senescence in the periphery of the doxorubicin treated mice was confirmed in the liver. The cell cycle inhibitor *p21* was upregulated in the liver of doxorubicin treated animals, confirming the presence of senescent cells in a peripheral organ (Figure 4C). *p16* expression was not increased in the liver of doxorubicin-treated mice, with the exception of one animal, which did not

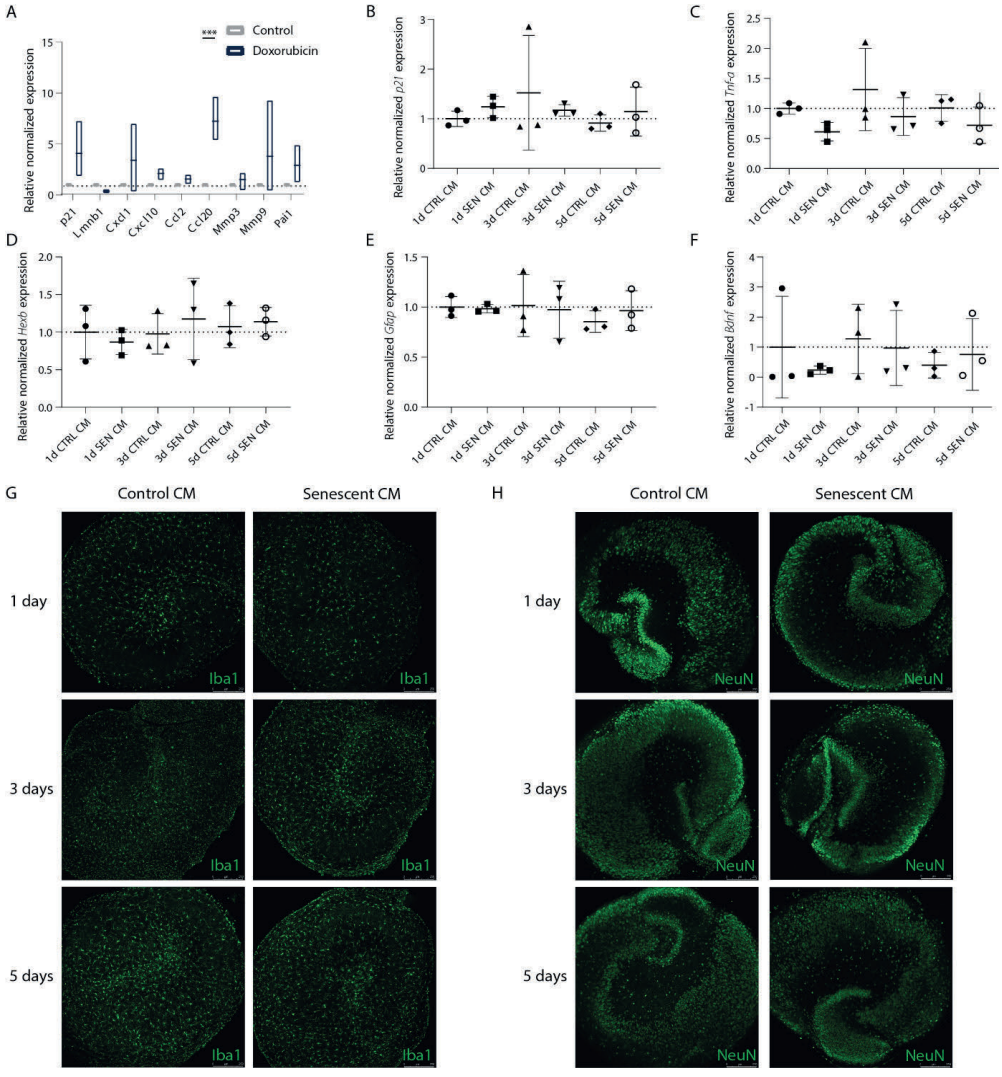

Figure 3: Effect of SASP on organotypic hippocampal slice cultures.

*A: Expression of senescence genes measured by qPCR in MEFs 8 days after doxorubicin induced senescence. ***p<0.001 B: p21 expression measured by qPCR in OHSCs treated for 1, 3 or 5 days with either conditioned medium from control or doxorubicin-treated MEFs. C: Tnf-a expression measured by qPCR in OHSCs treated for 1, 3 or 5 days with either conditioned medium from control or doxorubicin-treated MEFs. D: Hexb expression measured by qPCR in OHSCs treated for 1, 3 or 5 days with either conditioned medium from control or doxorubicin-treated MEFs. E: Gfap expression measured by qPCR in OHSCs treated for 1, 3 or 5 days with either conditioned medium from control or doxorubicin-treated MEFs. F: Bdnf expression measured by qPCR in OHSCs treated for 1, 3 or 5 days with either conditioned medium from control or doxorubicin-treated MEFs. G: Representative images of Iba1 staining in OHSCs treated for 1, 3 or 5 days with either conditioned medium from control or doxorubicin-treated MEFs. H: Representative images of NeuN staining in OHSCs treated for 1, 3 or 5 days with either conditioned medium from control or doxorubicin-treated MEFs.*

show an increase in *p21* compared to the control (Figure 4D).

Chemotherapy induces a temporal decrease in white blood cells, but less is known about the long-term effects of chemotherapy on blood cell type proportions. The cell numbers were analyzed based on the expression of blood cell type markers with flow cytometry. T-cells were identified as $CD3^{+}$ cells; B-cells as $B220^{+}$ cells; granulocytes as $CD3^{-}/B220^{-}/Gr\text{-}1^{+}$/side scatter $(SSC)^{High}$ cells; macrophages as $CD3^{-}/B220^{-}/Mac\text{-}1^{+}/SSC^{low}$ cells. No differences in the percentages of T-cells, B-cells, granulocytes or macrophages were observed in methotrexate treated animals (Figure 4E-H). While the number of animals was too low to detect any differences in T-cell and macrophage numbers, B-cell numbers were increased in doxorubicin treated mice compared to the vehicle treated controls and the number of granulocytes was decreased 6 months after treatment (Figure 4I-L). Together this data shows that doxorubicin has long-term effects on the immune cell composition.

Next, physical and cognitive functions of the mice were measured. Doxorubicin has been shown to reduce physical performance which was rescued by the removal of senescent cells (Demaria et al., 2017). Methotrexate-treated animals performed worse in a rotarod assay (Figure 4M), while grip strength was not altered by the treatment (Figure 4N), indicative of a reduction in endurance but not maximal strength of the muscles. One of the reported side-effects of methotrexate is altered behavior of mice in an open field test, namely less time spent in the middle of the arena (Gibson et al., 2019). The mice traveled the same distance in the open field arena during 10 minutes (Figure 4O), but methotrexate treated mice spent more time in the corners of the open field compared to controls, in agreement with the data of Gibson et al. (Figure 4P). Doxorubicin does not cross the blood-brain-barrier, but might have indirect effects on the CNS. The persistent alterations in blood cell type numbers suggests a long-lasting effect of the drug. To determine if CNS cells were affected by doxorubicin, we evaluated changes in neuroinflammation with the positron emission tomography (PET) tracer ^{11}C-PBR28. Binding of ^{11}C-PBR28 to benzodiazepine receptors (PBRs) is increased under neuroinflammatory conditions, due to the upregulation of the receptors on activated microglia (Imaizumi et al., 2007). PET scans were performed 2 to 22 weeks after treatment and the standard uptake value was measured. No difference in ^{11}C-PBR28 signal between doxorubicin treated mice and their

littermate controls was observed (Figure S3C). Next, we determined whether doxorubicin had an effect on mouse behavior using novel object recognition and open field tests. No differences were observed between the two groups in either the novel object recognition or the open field tests (Figure 4Q-S).

To determine the indirect effect of genotoxic stress induced senescence in the periphery on the brain, we studied gene expression in microglia isolated from the cortical and hippocampal regions of the CNS of doxorubicin treated animals compared to their littermate controls. RNA sequencing showed 693 differentially expressed genes in the cortex with LogFC >1 or <-1 and $p<0.05$ (Figure 5A) and 723 differentially expressed genes in the hippocampus with LogFC >1 or <-1 and $p<0.05$ (Figure 5B). Gene ontology analysis revealed an enrichment of genes involved in mTOR signaling and depletion of genes involved cell migration in cortical microglia of doxorubicin-treated mice (Figure 5C-D). Genes involved in the negative regulation of growth were enriched and involved in apoptosis signaling were depleted in hippocampal microglia of doxorubicin-treated mice (Figure E-F). Together with the data from the periphery, these data show that doxorubicin had effects on the immune cell numbers in the periphery and caused changes in gene expression of the resident immune cells of the brain.

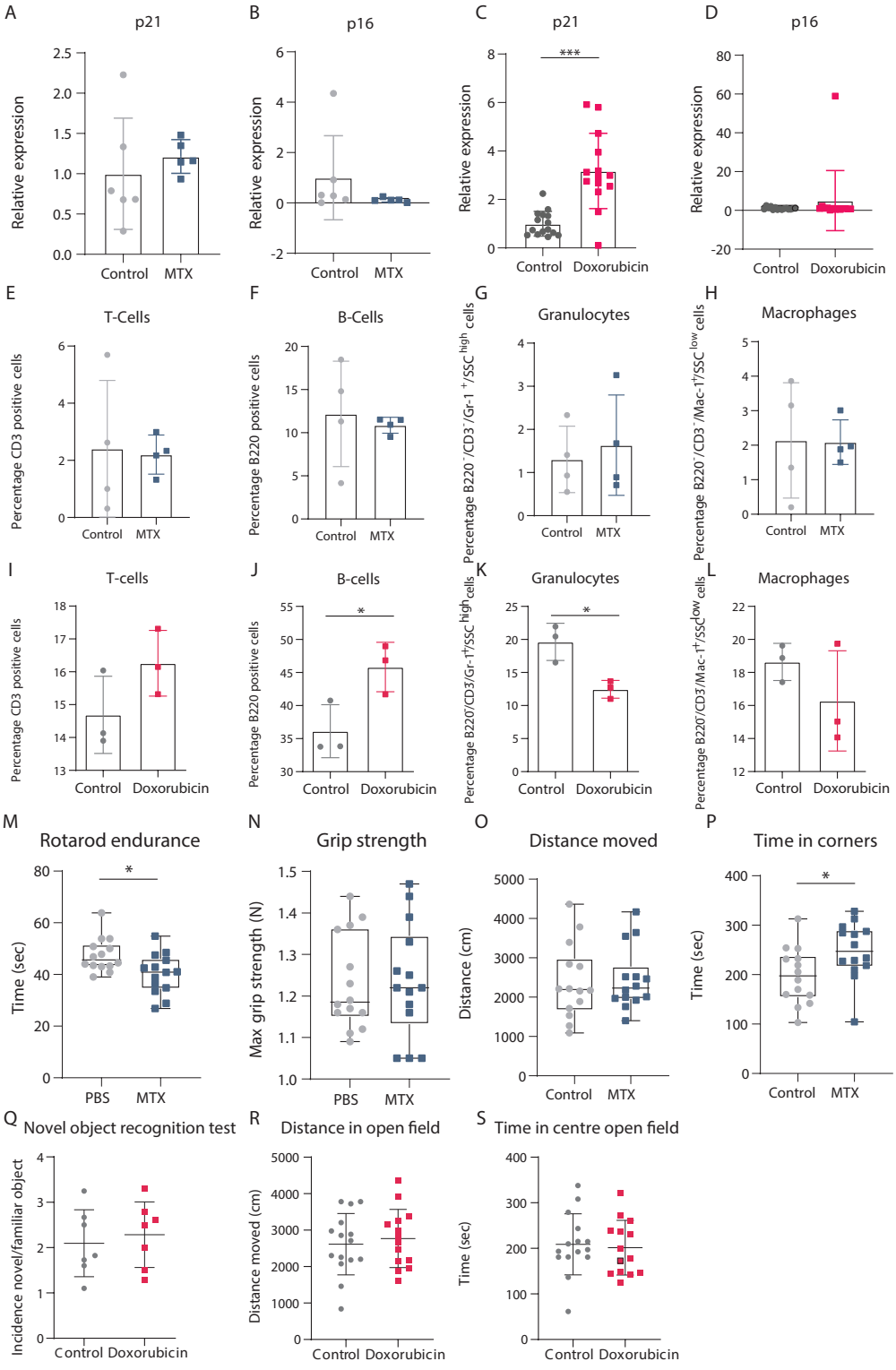
A
p21
Relative expression
Control
MTX
B
p16
Relative expression
Control
MTX
C
p21
***
Relative expression
Control
Doxorubicin
D
p16
Relative expression
Control
Doxorubicin
E
T-Cells
Percentage CD3 positive cells
Control
MTX
F
B-Cells
Percentage B220 positive cells
Control
MTX
G
Granulocytes
Percentage B220-/CD3-/Gr-1+/SSChigh cells
Control
MTX
H
Macrophages
Percentage B220-/CD3-/Mac-1+/SSClow cells
Control
MTX
I
T-cells
Percentage CD3 positive cells
Control
Doxorubicin
J
B-cells
*
Percentage B220 positive cells
Control
Doxorubicin
K
Granulocytes
*
Percentage B220-/CD3/Gr-1+/SSChigh cells
Control
Doxorubicin
L
Macrophages
Percentage B220-/CD3/Mac-1+/SSClow cells
Control
Doxorubicin
M
Rotarod endurance
*
Time (sec)
PBS
MTX
N
Grip strength
Max grip strength (N)
PBS
MTX
O
Distance moved
Distance (cm)
Control
MTX
P
Time in corners
*
Time (sec)
Control
MTX
Q
Novel object recognition test
Incidence novel/familiar object
Control
Doxorubicin
R
Distance in open field
Distance moved (cm)
Control
Doxorubicin
S
Time in centre open field
Time (sec)
Control
Doxorubicin

Figure 4: Methotrexate and doxorubicin exert variable effects on cognitive and physical functions *in vivo*.

*A: p21 expression measured by qPCR in liver tissue from mice treated with methotrexate compared to vehicle treated control mice. B: p16 expression measured by qPCR in liver tissue from mice treated with methotrexate compared to vehicle treated control mice. C: p21 expression measured by qPCR in liver tissue from mice treated with doxorubicin compared to vehicle treated control mice. ***p<0.001. D: p16 expression measured by qPCR in liver tissue from mice treated with doxorubicin compared to vehicle treated control mice. E: Percentage of CD3 positive cells isolated from blood of methotrexate treated mice and control mice. F: Percentage of B220 positive cells isolated from blood of methotrexate treated mice and control mice. G: Percentage of CD3/B220 negative, Gr-1 positive and side scatter high cells isolated from blood of methotrexate treated mice and control mice. H: Percentage of CD3/B220 negative, Mac-1 positive and side scatter low cells isolated from blood of methotrexate treated mice and control mice. I: Percentage of CD3 positive cells isolated from blood of doxorubicin treated mice and control mice. J: Percentage of B220 positive cells isolated from blood of doxorubicin treated mice and control mice. *p<0.05. K: Percentage of CD3/B220 negative, Gr-1 positive and side scatter high cells isolated from blood of doxorubicin treated mice and control mice. *p<0.05. L: Percentage of CD3/B220 negative, Mac-1 positive and side scatter low cells isolated from blood of doxorubicin treated mice and control mice. M: Riding time on the accelerating rotation rod of mice treated with methotrexate and control mice. *p<0.05. N: Maximal grip strength of mice treated with methotrexate and control mice. O: Distance moved in 10 min in the open field box by mice treated with methotrexate and control mice. P: Time spend in the corner of the open field box by mice treated with methotrexate and control mice. *p<0.05. Q: Incidence of nose point touching the novel over the familiar object in a novel object recognition test of mice treated with doxorubicin and control mice. R: Distance moved in 10 min in the open field box by mice treated with doxorubicin and control mice. S: Time spend in the center of the open field box by mice treated with doxorubicin and control mice. A-B: n=6 for controls and n=5 for the methotrexate treated group. C-D: n=14 per group. E-H: n=4 per group. I-L: n=3 per group. M-S: n=14 per group.*

Discussion

Taken together, this study showed that genotoxic stress can directly induce cellular senescence in glial cells and that genotoxic stress induced indirect changes in the brain. The question if these indirect effects are due to the senescent cells and if senescence can also be caused in the brain indirectly by genotoxic stress remain to be answered. To start to be able to answer this, we need to define what senescence is. If senescence is a process of irreversible growth arrest, then post-mitotic cells are already in this state. If we consider additional senescence-associated markers, such as the SASP and enhanced lysosomal activity, then also cells unable to proliferate can switch to a senescent state when they acquire these aberrant functions.

For glial cells, the markers that are used for senescent fibroblasts are the most appropriate identifiers of senescence so far. However, we need to take into account that activated glial cells gain a pro-inflammatory secretory phenotype that might be similar to the factors that are considered to be part of the SASP. Moreover, senescent cells over time express features similar to macrophages, such as phagocytosis, while macrophages over time express features of senescent cells, such as increased expression of p16 and increased lysosomal activity (Behmoaras and Gil, 2021). More research needs to be performed to understand the implications of these phenotypic changes. The effect of elimination of cells that accumulate senescence markers on the brain is a very important unresolved issue, especially after genotoxic insults, where more cells might have accumulated senescence-like markers. The extensive removal of cells in the CNS by senolytics might interfere with the structure and integrity of the brain.

The indirect effects of the SASP on the organotypic slice cultures were shown to be limited. However, little is known about the long-term effects of peripheral senescence on the brain. The SASP cannot only cause an inflammatory environment, but is also able to induce secondary senescence (Teo et al., 2019). These cells might not look like primary senescent cells and might contribute in a different fashion to disease development compared to the primary senescent cells. Cross talk between organs and especially between the periphery and the brain is important to understand in order to unravel the long-term effects of cancer treatments.

It has been shown that immediately after chemotherapy, and also after 12 months, cellular senescence markers are increased in breast cancer survivors (Sanoff et al., 2014). Not only direct effects on the CNS play an important role in the induction of chemo-brain, but also changes in the periphery can influence the neurocognition of cancer survivors. Even though doxorubicin does not pass the blood-brain-barrier (Colombo et al.), mice treated with doxorubicin display cognitive decline (Seigers et al., 2015), raising the possibility that peripheral cellular senescence is a key player in the induction of chemo-brain in breast cancer survivors. In our experiments, we could not reproduce the reported cognitive impairments in mice, suggesting that doxorubicin alone might not be enough to induce chemo brain, even though we did observe transcriptional changes in microglia.

Methotrexate treatment showed more direct effects on the brain both in our dataset as in the literature (Gibson et al., 2019). In contrast, the data on the doxorubicin-treated mice suggest a more indirect effect of the drug on the brain. The direct and indirect effects of doxorubicin on neurotoxicity have been discussed in a recent review article (Du et al., 2021). Even though doxorubicin has a limited capacity to penetrate the blood-brain-barrier, recent studies have shown multiple mechanisms by which doxorubicin might directly cause DNA-damage in neurons. On the other hand, it has also been demonstrated that doxorubicin induces damage in the periphery that might indirectly influence the brain via oxidative stress, inflammation, and nitrification stress. These stresses might be a result from the induction of senescence in the periphery. Therefore, a next study should investigate whether senolytic treatment, eliminating peripheral senescent cells, right after chemotherapy might ameliorate or even prevent the development of chemotherapy-induced cognitive impairment by decreasing the inflammation and other stressors induced by the SASP of senescent cells.

Figure 5: Doxorubicin induced transcriptional changes in microglia from cortex and hippocampus.

A: Volcano plot depicting differential expressed genes between microglia isolated from the cortex of control and doxorubicin treated mice. B: Volcano plot depicting the differential expressed genes between microglia isolated from the hippocampus of control and doxorubicin treated mice. C: GOs significantly enriched in the microglia from the cortex of doxorubicin treated mice. D: GOs significantly enriched in the microglia from the cortex of control mice compared to doxorubicin treated mice. E: GOs significantly enriched in the microglia from the hippocampus of doxorubicin treated mice. F: GOs significantly enriched in the microglia from the cortex of control mice compared to doxorubicin treated mice. n=5 per group.

Materials and methods

Mice

p16–3MR mice with a C57BL/6 background or wild type C57BL/6 were used for all experiments (Demaria et al., 2014). Mice were raised on a 12-hr light/dark cycle with food and water available *ad libitum* and were housed in groups. All experiments were performed in the Central Animal Facility (CDP) of the UMCG, with protocol (15339-03-002 and 15539-03-005) approved by the Animal Care and Use Committee (DEC) of the University of Groningen.

Doxorubicin

Mice were given an i.p. injection of 5 mg/kg on three consecutive days at the early adult age of 3-5 months

Methotrexate

Mice were given an i.p. injection of 100 mg/kg methotrexate (MTX) dissolved in PBS on P21, P28, and P35.

Open field

Anxiety was analyzed using an open field test. Animals were handled for 5 days consecutively for 2 min before the start of the experiment. The experimental chamber was 40x30x30 cm made of opaque Plexiglas. A camera was mounted above the chamber to record the animal's behavior. The mouse was allowed to explore the arena for 10 min. The camera footage was then analyzed using Ethovision analysis software. The animal's willingness to explore the center of the arena was assessed.

Novel Object Recognition Test

Cognition was analyzed using the novel object recognition task (NORT). Training of the NORT started 1 day after the open field test in the same chamber, but now with two identical objects: soda cans with paper rooftops. Each time the mouse was placed into the chamber, the mouse was placed in between the objects in the center of the chamber. During the training phase, the mouse was allowed to explore the identical objects for 15 min. During the testing phase 24 hours after the training phase, one of the familiar objects was replaced by a novel object, a glass vase. The mouse was returned to the experimental chamber and allowed to explore for 10 min. The objects used as novel and familiar were counterbalanced, as was the position of the novel object from

trial to trial, animal to animal. The camera footage was then analyzed using Ethovision analysis software, and any exploratory head gesture within 2 cm of the Lego object was measured. Only animals that explored the objects for a minimum of 30 s were included in the analysis. The Recognition Ratio was determined by taking the ratio of the amount of time spent investigating the novel object compared to the time spent investigating the familiar object.

Rotarod

For the rotarod test, mice were placed on the beam of a rotarod (IITC Rotarod) facing in the opposite orientation to rotation. The speed was gradually accelerated to a maximum of 30 rpm. The latency before falling was measured for 4 trials at 1 h intervals.

Maximal grip strength

A Grip Strength Meter was used to measure forelimb grip strength. As a mouse grasped the bar, the peak pull force in Newton (N) was recorded on a digital force transducer. The mouse was allowed to grasp the bar mounted on the force gauge. The gauge was reset to 0 N after stabilization and the mouse's tail was slowly pulled back by a researcher. Tension was recorded by the gauge at the time the mouse released its forepaws from the bar. We performed 3 sets of 5 consecutive measurements. From each set, the highest number was recorded.

Positron Emission Tomography (PET)

[11C]-PBR28 was synthesized following a previously described procedure (Parente et al., 2016). The mice were anesthetized with isoflurane (5% for induction, 1–2.5 % for maintenance) mixed with oxygen. Mice were i.v. injected in the penile vein, therefore only male mice were used, with 7-9 Mbq [11C]-PBR28 and were then placed in a small animal PET scanner (Focus 220, Siemens Healthcare, USA) with their head in the center of the field of view. A 30 min static scan was performed 30 min after the injection. A transmission scan was acquired using a ^{57}Co point source for attenuation and scatter correction. Analysis was performed in PMOD.

Blood cell sort

Blood was taken via heart puncture with a heparinized syringe and stored on ice. Red blood cells were lysed for 10 min lysis with erylysis buffer at room temperature. The samples were centrifuged at 450 rcf and supernatant was

discarded. Cell pellets were incubated with the antibodies CD3-APC, Gr-1-PECy7, Mac-1 PECy7, and B220-FITC all from Biolegend, and analyzed with flow cytometry.

Cell isolation from mouse brain tissue

Microglia were isolated from adult mouse brain using an enzymatic protocol at 4°C. The brains were isolated, hippocampus and cortex were separated, and dissociated by three rounds of GentleMACS (m_brain_01, m_brain_02, and m_brain_03) in enzyme mix of 15 mg/ml Protease (Sigma P5380), 1 mM L-cysteine hydrochloride (Sigma C7477), and 0.5 µg/µl DNase (Roche 10104159001) with 10 min incubation in the mix on ice in between GentleMACS programs. The homogenized brain samples were passed through a 100 µM cell strainer to obtain a single cell suspension. The cells were centrifuged at 300 rcf for 10 min at 4°C and the pellet was resuspended in 24% Percoll gradient buffer. 3 mL dPBS was pipetted onto the gradient buffer and myelin was removed by centrifuging at 950 rcf for 20 min at 4°C. The cell pellets were incubated with DAPI and Draq5. Cell pellets were incubated with the antibodies CD11b-BV421 (clone M1/70, Biolegend, San Diego, CA, USA), CD45-FITC (clone 30-F11, Biolegend, San Diego, CA, USA), CD49d-PE (clone R1-2, Miltenyi Biotec), PI and Draq5. Microglia were FACS sorted as PI^{neg} $Draq5^{pos}$ $CD11b^{high}$ $CD45^{int}$ $CD49d^{neg}$ events. Bulk samples were sorted from individual mice (n=5 for all groups).

Real-Time PCR

Total RNA was prepared using the AllPrep DNA/RNA Micro Kit (Qiagen, 80284). RNA was reverse transcribed into cDNA using a kit (Applied Biosystems). Quantitative RT-PCR (qRT- PCR) reactions were performed as described (Demaria et al., 2010) using the Universal Probe Library system (Roche). Primers used are listed in the tables below.

Gene #probe	Forward	Reverse
mCxcl1 #83	GACTCCAGCCACACTCCAAC	TGACAGCGCAGCTCATTG
mMmp9 #83	AGACGACATAGACGGCATCC	TCGGCTGTGGTTCAGTTGT
mMmp3 #89	TTTTGGCCATCTCTTCCATC	CTCCTCGTGCCCTCGTATAG
mp16 #91	AATCTCCGCGAGGAAAGC	GTCTGCAGCGGACTCCAT
mp21 #16	AACATCTCAGGGCCGAAA	TGCGCTTGGAGTGATAGAAA
mLmnb1 #15	GGGAAGTTTATTCGCTTGAAGA	ATCTCCCAGCCTCCCATT
mCxcl10 #3	GCTGCCGTCATTTTCTGC	TCTCACTGGCCCGTCATC
mCcl2 #62	CATCCACGTGTTGGCTCA	GATCATCTTGCTGGTGAATGAGT
mCcl20 #73	AACTGGGTGAAAAGGGCTGT	GTCCAATTCCATCCCAAAAA
mPai-1 #5	TTCCTCTCTTTTCATTATGCACTG	CATTTGGGGCCCTATGGTA
mGdnf #70	TCCAACTGGGGGTCTACG	GACATCCCATAACTTCATCTTAGAGTC
mIl6 #78	TCTAATTCATATCTTCAACCAAGAGG	TGGTCCTTAGCCACTCCTTC
mBdnf-1 #80	GCATCTGTTGGGGAGACAAG	TCACCTGGTGGAACATTGTG
mHprt1 #62	ATCACATTGTGGCCCTCTG	GTCATGGGAATGGATCTATCACT
mHmbs #91	AGAAAAGTGCCGTGGGAAC	TGTTGAGGTTTCCCCGAAT
mHexb #41	CCATTGTTTGGCAAGAAGTTT	TTCCACACTTCGACTACTGTGC
mGfap #64	ACAGACTTTCTCCAACCTCCAG	CCTTCTGACACGGATTTGGT
mTnfa #25	CTGTAGCCCACGTCGTAGC	TTGAGATCCATGCCGTTG
mIl1b #38	AGTTGACGGACCCCAAAAG	AGCTGGATGCTCTCATCAGG

Table 2: Mouse primers

Gene #probe	Forward	Reverse
rp21 #16	GACATCTCAGGGCCGAAA	GGCGCTTGGAGTGATAGAAA
rp16 #42	GGGCTTCCTAGACACTCTGGT	GTGATGTCCCCGCTCTAGG
rLmnb1 #55	GAGGATGTGAAGGTTGTGTTGA	TGAAGACTGTGCTTCTCTGAGC
rIl6 #106	CCTGGAGTTTGTGAAGAACAACT	GGAAGTTGGGGTAGGAAGGA
rHprt1 #22	GGTCCATTCCTATGACTGTAGATTTT	AACAATCAAGACGTTCTTTCCAG
rHmbs #49	AGGATGGGCAACTGTACCTG	CCTCTGGACCATCTTCTTGC
rp53 #69	GCTCCCCTGAAGACTGGATAA	CTGTGGTGGGCAGAATATCAT
rTnfa #15	TCTGTGCCTCAGCCTCTTCT	GGCCATGGAACTGATGAGA
rIl-1b #42	ACAGACCCCAAAAGATTAAGGA	CGAGATGCTGCTGTGAGATT
rTgf-b #56	TCAGACATTCGGGAAGCAGT	ACGCCAGGAATTGTTGCTAT
rMbp1 #13	TACCCTGGCTAAAGCAGAGC	GGGAGCCGTAGTGGGTAGTT
rOlig1 #4	GGTGGACAAACCCAGCTC	AGCTGCCTTGCTGTGGTTA
rOlig2 #21	CAGAGACCCGAGCCAACA	TCCTTTTTCAACCTTCCGAAT
rPdgfra #9	CCCTGGAGAGGTGAGAAACA	TTGATGGACGGGAGTTTGAT

Table 3: Rat primers

Bulk RNAseq library construction and sequencing

RNA was isolated from cell pellets with the AllPrep DNA/RNA Micro Kit (Qiagen, 80284). RNA concentrations were measured on a Qubit using a HS RNA kit. 2,5 ng of the samples was used for library preparation with the Lexogen QuantSeq 3' mRNA-Seq Library Prep Kit (FWD) from Illumina. All libraries were pooled equimolarly and sequenced on a NextSeq 500 at the sequencing facility in the UMCG.

Bulk RNAseq data analysis

Data preprocessing was performed with the Lexogen Quantseq 2.3.1 FWD UMI pipeline on the BlueBee Genomics Platform (1.10.18). Count files were loaded into R and DAFS filtering was performed to remove lowly expressed genes (George and Chang, 2014). A negative binomial generalized log-linear model was used to model gene expression levels, as implemented in edgeR, differentially expressed genes were determined using a likelihood ratio test (Robinson, McCarthy and Smyth, 2010). Thresholds were set at abs(logFC) > 1 and $p < 0.05$. Volcano plots were made with the CRAN packages 'ggplot2' and 'ggrepel'. Gene ontology analysis was performed on significantly differentially expressed genes ($p < 0.05$ and logFC > 0.1) using Metascape.

Primary cell cultures

Primary rat microglia, astrocytes and OPC cultures were prepared as previously described (Lentferink et al., 2018). Microglia were maintained at 37°C in a 5 % CO_2 atmosphere in microglia medium containing DMEM 41965-062, 100 U penicillin and streptomycin, 4mM L-glutamine, 5 ml pyruvate and 10% FCS. Astrocytes were maintained at 37°C in a 5 % CO2 in O2A medium containing DMEM 41965-062, 100 U penicillin and streptomycin, 4mM L-glutamine, and 10% FCS. OPCs were synchronized to the bipolar early OPC stage by addition of 10 ng/ml platelet-derived growth factor-AA (PDGF-AA; Peprotech, cat. no. 100–13A) and 10 ng/ml human fibroblast growth factor-2 (FGF-2; Peprotech, cat. no. 100-18B) 1 hour after plating. After 2 days OPCs were allowed to differentiate in Sato medium supplemented with 0.5% fetal bovine serum (FBS). For inducing ionizing radiation-induced senescence, cells were exposed to 0.5, 2.5, 5, or 10 Gy from a Cesium-137 source according to the instruction manual (IBL 637 Cesium-137γ-ray machine, UMCG), and analyzed 10 days later. Paraquat (36541) treatment of 20, 40 or 80 uM was added 1 day after

plating and effects were measured 10 days later.

Primary mouse astrocytes were prepared after microglia shake off described previously by Schaafsma and colleagues (Schaafsma et al., 2015). Astrocytes were maintained at 37°C in a 5 % CO2 in Dulbecco's Modified Eagle Medium (DMEM) high glucose, GlutaMAX (10569-010, Gibco) supplemented with 10 % (v/v) fetal bovine serum (FBS) (10270106, Gibco) and 100 units/ml penicillin and 100 µg/ml streptomycin. Astrocytes were subjected to 48 hours of 10 uM or other concentrations stated in the figure of methotrexate (J66364.MD) and analyzed 7 days after treatment.

Cell culture

BV2, murine microglia cells, and BJ cells were maintained at 37°C in a 5 % CO2 and 5% O2 atmosphere. Cells were cultured in Dulbecco's Modified Eagle Medium (DMEM) high glucose, GlutaMAX (10569-010, Gibco) supplemented with 10 % (v/v) fetal bovine serum (FBS) (10270106, Gibco) and 100 units/ml penicillin and 100 µg/ml streptomycin. For inducing ionizing radiation-induced senescence, cells were grown to 70-80% confluency, exposed to 5, 10, or 20 Gy from a Cesium-137 source according to the instruction manual (IBL 637 Cesium-137γ-ray machine, UMCG), and analyzed 7 days later. Control cells were mock irradiated. The medium of treated cells was replaced every 48 hours.

Edu incorporation assay

EdU incorporation assay was performed according to the protocol of Alejandra Hernandez-Segura and colleagues (Hernandez-Segura et al., 2018). In short, the cells were washed twice with 1x PBS and fixed with 4% formaldehyde, in PBS for 10 min at RT. Then, the cells were incubated for 5 min in 100 mM Tris pH 7.6, and permeabilized in 0.1 % Triton X-100 in PBS for 10 min. After washing 3x with 1x PBS, the cells were incubated for 30 min with EdU staining solution in the dark. Afterwards, cells were washed three times with 1x PBS, and mounted with mounting media including 2 µg/ml DAPI onto coverslips. The samples were imaged with a fluorescence microscope (DMI4000 B, Leica), and quantified with Fiji. For quantification at least 100 cells were counted of DAPI and EdU, and the percentage of cells that incorporated EdU was quantified by using the following formula: EdU positive cells (%) = (EdU positive cell count (Cy3)/total cell count (DAPI)) * 100.

SA-β-gal staining

SA-β-gal staining was performed according to Alejandra Hernandez-Segura, et al. (Hernandez-Segura et al., 2018). In short, the cells were washed twice with 1x PBS and fixed with 2% formaldehyde + 0.2% glutaraldehyde in PBS for 5 min at RT. Then washed twice with 1x PBS before incubation with SA-β-gal staining solution at 37 °C for 5-6 hours. Afterwards, the cells were washed with 1x PBS, and samples were taken with EVOS xl core (v. 1.0.198, life sciences). For quantification at least 100 cells were counted and the percentage of SA-β-gal positive cells was evaluated.

Western blot

Protein samples were prepared by washing the cells twice with cold PBS. Whereafter they were collected in PBS and centrifuged at 4 degrees at max speed for 30 seconds. Supernatant was removed after which the cell pellet was snap frozen. RIPA buffer (ab156034) + protease and phosphatase inhibitor (A32959) was added to the pellet (35-50ul) whereafter it was sonicated for 7 cycles 30 sec on 30 sec off. Concentration was measured using a Pierce BCA assay kit from Thermo Fisher Scientific (10741395). 40 ng of protein plus laemmli buffer was loaded in 12 µl in a 4–20% Mini-PROTEAN® TGX™ Precast Gel (4561096). The gel ran at 80 volts and switched to 100 volts after 15 min. Semi dry transfer with 0.2 µm PVDF (1704273) Trans-Blot Turbo Transfer System was performed according to the manufacturers protocol. The membrane was cut at 70 kb. The top half was incubated with 5% milk in TBS-T for an hour and overnight with 1:2000 monoclonal Anti-Vinculin antibody produced in mouse, clone hVIN-1, ascites fluid (V9131). The bottom half was incubated with 5% BSA TBS-T for an hour and overnight with 1:1000 anti-CDKN2A/p16INK4a antibody [EPR20418] (ab211542). After washing in TBS-T, membranes were incubated for an hour with 1:1000 goat-anti-mouse peroxidase conjugated immunoglobulins DAKO P0447 or goat-anti-rabbit peroxidase conjugated immunoglobulins DAKO P0448. The signals were visualized by chemiluminescence (ECL, Amersham Life Technologies) using ImageQuant LAS 4000 mini imaging machine (GE Healthcare Bioscience AB). Fiji was used for the quantification of the bands.

Conditioned medium

MEFs P7 were maintained at 37°C in a 5 % CO_2 and 5% O_2 atmosphere. Cells were cultured in Dulbecco's Modified Eagle Medium (DMEM) high glucose, GlutaMAX (10569-010, Gibco) supplemented with 10 % (v/v) fetal bovine serum (FBS) (10270106, Gibco) and 100 units/ml penicillin and 100 µg/ml streptomycin. For induction of senescence, cells were treated with 250 nM Doxo for 24 hours. After 7 days, the medium was changed to DMEM+0.2% FBS. After 24 hours, the medium was collected and adjusted to cell number. The conditioned medium was concentrated using Amicon centrifugal spin filter units (MWCO 3.5 kDa). The medium was centrifugated for 40 minutes at 4 degrees 3900g in the spin filter units.

Preparation and staining of OHSC

Organotypic hippocampal slice cultures were prepared as described previously (Zhang et al., 2021) from C57BL/6 mice according to protocol (15360-02-001) approved by the Animal Care and Use Committee (DEC) of the University of Groningen. The slice cultures were kept at 35°C in a humidified atmosphere (5% CO2). On the first day after preparation, OHSCs were treated with conditioned medium for 48h. OHSCs were kept for up to 5 days and the culture medium with conditioned medium was refreshed every 2 days. After fixation with 4% PFA overnight at 4°C, OHSCs were processed for immunofluorescence staining. Slices were blocked for 1 hr with 5% normal donkey serum and thereafter incubated with a primary antibody against Iba1 (1:1,000; Wako, 019-19741) or NeuN (1:1000; chemicon, Mab377) overnight at 4°C. On the next day, after washing thrice with 1× PBS, Alexa Fluor 488 donkey anti-rabbit (1:333; Invitrogen, A21206) or Alexa Fluor 488 donkey anti-mouse (1:333; Invitrogen, A21202) secondary antibody was added. After 1 hr of secondary antibody incubation, sections were washed and incubated in Hoechst solution (1 µg/ml, Sigma-Aldrich, 14530) for 5 min. After washing, the slides were mounted with Mowiol mounting medium on glass slides. Image acquisition was performed using a Leica SP8 confocal microscope system (TCS SP8, Leica Microsystems).

Statistics

GraphPad Prism 8 was used for the statistical analysis of all experiments except for the RNA sequencing. Ordinary one-way ANOVA with multiple comparisons was performed for grouped data and unpaired t-test to compare chemotherapy treated mice with their littermate controls.

References

Behmoaras, J., and Gil, J. (2021). Similarities and interplay between senescent cells and macrophages. J. Cell Biol. 220.

Chinta, S.J., Woods, G., Demaria, M., Rane, A., Zou, Y., McQuade, A., Rajagopalan, S., Limbad, C., Madden, D.T., Campisi, J., et al. (2018). Cellular Senescence Is Induced by the Environmental Neurotoxin Paraquat and Contributes to Neuropathology Linked to Parkinson's Disease. Cell Rep. 22, 930–940.

Colombo, T., Zucchetti, M., and D 'incalci, M. Cyclosporin A Markedly Changes the Distribution of Doxorubicin in Mice and Rats1. 269.

Demaria, M., Ohtani, N., Youssef, S.A., Rodier, F., Toussaint, W., Mitchell, J.R., Laberge, R.-M., Vijg, J., Van Steeg, H., Dollé, M.E.T., et al. (2014). An Essential Role for Senescent Cells in Optimal Wound Healing through Secretion of PDGF-AA. Dev. Cell 31, 722–733.

Demaria, M., O'Leary, M.N., Chang, J., Shao, L., Liu, S., Alimirah, F., Koenig, K., Le, C., Mitin, N., Deal, A.M., et al. (2017). Cellular Senescence Promotes Adverse Effects of Chemotherapy and Cancer Relapse. Cancer Discov. 7, 165–176.

Du, J., Zhang, A., Li, J., Liu, X., Wu, S., Wang, B., Wang, Y., and Jia, H. (2021). Doxorubicin-Induced Cognitive Impairment: The Mechanistic Insights. Front. Oncol. 11.

Freund, A., Laberge, R.-M., Demaria, M., and Campisi, J. (2012). Lamin B1 loss is a senescence-associated biomarker. Mol. Biol. Cell 23, 2066.

Genestier, L., Paillot, R., Fournel, S., Ferraro, C., Miossec, P., and Revillard, J.P. (1998). Immunosuppressive properties of methotrexate: apoptosis and clonal deletion of activated peripheral T cells. J. Clin. Invest. 102, 322.

Gibson, E.M., Nagaraja, S., Ocampo, A., Tam, L.T., Wood, L.S., Pallegar, P.N., Greene, J.J., Geraghty, A.C., Goldstein, A.K., Ni, L., et al. (2019). Methotrexate Chemotherapy Induces Persistent Tri-glial Dysregulation that Underlies Chemotherapy-Related Cognitive Impairment. Cell 176, 43-55.e13.

Han, R., Yang, Y., Dietrich, J., Luebke, A., Mayer-Pröschel, M., and Noble, M. (2008). Systemic 5-fluorouracil treatment causes a syndrome of delayed myelin destruction in the central nervous system. J. Biol. 7.

Hernandez-Segura, A., Brandenburg, S., and Demaria, M. (2018). Induction and validation of cellular senescence in primary human cells. J. Vis. Exp. 2018, 57782.

Imaizumi, M., Kim, H., Zoghbi, S., Briard, E., Hong, J., Musachio, J., Ruetzler, C., Chuang, D., Pike, V., Innis, R., et al. (2007). PET imaging with [11C]PBR28 can localize and quantify upregulated peripheral benzodiazepine receptors associated with cerebral ischemia in rat. Neurosci. Lett. 411, 200–205.

Jun, J. Il, and Lau, L.F. (2010). The matricellular protein CCN1 induces fibroblast senescence and restricts fibrosis in cutaneous wound healing. Nat. Cell Biol. 12, 676–685.

Kovalchuk, A., and Kolb, B. (2017). Chemo brain: From discerning mechanisms to lifting the brain fog—An aging connection. Cell Cycle 16, 1345.

Krizhanovsky, V., Yon, M., Dickins, R.A., Hearn, S., Simon, J., Miething, C., Yee, H., Zender, L., and Lowe, S.W. (2008). Senescence of activated stellate cells limits liver fibrosis. Cell 134, 657–667.

Lentferink, D.H., Jongsma, J.M., Werkman, I., and Baron, W. (2018). Grey matter OPCs are less mature and less sensitive to IFNγ than white matter OPCs: consequences for remyelination. Sci. Rep. 8.

Muñoz-Espín, D., Cañamero, M., Maraver, A., Gómez-López, G., Contreras, J., Murillo-Cuesta, S., Rodríguez-Baeza, A., Varela-Nieto, I., Ruberte, J., Collado, M., et al. (2013). Programmed cell senescence during mammalian embryonic development. Cell 155, 1104.

Parente, A., Feltes, P.K., Vállez García, D., Sijbesma, J.W., Moriguchi Jeckel, C.M., Dierckx, R.A., de Vries, E.F., and Doorduin, J. (2016). Pharmacokinetic Analysis of 11C-PBR28 in the Rat Model of Herpes Encephalitis: Comparison with (R)-11C-PK11195. J. Nucl. Med. 57, 785–791.

Sanoff, H.K., Deal, A.M., Krishnamurthy, J., Torrice, C., Dillon, P., Sorrentino, J., Ibrahim, J.G., Jolly, T.A., Williams, G., Carey, L.A., et al. (2014). Effect of Cytotoxic Chemotherapy on Markers of Molecular Age in Patients With Breast Cancer. JNCI J. Natl. Cancer Inst. 106, dju057.

Schaafsma, W., Zhang, X., van Zomeren, K.C., Jacobs, S., Georgieva, P.B., Wolf, S.A., Kettenmann, H., Janova, H., Saiepour, N., Hanisch, U.K., et al. (2015). Long-lasting pro-inflammatory suppression of microglia by LPS-preconditioning is mediated by RelB-dependent epigenetic silencing. Brain. Behav. Immun. 48, 205–221.

Seigers, R., Loos, M., Van Tellingen, O., Boogerd, W., Smit, A.B., and Schagen, S.B. (2015). Cognitive impact of cytotoxic agents in mice. Psychopharmacology (Berl). 232, 17–37.

Serrano, M., Lin, A.W., McCurrach, M.E., Beach, D., and Lowe, S.W. (1997). Oncogenic ras provokes premature cell senescence associated with accumulation of p53 and p16INK4a. Cell 88, 593–602.

Siegel, R.L., Miller, K.D., and Jemal, A. (2018). Cancer statistics, 2018. CA. Cancer J. Clin. 68, 7–30.

Tao, J.J., Visvanathan, K., and Wolff, A.C. (2015). Long term side effects of adjuvant chemotherapy in patients with early breast cancer. The Breast 24, S149–S153.

Teo, Y.V., Rattanavirotkul, N., Olova, N., Salzano, A., Quintanilla, A., Tarrats, N., Kiourtis, C., Müller, M., Green, A.R., Adams, P.D., et al. (2019). Notch Signaling Mediates Secondary Senescence. Cell Rep. 27, 997-1007.e5.

Walczak, P., and Janowski, M. (2019). Chemobrain as a Product of Growing Success in Chemotherapy - Focus on Glia as both a Victim and a Cure. Neuropsychiatry (London). 9.

Watanabe, S., Kawamoto, S., Ohtani, N., and Hara, E. (2017). Impact of senescence-associated secretory phenotype and its potential as a therapeutic target for senescence-associated diseases. Cancer Sci. 108, 563–569.

Zhang, X., Heng, Y., Kooistra, S.M., Weering, H.R.J. van, Brummer, M.L., Gerrits, E., Wesseling, E.M., Brouwer, N., Nijboer, T.W., Dubbelaar, M.L., et al. (2021). Intrinsic DNA damage repair deficiency results in progressive microglia loss and replacement. Glia 69, 729.

Supplemental figures

A

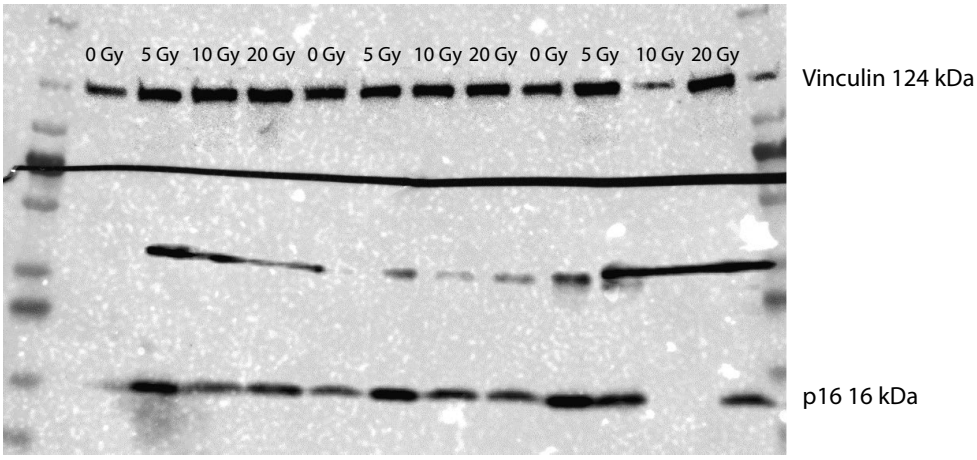

Supplemental figure 1: Western blot for p16 of irradiated BV2 cells.

A: Image of the total western blot of the three biological triplicates of BV2 cells subjected to 0, 5, 10 or 20 Gy of ionizing radiation.

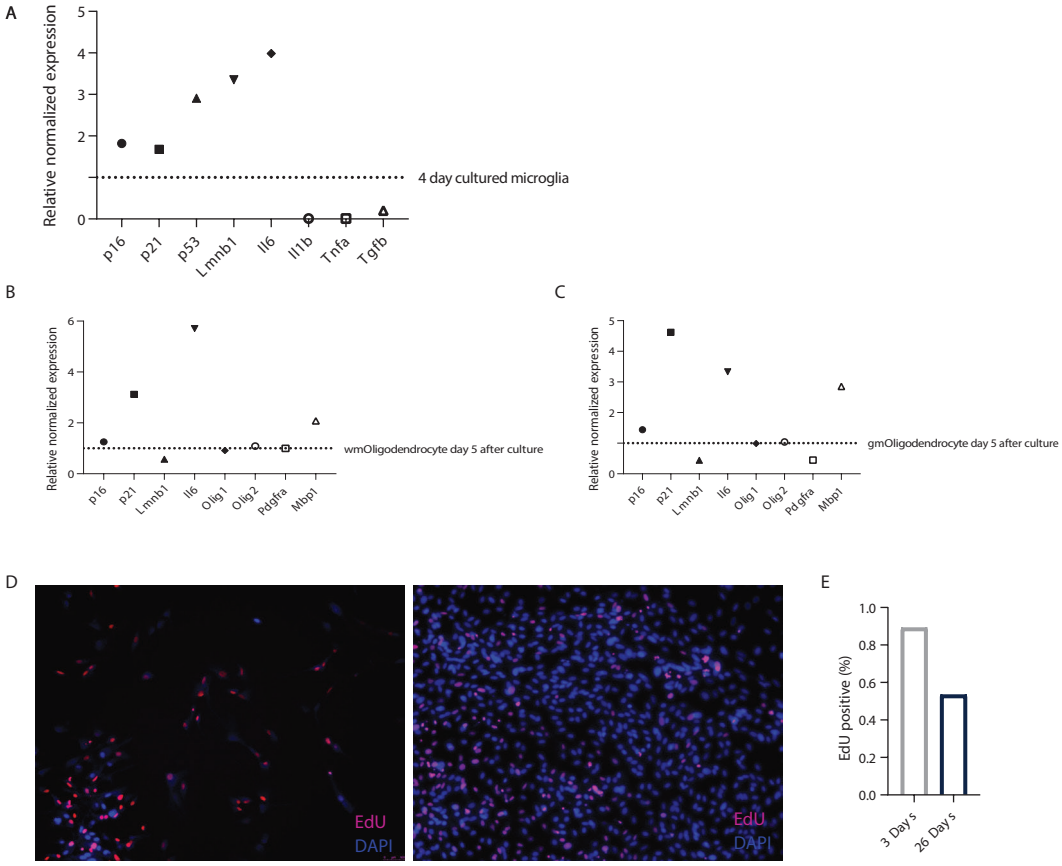

Supplemental figure 2: Culture stress induced senescence in glial cells.

A: Expression of senescence genes measured with qPCR in primary rat microglia of 25 days compared to 4 days in culture. B: Expression of senescence and oligodendrocyte genes measured with qPCR in primary rat white matter oligodendrocytes of 21 days compared to 5 days in culture. C: Expression of senescence and oligodendrocyte genes measured with qPCR in primary rat grey matter oligodendrocytes of 21 days compared to 5 days in culture. D: Representative images of EdU staining in primary rat astrocytes 3 and 26 days in culture. E: Quantification of Edu incorporation in primary rat astrocytes 3 and 26 days in culture.

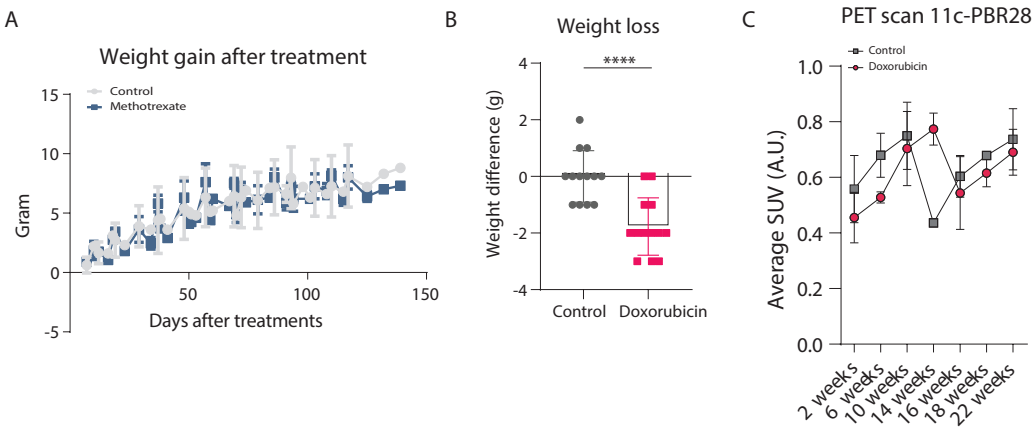

Supplemental figure 3: Doxorubicin induces weight loss in contrast to methotrexate, but no increased neuroinflammation.

*A: Weight gain over time of mice treated with methotrexate and control mice. B: Difference in weight of mice before and 6 weeks after doxorubicin treatment. ****p<0.0001. C: Average uptake of 11c-PBR28 in the brains of mice treated with doxorubicin and their controls over a period of 22 weeks. SUV= standard uptake value. A: n=6 for controls and n=5 for the methotrexate treated group. B: n=14 per group. C= n=3 per group.*

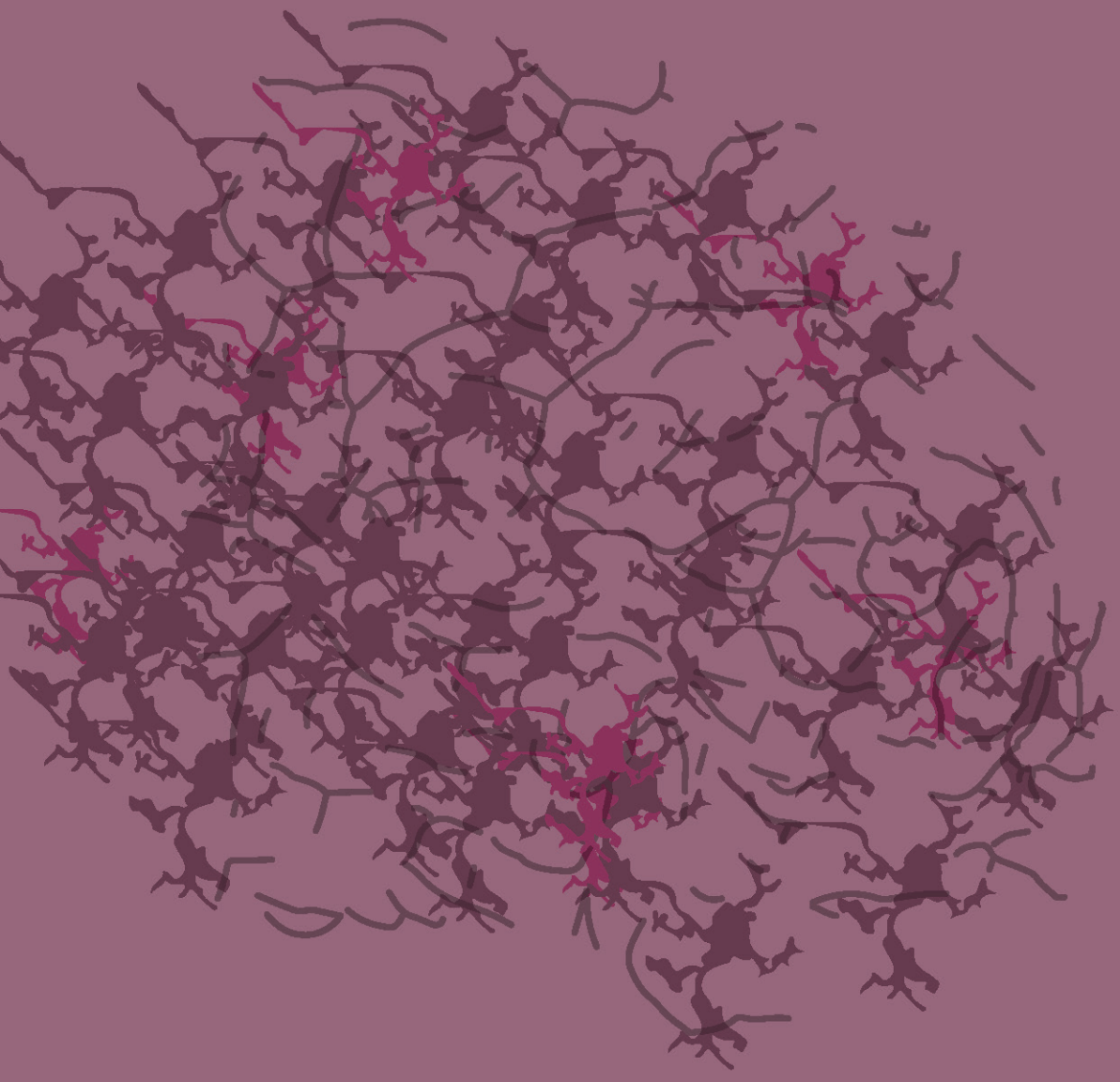

Chapter 5

Summary and general discussion

Summary

With the increasing evidence of the beneficial effects of the elimination of senescent cells during ageing, and the growing number of clinical trials investigating the effect of senolytics in the human body, it is important to understand the impact these drugs might have on the CNS. To understand this, we need to expand our knowledge on the cell types in the CNS that become senescent and if this process is beneficial or detrimental for the ageing brain. In this thesis, we investigate the natural and accelerated ageing phenotype of CNS cells.

In chapter 1, I describe the current knowledge on how cellular senescence develops in the CNS. First, I give a general overview of what the most common senescence-associated phenotypes are. Next, I describe the cellular composition of the brain, the role of glial cells and age-related changes. Last, I portray the evidence of cellular senescence in neurodegeneration and brain ageing.

In chapter 2, we study the effect of modulating lysosomal activity in senescent human fibroblasts. We show that three lysosomal modulating agents affect activity of the senescence-associated β-galactosidase, but not lead to changes in growth arrest or SASP. In addition, we show that pre-treatment of fibroblasts with one of the agents reduces senescence induction by the CDK4/6 inhibitor palbociclib, which action is related to lysosomal trapping.

In chapter 3, we use the p16-3MR mouse model to identify p16 expressing cells in the aged brain. $p16^{High}$ cells were sorted from brains of young and old mice and characterized using bulk and single cell sequencing. We show an increased number of $p16^{High}$ cells in the brain of old mice compared to the brain of young mice. Using bulk sequencing, we show that the differentially expressed genes between the $p16^{High}$ and $p16^{low}$ cells are mostly related to phagocytosis and inflammation. With cluster analysis of the single cell data, we show an enrichment of microglia in the $p16^{High}$ population. We confirm that microglia in wild-type mice and human brain have high *p16/CDKN2A* expression. With additional clustering within the microglia population of the single cell data, we identify two novel distinct sub-populations enriched in the $p16^{High}$ microglia. These previously unidentified microglia clusters change in abundance over time. Cluster 1 is stably present, but decreases with old age

and cluster 2 increases during the course of ageing.

In chapter 4, we investigate the effects of genotoxic stress-induced senescence on glial cells. We find that genotoxic stress induced the expression of senescence-associated markers in cultured glial cells. We measure indirect effects of SASP on brain cells with the use of organotypic hippocampal slice cultures. We find no changes in gene expression or cell numbers in the slice cultures treated with conditioned medium from senescent fibroblasts compared to slice cultures exposed to conditioned medium from proliferating fibroblasts. We measure the effects of two chemotherapeutics, methotrexate and doxorubicin, *in vivo* to investigate direct and indirect effects on the brain. Methotrexate reduces muscle endurance of mice and increases altered behavior in an open field test, but we observe no changes in senescence markers. In contrast, doxorubicin increases *p21* expression and influences the white blood cell composition, but we find no changes in cognitive function. Microglia isolated from doxorubicin treated mice do show differentially expressed genes compared to their littermate control, which is related to mTOR signaling and negative regulation of growth.

General discussion

Markers for cellular senescence

Cellular senescence was first reported as a cell state of irreversible growth arrest (Hayflick and Moorhead, 1961). The identification of senescence-associated phenotypes has increased over the years, but so far, no marker to identify senescence is specific for senescence and sufficient to detect this particular cell faith. This is partly due to the heterogeneity of senescent cells (Hernandez-Segura et al., 2017). On the other hand, extrinsic factors can change senescence phenotypes such as lysosomal modulation changed β-galactosidase activity in chapter 2. In this chapter we also found that one of the lysosomal genes, *LAPTM4A*, was highly expressed in senescent cells and that this expression was not changed by lysosomal modulation. This shows potential for this gene as a senescence marker, however the expression needs to be confirmed in other cell types and with other types of senescence induction.

Senescent cells show increased dye uptake

To study which cells in the CNS become senescent, we purify $p16^{High}$ cells from brains of naturally aged mice in chapter 3. During sorting of $p16^{High}$ cells and analysis of the FACS plots, increased levels of DAPI were observed in $p16^{High}$ cells compared to $p16^{Low}$ cells in both young and old animals (Figure 1A-B). DAPI normally only enters the nuclei of dead cells, however the level of DAPI in $p16^{High}$ cells was below the threshold that was set to identify dead cells. To confirm this finding, IMR90 fibroblasts exposed to 10 Gy of gamma irradiation were stained with both Hoechst, penetrating live cells, and DAPI, penetrating permeabilized membranes. The ratio DAPI over Hoechst was quantified and showed a higher ratio in the irradiated cells versus the controls (Figure 1C-D). In addition, the uptake of trypan blue by irradiated IMR90 cells was measured and increased compared to proliferating control cells (Figure 1E). The percentafe of cells lost during replating was lower than the difference in trypan blue uptake, suggesting that cell death is not the cause of dye uptake in senescent cells (Figure 1F). Together this data suggest that the cell membrane of senescent cells is more permeable compared to proliferating cells.

LAPTM4A, the lysosomal gene found upregulated in senescent fibroblast in chapter 2, has been shown to be involved in the synthesis of glycosphingolipids, which are components of the cell membrane (Yamaji et al., 2019). The increased expression of this gene in senescent cells might alter glycosphingolipid synthesis and thereby influence the composition and integrity of the cell membrane resulting in a more permeable membrane.

Markers for senescent cells in the CNS

Post-mitotic neurons have been shown to accumulate features of senescence (Moreno-Blas et al., 2019; Riessland et al., 2019). This, in combination with the results from chapter 4, where glial cells have been shown to portray a senescence phenotype, implies that both mitotic and post-mitotic cells can become senescent. The differences between senescence of mitotic and post-mitotic cells is not fully understood. To identify these differences and their consequences, further studies should be performed on the validity of senescence-associated phenotypes and their functional ramifications in the

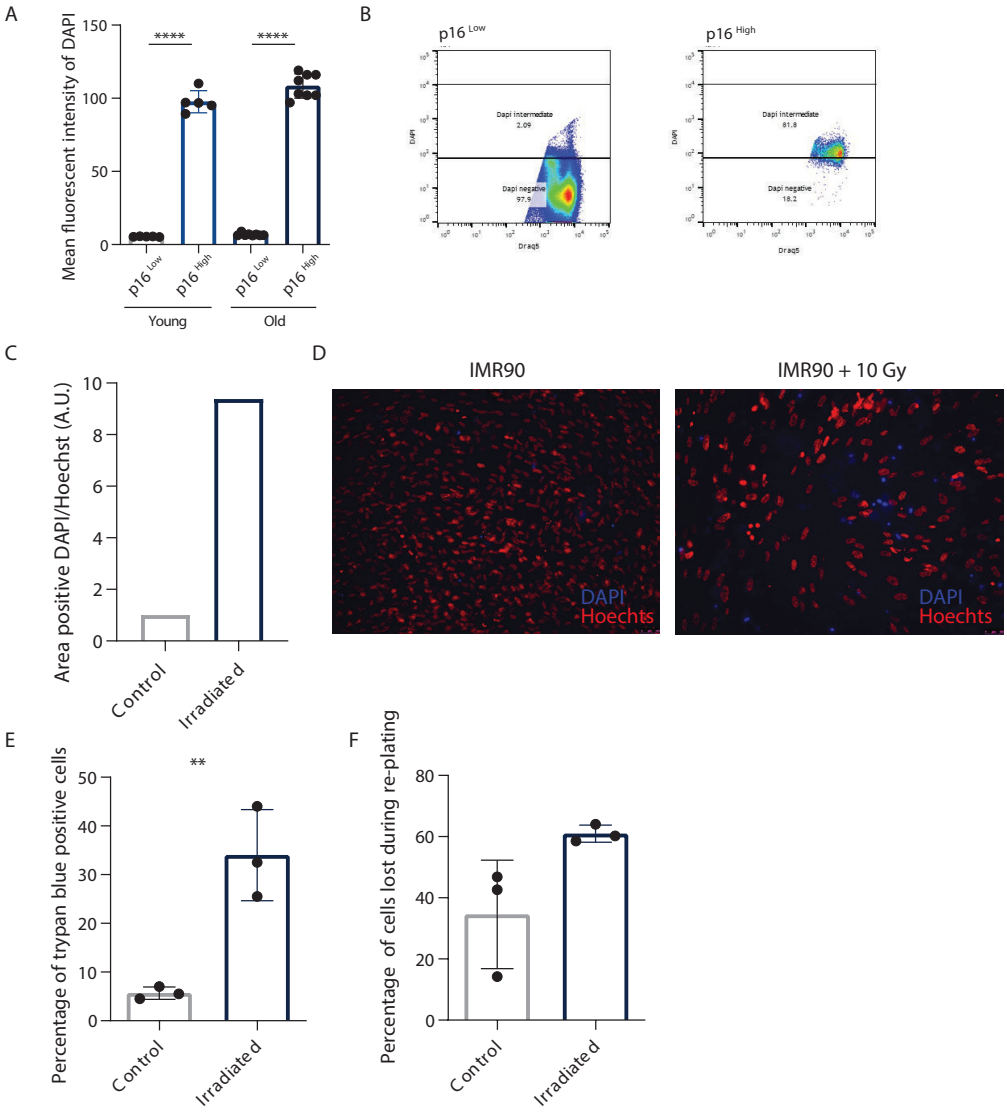

Figure 1: Increased uptake of dyes by senescent cells.

*A: Quantification of mean fluorescent intensity of DAPI in $p16^{High}$ and $p16^{Low}$ cells isolated from brains of 7-12-week (defined young) and 105-116-week (defined old) mice. B: Representative FACS plots showing the distribution of cells in the DAPI channel with the DAPI positive cells (defined as dead cells) removed from the plots. C: Area positive of DAPI divided by the area positive for Hoechst in IMR90 fibroblast with or without 10 Gy of gamma irradiation 1 week before staining. D: Representative images of IMR90 cells stained with DAPI and Hoechst 1 week after (mock) irradiation. E: Quantification of percentage of trypan blue positive IMR90 cells 1 week after 10 Gy irradiation. **p<0.01 F: Quantification of percentage of IMR90 cells before plating minus after replating 1 week after 10 Gy irradiation.*

brain.

Most studies on senescence in the brain so far have been performed in mice. It is important to be able to understand the role of senescent cells in human brains as well. The difficulty of not being able to take the CNS from living donors is the delay of the postmortem tissues and co-morbidities of donors. Markers of senescence detect damage such as DNA-damage and alterations in morphology of cells and nuclei. However, in postmortem tissues it is difficult to know if a damage is caused by a disease or ageing or if the damage accumulated during or after death of the donor. It is important to keep this in mind when translating the results found in murine studies to the human situation. More models closer to the human brain, such as brain organoids that are being developed, might help to elucidate the function of senescent brain cells in a complex environment. As an alternative, specimens obtained after brain surgery to treat epilepsy or remove brain tumors might add value to senescence research, because there is no time delay between the surgery and sample collection and processing.

Implications for senescent cells in the brain

In addition to differences between mitotic and post-mitotic cells, there are also differences in senescence marker expression within cell types of the CNS as a result of different stimuli. In chapter 3, p16 expression was increased by ageing in microglia, but other senescence markers were not increased in the transcriptome of these cells. The transcriptional profile of p16 expressing microglia did differ from the other microglia present in the aged murine brain. In chapter 4, senescence markers were induced in microglia, astrocytes and oligodendrocytes by genotoxic stress. The type of stressor seemed to determine the expression of the senescence markers in the glial cells, indicating that there is not only one senescence phenotype. Together, this shows that the induction of senescence phenotypes is different by different stressors. The effect of the different phenotypes of senescent cells in the CNS remain unknown. Some of the phenotypes might be beneficial, while other senescent phenotypes might induce neurotoxicity and neurodegeneration. Identification and elucidation of the roles of senescent cells in the CNS should elucidate which senescent cells are protective and should be protected from elimination while the other phenotypes might be targeted for removal to ameliorate brain degeneration.

Direct versus indirect induction of senescence

Cellular senescence in the CNS can be induced by stressors directly such as ageing of the cells and genotoxic stress, but also indirectly due to SASP expression of peripheral cells. However, this area is not yet explored in detail. In chapter 4, the effect of doxorubicin-induced senescence on microglia suggest that factors secreted by senescent cells can influence glial cells in the brain. Further studies need to confirm the effect of senescent cells on the brain and the degree of influence that the periphery can have on the brain. Interestingly, removal of peripheral senescence cells has been shown to improve cognitive function (Ogrodnik et al., 2021).
Secondary senescence in the brain due to peripheral senescent cells by the secretion of SASP factors is another area that has not been explored. Does the SASP activate glial cells and do brain cells become senescent due to the SASP? These questions remain to be answered.

The interplay between the blood-brain-barrier and senescence

The blood-brain-barrier (BBB) plays an important role in protecting the brain from damaging agents that might circulate in the vascular system and thereby also in the indirect effects of senescent cells on the brain. The BBB loses integrity with age (Montagne et al., 2015) and senescent cells accumulate with ageing (Baker et al., 2016). Together, this increases the vulnerability of the brain to the SASP. Furthermore, senescent cells have been shown to contribute to the loss of blood brain barrier functioning exacerbating this issue (Yamazaki et al., 2016). To date, not much is known on the effects of senescent cell removal on the BBB. In addition, no studies have investigated if senescent cells also infiltrate the CNS, especially when the BBB is leakier. Future experiments studying senescence in the CNS should also take the BBB into account for example by mapping senescent cells in the brain over time.

Future prospects

Permeability of senescent cells

First, senescent cells should be further characterized to improve identification and targeting of senescent cells. The cell membrane is a part of the senescent cell that should be further investigated. To test the permeability of senescent cell membranes, experiments such as lipidomics of the cell membrane of senescent cells and live cell imaging of uptake of (fluorescent) particles should be performed. If the experiments confirm the more penetrable membranes of senescent cells, this feature could be exploited as a means to detect senescent cells, but possible also help with targeting drugs specifically to these cells.

Senescent glial cell function

To delineate the effect of the senescence program on glial cell function, senescent glial cells need to be further investigated. In chapter 3, $p16^{High}$ microglia have been identified in the aged brain together with their transcriptional profile. To investigate their function, these cells could be specifically removed using the p16-3MR transgenic mice. To make the mouse more specific for microglia, the p16-3MR should be activated by a microglia-specific promotor Cx3cr1 using a cre/loxp system. A stop codon would be incorporated in the *p16* promotor of the p16-3MR construct and would be floxed. Only microglia, which have active Cx3cr1 expression, express Cre which results in the removal of the stop codon. In turn, p16 expression would result in the upregulation of the kill switch. Thereby the $p16^{High}$ microglia can be specifically ablated without affecting other cell types. The morphology of the glial cells together with their response to inflammatory stimuli such as LPS should be measured. Similar experiments should be performed in stress or disease induced senescence in the brain. In addition to the in vivo experiments, functional experiments of senescent cells in vitro such as phagocytosis assays and chemotaxis assays of p16 overexpressing microglia might further elucidate the effect of senescence on glia cell function.

Senescent cell markers in the CNS

Another strategy to isolate and investigate p16^{High} microglia is to find a specific marker that can be used to purify these cells from non-transgenic mice. The novel Cx3cr1-Cre/p16-3MR/loxp mouse model should be used to find and validate such a marker by purifying p16^{High} microglia and characterize surface proteins that are specifically expressed on these cells. This marker can then also be used to investigate p16^{High} microglia purified from human brain tissue and study if these cells are similar across species.

In addition to the marker found by investigating p16^{High} microglia, also other promising senescence markers should be explored. In chapter 2, the *LAPTM4A* gene was identified as a promising candidate. Further studies should characterize if the protein is also increased in senescent cells and if this is the case only in fibroblast or also in other cell types. When in vitro studies confirm the upregulation of *LAPTM4A* in senescent cells, a mouse model expressing the 3MR construct after the *LAPTM4A* promotor instead of the *p16* promotor should be constructed to be able to visualize where in the body this protein in upregulated and what the effect is of eliminating specifically *LAPTM4A* expressing cells to investigate if this might be a novel target for senescent cells and ameliorate age related diseases.

Senescence in human the brain with ageing and disease

The largest gap in our understanding of senescence in the CNS resides in the translation of senescent cells that have been identified in the animal models to the human situation. First, we need to determine if cells of the human CNS become senescent. Next, the factors correlated to senescence need to be identified, such as ageing and neurodegenerative diseases. To investigate the cell types in the aged and diseased human brain tissues that express senescence markers in more detail, experiments performing multi-omics approaches in combination with spatial resolution such as spatial transcriptomics and RNA in situ hybridization should be performed. The roles of these cells should then be further investigated. *In vitro* models with human brain cells, such as induced pluripotent stem cell derived co-cultures of neurons and glial cells might give

the first insight into the functional differences between senescent brain cells and the effect they have on the surrounding environment.

Indirect effects of senescent cells on the CNS

In line with this, different stimuli might induce different sets of SASP factors in brain cells. Similar in vitro studies could identify the beneficial and detrimental factors for brain cells and this knowledge can be used for future treatments of neurodegenerative diseases. Instead of removing senescent cells per se, the elimination of specific detrimental factors or induction of beneficial ones might ameliorate brain degeneration. Experiments investigating the SASP factors that enter the brain from the periphery and their effect on the brain cells should be performed to test if detrimental factors enter the CNS. This might be done by transplanting senescent cells into the periphery of mice and measure the cytokine and chemokine levels in the CNS. In addition, the morphology and transcriptional profile of brain cells, senescence marker expression and cognitive functioning should be determined.

Effect of therapies on senescence in the CNS

The effects of therapies, that patients receive to treat other diseases such as cancer, on senescence in the CNS is unknown. Further studies are needed to identify which therapies cause senescence. Do they cause senescence in the periphery and thereby affect the brain or do they also cause senescence in the CNS directly? What are the consequences of these senescent cells? Do these cells secrete different types of SASP due to different treatments? All these questions remain to be answered. We could start answering these questions by studying brain tissues from tissue repositories such as the Netherlands Brain Bank and correlate the medical information about therapies received by the donor to senescence load. There are donors that have received treatments against cancer such as irradiation and chemotherapy, which are expected to induce senescence in the brain, and studying these tissues might confirm the results found in animal models.

The effects of senescent cell removal on the CNS

Removing senescent cells from the periphery has been proven beneficial in

mice (Baker et al., 2011; Chang et al., 2016; Demaria et al., 2017). Moreover, the effectiveness of senolytics, drugs that specifically remove senescent cells, has been proven in humans for diseases such as idiopathic pulmonary fibrosis, diabetes mellitus, and chronic kidney disease (Ellison-Hughes, 2020). The effect of elimination of senescent cells on the CNS has to be researched in more detail to prevent potential side-effects of senolytic drugs on the brain and maybe even exploit these treatments to prevent or ameliorate neurodegeneration.

All the steps from senescence marker to senescence brain cell function and elimination will answer the question: Should we remove senescent brain cells or in other words, to eliminate or not to eliminate?

Conclusion

Senescent cells are present in both the aged murine and human CNS. The role of these cells in the CNS have to be studied further to investigate if the cells should be eliminated or play a crucial role for the maintenance of the brain. Senescent glial cells might be harmful to the ageing brain, while senescent neurons and neuron progenitor cells removal might further deteriorate the cognitive functioning of the CNS. With an eye on recent senolytic developments in clinical trials, it has to be considered that there is a lack of knowledge on the effect of removal of senescent brain cells. More studies have to be performed to discover how effectively these drugs cross the BBB, enter the CNS and what the consequences of elimination of senescent brain cells might be. The question remains: is clearance of senescent cells from the CNS beneficial for brain function or might this further progress CNS pathology in the ageing brain?

References

Baker, D.J., Wijshake, T., Tchkonia, T., Lebrasseur, N.K., Childs, B.G., Van De Sluis, B., Kirkland, J.L., and Van Deursen, J.M. (2011). Clearance of p16 Ink4a-positive senescent cells delays ageing-associated disorders. Nature 479, 232–236.

Baker, D.J., Childs, B.G., Durik, M., Wijers, M.E., Sieben, C.J., Zhong, J., A. Saltness, R., Jeganathan, K.B., Verzosa, G.C., Pezeshki, A., et al. (2016). Naturally occurring p16 Ink4a-positive cells shorten healthy lifespan. Nature 530, 184–189.

Chang, J., Wang, Y., Shao, L., Laberge, R.-M., Demaria, M., Campisi, J., Janakiraman, K., Sharpless, N.E., Ding, S., Feng, W., et al. (2016). Clearance of senescent cells by ABT263 rejuvenates aged hematopoietic stem cells in mice. Nat. Med. 22, 78–83.

Demaria, M., O'Leary, M.N., Chang, J., Shao, L., Liu, S., Alimirah, F., Koenig, K., Le, C., Mitin, N., Deal, A.M., et al. (2017). Cellular Senescence Promotes Adverse Effects of Chemotherapy and Cancer Relapse. Cancer Discov. 7, 165–176.

Ellison-Hughes, G.M. (2020). First evidence that senolytics are effective at decreasing senescent cells in humans. EBioMedicine 56.

Hayflick, L., and Moorhead, P.S. (1961). The serial cultivation of human diploid cell strains. Exp. Cell Res. 25, 585–621.

Hernandez-Segura, A., de Jong, T. V, Melov, S., Guryev, V., Campisi, J., and Demaria, M. (2017). Unmasking Transcriptional Heterogeneity in Senescent Cells.

Montagne, A., Barnes, S.R., Sweeney, M.D., Halliday, M.R., Sagare, A.P., Zhao, Z., Toga, A.W., Jacobs, R.E., Liu, C.Y., Amezcua, L., et al. (2015). Blood-brain barrier breakdown in the aging human hippocampus. Neuron 85, 296–302.

Moreno-Blas, D., Gorostieta-Salas, E., Pommer-Alba, A., Muciño-Hernández, G., Gerónimo-Olvera, C., Maciel-Barón, L.A., Konigsberg, M., Massieu, L., and Castro-Obregón, S. (2019). Cortical neurons develop a senescence-like phenotype promoted by dysfunctional autophagy. Aging (Albany. NY). 11, 6175–6198.

Ogrodnik, M., Evans, S.A., Fielder, E., Victorelli, S., Kruger, P., Salmonowicz, H., Weigand, B.M., Patel, A.D., Pirtskhalava, T., Inman, C.L., et al. (2021). Whole-body senescent cell clearance alleviates age-related brain inflammation and cognitive impairment in mice. Aging Cell.

Riessland, M., Kolisnyk, B., Kim, T.W., Cheng, J., Ni, J., Pearson, J.A., Park, E.J., Dam, K., Acehan, D., Ramos-Espiritu, L.S., et al. (2019). Loss of SATB1 Induces p21-Dependent Cellular Senescence in Post-mitotic Dopaminergic Neurons. Cell Stem Cell.

Yamaji, T., Sekizuka, T., Tachida, Y., Sakuma, C., Morimoto, K., Kuroda, M., and Hanada, K. (2019). A CRISPR Screen Identifies LAPTM4A and TM9SF Proteins as Glycolipid-Regulating Factors. IScience 11, 409–424.

Yamazaki, Y., Baker, D.J., Tachibana, M., Liu, C.-C., van Deursen, J.M., Brott, T.G., Bu, G., and Kanekiyo, T. (2016). Vascular Cell Senescence Contributes to Blood-Brain Barrier Breakdown. Stroke 47, 1068–1077.

5

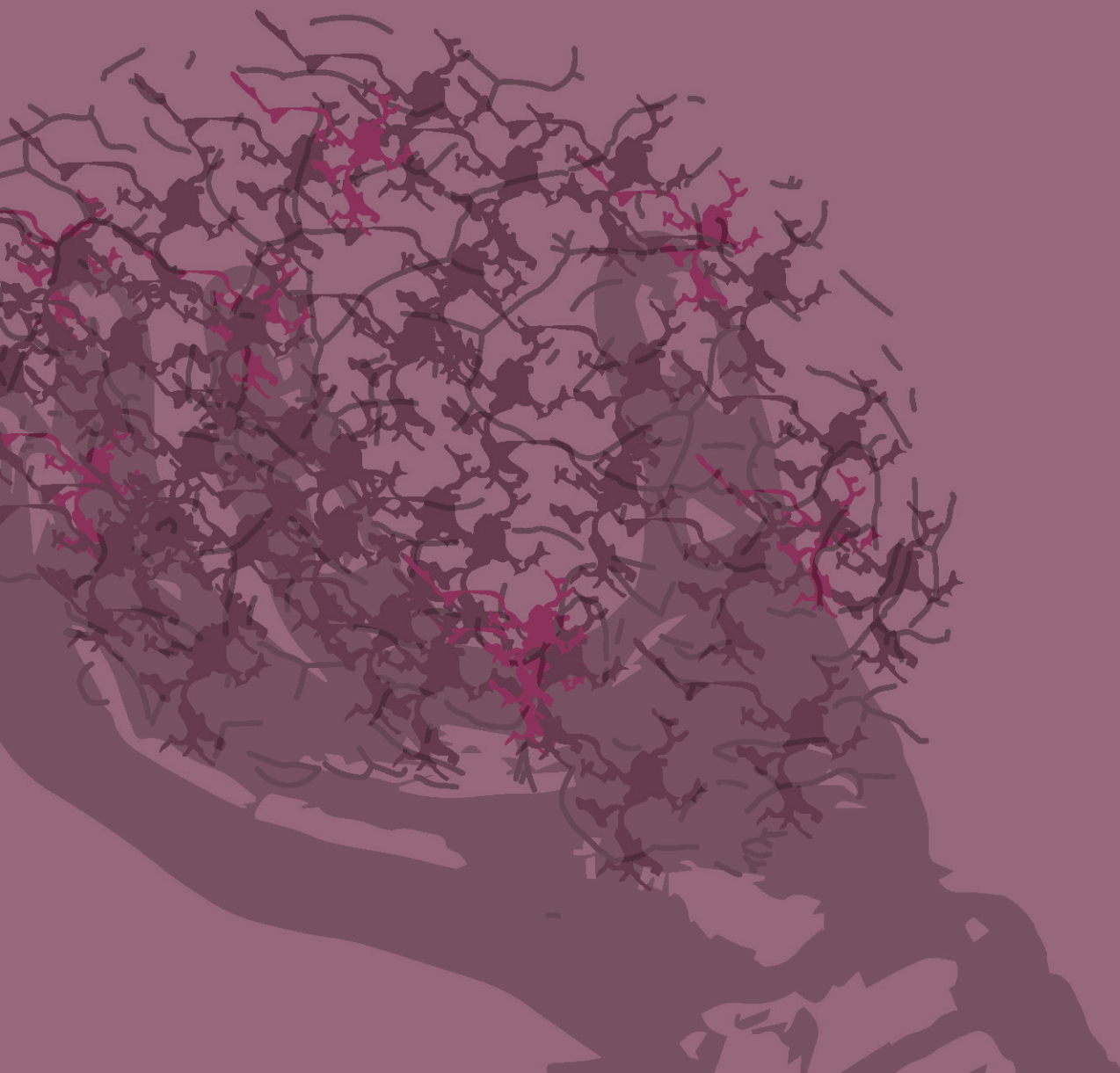

Chapter 6

Appendices

I List of abbreviations

II Nederlandse samenvatting

III Acknowledgements

IV About the author

V List of publications

List of abbreviations

AD	Alzheimer’s disease
ALS	Amyotrophic lateral sclerosis
APP	Amyloid precursor protein
BBB	Blood brain barrier
CAM	CNS associated macrophages
CCL	Chemokine (C-C motif) ligand
CDK	Cyclin dependent kinase
CDP	Central animal facility
CNS	Central nervous system
CXCL	Chemokine (C-X-C motif) ligand
DAM	Disease associated microglia
DAPI	4’,6-diamidino-2-phenylindole
DDR	DNA damage response
DEC	Animal care and use committee
DMEM	Dulbecco's modified eagle medium
EAE	Experimental autoimmune encephalomyelitis
EdU	5-ethynyl-2'-deoxyuridine
ELISA	Enzyme-linked immunosorbent assay
EV	Extracellular vesicles
FACS	Fluorescence-activated cell sorting
FBS	Fetal bovine serum

FUS	Fused in sarcoma
GRP	Glial restricted progenitor
Gy	Gray
HMBG	High-mobility group box
HOM	Homeostatic microglia
HSV	Herpes simplex virus
HVG	Highly variable feature
IFN	Interferon microglia
IL	Interleukin
LAPTM4A	Lysosomal-associated transmembrane protein 4A
LLOMe	L-Leucyl-L-Leucine-O-Methyl esther
logFC	Log fold change
MEF	Mouse embryonic fibroblast
MMP	Matrix metalloproteinase
mRFP	Monomeric red fluorescent protein
MTX	Methotrexate
MS	Multiple sclerosis
N	Newton
NK	Natural killer
NORT	Novel object recognition task
OHSC	Organotypic hippocampal slice cultures
OPC	Oligodendrocyte progenitor cell
PAI	Plasminogen activator inhibitor

PBR	Benzodiazepine receptors
PCA	Principal component analysis
PD	Parkinson's disease
PET	Positron Emission Tomography
PSEN	Presenilin
qRT-PCR	Quantitative real-time poly chain reaction
ROS	Reactive oxygen species
SA-β-gal	Senescence-associated β-galactosidase
SASP	Senescence associated secretory phenotype
SOD	Superoxide dismutase
tTK	Thymidine kinase
UM	Unknown microglia
UMAP	Uniform manifold approximation and projection
WGCNA	Weighed gene correlation network analysis

Nederlandse samenvatting

Met het toenemende bewijs van de gunstige effecten van de eliminatie van senescente cellen tijdens het ouder worden en het groeiende aantal klinische onderzoeken naar het effect van senolytica in het menselijk lichaam, is het belangrijk om de impact te begrijpen die deze medicijnen kunnen hebben op het centraal zenuw stelsel (CZS). Om dit te begrijpen, moeten we onze kennis uitbreiden over de celtypen in het CZS die senescent worden en of dit proces gunstig of nadelig is voor het ouder wordende brein. In dit proefschrift onderzoeken we het natuurlijke en versnelde verouderingsfenotype van CZS-cellen.

In hoofdstuk 1 beschrijf ik de huidige kennis over hoe cellulaire veroudering zich ontwikkelt in het CZS. Eerst geef ik een algemeen overzicht van wat de meest voorkomende senescentie-geassocieerde fenotypes zijn. Vervolgens beschrijf ik de cellulaire samenstelling van de hersenen, de rol van gliacellen en leeftijdsgebonden veranderingen. Ten slotte geef ik een overzicht van het bewijs van cellulaire senescentie bij neurodegeneratie en hersenveroudering.

In hoofdstuk 2 bestuderen we het effect van het moduleren van de lysosomale activiteit in senescente menselijke fibroblasten. We laten zien dat drie lysosomale modulerende middelen de activiteit van de senescentie-geassocieerde β-galactosidase beïnvloeden, maar niet leiden tot veranderingen in groeistop of het senescent geassocieerde secretie fenotype (SASP). Bovendien laten we zien dat voorbehandeling van fibroblasten met een van de middelen de senescentie-inductie door de CDK4/6-remmer palbociclib vermindert, welke werking gerelateerd is aan lysosomale accumulatie.

In hoofdstuk 3 gebruiken we het p16-3MR muismodel om in verouderde hersenen p16 tot expressie brengende cellen te identificeren. Cellen met hoge p16 expressie ($p16^{Hoog}$-cellen) werden gesorteerd uit de hersenen van jonge en oude muizen en gekarakteriseerd met behulp van bulk- en single-cell sequencing. We laten een verhoogd aantal $p16^{Hoog}$ cellen zien in de hersenen van oude muizen in vergelijking met de hersenen van jonge muizen. Met behulp van bulksequencing laten we differentieel tot expressie gebrachte genen zien tussen de $p16^{Hoog}$ en $p16^{Laag}$ cellen die meestal verband houden met

fagocytose en ontsteking. Met clusteranalyse van de single cell data laten we een verrijking zien van microglia in de p16^{Hoog} populatie. We bevestigen dat microglia in wildtype muizen en menselijke hersenen een hoge *p16/CDKN2A*-expressie hebben. Met extra clustering binnen de microglia-populatie van de single cell gegevens, identificeren we twee nieuwe verschillende subpopulaties verrijkt in de p16^{Hoog} microglia. Deze voorheen niet-geïdentificeerde microglia-clusters veranderen in de loop van de tijd in hoeveelheid. Cluster 1 is stabiel aanwezig, maar neemt af met de leeftijd en cluster 2 neemt toe in het verouderingsproces.

In hoofdstuk 4 onderzoeken we de effecten van genotoxische stress geinduceerde senescentie op gliacellen. We vinden dat genotoxische stress de expressie van senescentie-geassocieerde markers in gekweekte gliacellen induceert. We meten indirecte effecten van SASP op hersencellen met behulp van organotypische hippocampale slice-culturen. We vinden geen veranderingen in genexpressie of celaantallen in de slice-culturen die zijn behandeld met geconditioneerd medium van senescente fibroblasten in vergelijking met slice-culturen die zijn blootgesteld aan geconditioneerd medium van prolifererende fibroblasten. We meten de effecten van twee chemotherapeutica, methotrexaat en doxorubicine, *in vivo* om directe en indirecte effecten op de hersenen te onderzoeken. Methotrexaat vermindert het spieruithoudingsvermogen van muizen en verhoogt veranderd gedrag in een open veldtest, maar we zien geen veranderingen in senescentiemarkers. Doxorubicine daarentegen verhoogt de *p21*-expressie en beïnvloedt de samenstelling van de witte bloedcellen, maar we vinden geen veranderingen in de cognitieve functie. Microglia geïsoleerd uit met doxorubicine behandelde muizen vertonen differentieel tot expressie gebrachte genen in vergelijking met hun nestgenoten, wat gerelateerd is aan mTOR-signalering en negatieve groeiregulatie.

In hoofdstuk 5 wordt de data uit hoofdstukken 2 tot en met 4 bediscussieerd en de experimenten en perspectieven voor de toekomst beschreven.

Conclusie

Senescente cellen zijn aanwezig zowel in het CZS van verouderde muizen- als het menselijke CZS. De rol van deze cellen in het CZS moet verder worden bestudeerd om te onderzoeken of de cellen een cruciale rol spelen voor het onderhoud van de hersenen of moeten worden geëlimineerd. Senescente gliacellen kunnen schadelijk zijn voor de ouder wordende hersenen, terwijl het verwijderen van verouderde neuronen en neuronvoorlopercellen de cognitieve werking van het CZS verder kan verslechteren. Met het oog op recente senolytische ontwikkelingen in klinische onderzoeken, moet er rekening worden gehouden met het feit dat er een gebrek is aan kennis over het effect van eliminatie van verouderende hersencellen. Er moeten meer studies worden uitgevoerd om te ontdekken hoe effectief synolytica de BBB passeren, het CZS binnendringen en wat de gevolgen kunnen zijn van de eliminatie van verouderde hersencellen. De vraag blijft: is de eliminatie van senescente cellen uit het CZS gunstig voor de hersenfunctie of kan dit de CZS-pathologie in de verouderende hersenen verder bevorderen?

Acknowledgements

With the thesis completed, it is time to thank all the people that supported me during this period of my life.

First of all, I would like to thank **prof. dr. Bart J.L. Eggen** and **prof. dr. Marco Demaria** for the supervision during my PhD project. It was a bumpy ride, but with your help we managed to get everything back on track. I am glad that I was able to start a collaboration between both your labs and hope that this will continue after I have left the UMCG.

Yearly assistance provided by **prof. dr. Eddy A. van der Zee** and **dr. Peter de Keizer** helped me taking a step back and looking at my project from a different perspective. I would like to thank you both for being part of my supervisory committee and for always showing interest in my work.

In addition, I would like to thank the members of the reading committee **Prof. dr. Dineke Verbeek**, **prof. dr. Vassilis Gorgoulis** and **prof. dr João Malva** for taking the time to read and for providing feedback on my thesis.

I would like to thank my paranymphs **Josephine Hartung** and **Sharon Eskandar** for standing by my side during the PhD and the defense itself. **Jooosi**, thank you for always helping me with techniques in the lab as well as being super supportive during the whole project. Besides the lab, we spend a lot of time playing pool, going out or just making risotto and chilling on the couch. I enjoyed every minute of it and there will be many more. Best of luck with the last part of you PhD, you can do it! **Sharon**, you are the most outgoing person I know. Our conversations helped me a lot with growing as a person and believing more in myself. Thank you for being my quarantine buddy. Good luck with your medical rotations and finishing your PhD. I hope I can have you as my gynecologist in the future!

Working in between two labs was not always easy, but it did provide me with the privilege of having many people to discuss my project and personal matters. At the neuroscience department in the section medical physiology or now called department of the Biomedical Sciences of Cells & Systems, section Molecular Neurobiology, I started as a master student under the supervision

of **dr. Susanne M. Kooistra**. **Suus**, thank you for a great internship and always helping me with all of my questions also after the internship. Coming back as a PhD student was a very warm welcome back by everyone at the department. I would like to thank everyone in the department for contributing to this supportive and fun work environment. The staff: **Trix**, **Nieske**, **Eef**, **Hilmar**, **Tjalling**, **Michel**, **Rob**, **Inge Z**, **Inge H**, **Maaike**, **Naomi** and **Sharon B**. **Sharon**, I am very happy to be able to call you my girlfriend. It all started with the folding of 1000 origami cranes. I hope we will have a very fun and happy 53 years together with a lot of good food, good books, and amazing holidays.

The PhD students and postdocs rotate over the years: **Roeland**, **Marissa**, **Javier**, **Leroy**, **Yang**, **Xiaoming**, **Laura**, **Malte**, **Takuya**, **Tiago**, **Chairi**, **Sharon E**, **Jody**, **Marion**, **Wendy**, **Pauline**, **Rianne**, **Astrid**, **Anneke**, **Emma**, **Mirjam** and **Marina**. Together you made sure that there was always someone to answer questions about experiments and reagents, but also made sure there were always people to hang out with after office hours.

I was very lucky to share my office space with amazing people. First, **Xiaoming**, **Yang,** and **Chairi**. Later also **Sharon** and **Jody**. We had a great time together talking about everything and nothing. I could not have wished for better office mates. Thank you guys! **Chairi**, as a bit of the outlaws of the department, we could always confide in each other. I am very grateful for our friendship and am sure that it will last long after our PhD journeys have finished. I hope that you will find a position in the pharmaceutical industry that suits you and I wish you all the best for the next steps in your career and in life! **Jody**, we started to hang out relatively recently due to the move of the 10th floor to the 8th. Nevertheless, I am very happy that you joined our office and that we persevered through our Spanish course together. It might have been not such a good idea of me, but I am glad that we did it anyway and could struggle together. I wish you the best of luck with your PhD, but also with other adventures such as podcasts and horror movies.

Laura, I was very honored to be chosen as one of your paranymphs. I enjoyed our many activities together such as swimming, running and yoga. Enjoy your sabbatical and I hope to be able to enjoy many more yoga sessions with you as the instructor!

Emma, thank you for your help with the bioinformatic analysis of my article and fun adventures in the city center. I see a very successful future for you. Enjoy your post-doc in Stockholm!

Takuya, together we climbed many walls with many different routes. You motivated me to always go one boulder or grip further than I thought I could do. I wish you a lot of fun and nice experiences with traveling the world!

Marion, as the 6 members of the nicest offices at the 8th floor, we made a great team. I enjoyed a lot hanging out together after work and playing games such as saboteur. Good luck with your PhD and many hobbies. Don't forget to also do nothing sometimes!

The second half of my time I have spent at the European Research Institute of the Biology of Ageing (ERIBA). My lab members: **Alejandra**, **Jas**, **Thijmen**, **Eleni, Martha**, **Boshi**, **Jamil**, **Sebastian**, **Simone**, **Lotte**, **Michela**, **Willem**, **Yao**, and **Abel**. **Jamil,** you helped me integrate after our animal course together. I enjoyed our Berlin and Jena conference trip together a lot. I wish you the best of luck as post-doc in the lab!

Ale, we developed our friendship very quickly after I had proven to be a worthy Dutchy. I will always treasure the time we spend in Mexico together at the time of your wedding. I look forward to seeing what next steps you will take in your career. For now, best of luck at the RIVM as a proper Dutch person and enjoy your life in Nieuwegein.

Elaaa **Eleni**, thank you for listening to me complain all the time and making sitting behind our desks together a good time to look back on. I am happy you found your job as a project leader in the UMCG, so that we can spend more time in Groningen together.

Lotte, as my pole buddy, we already worked well together by supporting and catching each other at the pole. Thank you for all your help with the genotyping of mice and general lab stuff. Good luck at the lab and with possible future adventures!

Boshi, it was an honor to be your paranymph. Happy to see your paper was finally published! I wish you good luck with your carreer.

Abel, I enjoyed the dinners at your place a lot. Please still message me whenever you have an excess of hello fresh food. Lots of luck with your postdoc as a Dutch citizen!

Martha, thank you for your help with my Spanish tests and being a very nice colleague who actually refills things that are empty! I hope you will have a beautiful wedding and that your time here was successful, so that you will develop your career further in Spain.

Next, I want to thank my students: Bachelor students **Loes** and **Jade** and Master students **Teodora** and **Jurgen.** You helped me look at my project with a different perspective and contributed to this thesis with your experiments in the lab.

Next to lab members, also colleagues of the institute make the days at ERIBA more enjoyable. **Gloria**, I want to thank you for teaching me Spanish over the past couple of years. Gracias, muy amable! Together with **Wytse**, we planned a great trip through Mexico with as highlight Dia de los Muertos in Oaxaca.

For everyone at the first floor, thank you for the many nice activities we did together from pub quizzes to karaoke nights: **Gertrud**, **Hidde**, **Britt**, **Tobias**, **Leen**, **Anita**, **Mandy**, **Wytse**, **Renée**, **Kaila**, **Lisette,** and **Lale**.

Froukje, **Annabet** en **Bente**, als huisgenoten wil ik jullie graag bedanken voor een fijne sfeer in huis waarin ik altijd kon praten over de hoogte, maar ook dieptepunten van mijn project.

Mem en Gjalt, ik wol jim graach bedanke foar olle geselliche wiekeinen en steunende telefoantsjes.

About the author

Nynke Talma was born on the 19th of June 1994 in Leeuwarden. After finishing high school (VWO) in 2012 in Harlingen, she moved to Groningen to study Life Science and Technology at the University of Groningen (RUG). After obtaining her bachelor degree, she was selected for the master Medical Pharmaceutical Drug Innovation (MPDI) during which she did an internship for six months at the Buck Institute for Research on Ageing in Novato, California, USA, researching cellular senescence. With her knowledge obtained during this internship in combination with the knowledge from the previous internship at the neuroscience department in the section medical physiology, she wrote an application for a PhD project combining the two subjects: cellular senescence in the brain. This PhD project was granted a scholarship and the end result of the PhD project is described in this thesis. Currently she is working as a Scientific Official Secretary at the BEBO foundation in Assen.

List of publications

Identification of distinct and age-dependent p16High microglia subtypes

Talma, N. , Gerrits, E. , Wang, B. , Eggen, B. J. L. & Demaria, M. , 1-Oct-2021 , (E-pub ahead of print) In: Aging Cell. 13 p. , e13450.

P16-expressing microglial cells with distinct transcriptional profiles accumulate in the aging brain

Talma, N. , Gerrits, E. , Wang, B. , Eggen, B. J. & Demaria, M. , Jul-2021 , In: Glia. 69 , p. E262-E263 2 p.

A Senescence-Centric View of Aging: Implications for Longevity and Disease

Borghesan, M. , Hoogaars, W. M. H. , Varela-Eirin, M. , Talma, N. & Demaria, M. , Oct-2020 , In: Trends in Cell Biology. 30 , 10 , p. 777-791 15 p.

Pharmacokinetic Analysis of Monoamine Oxidase-B Tracer [C-11]-Deprenyl in Rats

Giacobbo, B. L. , Moraga-Amaro, R. E. , Schildt, A. , Sijbesma, J. W. A. , Talma, N. , Dierckx, R. A. J. O. , Doorduin, J. & de Vries, E. F. J. , Oct-2018 , In: European Journal of Nuclear Medicine and Molecular Imaging. 45 , p. S623 1 p.

Targeting senescence to delay progression of multiple sclerosis

Oost, W. , Talma, N. , Meilof, J. F. & Laman, J. D. , Nov-2018 , In: Journal of Molecular Medicine. 96 , 11 , p. 1153-1166 14 p.

Neuroprotective hypothermia - Why keep your head cool during ischemia and reperfusion

Talma, N. , Kok, W. F. , Veij Mestdagh, de, C. , Shanbhag, N. C. , Bouma, H. R. & Henning, R. H. , Nov-2016 , In: Biochimica et Biophysica Acta-General Subjects. 1860 , 11 , p. 2521-2528 8 p.